DOKUZ EYLÜL UNIVERSITY

GRADUATE SCHOOL OF NATURAL AND APPLIED SCIENCES

NUMERICAL AND EXPERIMENTAL INVESTIGATION OF MIXED CONVECTION IN REFRIGERATORS

by

Mete ÖZŞEN

July, 2011

İZMİR

NUMERICAL AND EXPERIMENTAL INVESTIGATION OF MIXED CONVECTION IN REFRIGERATORS

A Thesis Submitted to the Graduate School of Natural and Applied Sciences of Dokuz Eylül University In Partial Fulfillment of the Requirements for the Degree of Master of Science in Mechanical Engineering, Energy Program

by

Mete ÖZŞEN

July, 2011

İZMİR

THESIS EXAMINATION RESULT FORM

We have read the thesis entitled **"NUMERICAL AND EXPERIMENTAL INVESTIGATION OF MIXED CONVECTION IN REFRIGERATORS"** completed by **METE ÖZŞEN** under supervision of **ASSOC. PROF. DR. DİLEK KUMLUTAŞ** and we certify that in our opinion it is fully adequate, in scope and in quality, as a thesis for the degree of Master of Science.

Assoc. Prof. Dr. Dilek KUMLUTAŞ

Supervisor

Prof. Dr. İsmail H. TAVMAN

(Jury Member)

Yard. Doç. Dr. M. Turhan ÇOBAN

(Jury Member)

Prof. Dr. Mustafa SABUNCU
Director
Graduate School of Natural and Applied Sciences

ACKNOWLEDGMENTS

First of all, I would like to thank to my supervisor, Assoc. Prof. Dr. Dilek KUMLUTAŞ, for providing study environment and computational power for this numerical study in the university and also her advises and guidance throughout my study.

Also, I would like to thank to Assist. Ziya Haktan KARADENİZ and my friends in the Masters Degree Program of Energy, for sharing their knowledge and help.

Also I would like to thank to M.Sc. Mechanical Engineer Umut YILMAZ who works in the Innovation & Concept Department of the Vestel White Goods Company for helping the experimental studies.

Finally, I would like to gratefully thank to my family for their patience and unconditional support in every part of my life.

This study is supported by the Republic of TURKEY Ministry of Industry and Trade, with the 00457.STZ.2009-2 encoded SANTEZ project and Vestel White Goods Company.

Mete ÖZŞEN

NUMERICAL AND EXPERIMENTAL INVESTIGATION OF MIXED CONVECTION IN REFRIGERATORS

ABSTRACT

This study includes investigation of the temperature and flow fields which influence thermal condition of the domestic refrigerator. For this purposes, firstly domestic refrigerators were explained, classified and the improvement methods were specified. Suitability of the observed temperatures in the domestic refrigerators which were in the market and investigation methods of the domestic refrigerators was specified according to the studies which were in the literature. Then the numerical method was basically explained and steps of the Computational Fluid Dynamics (CFD) with Heat Transfer analysis, assumptions and implemented boundary conditions were specified. Then, the experimental and numerical studies were carried out on the static (natural convection driven) and brewed (static with fan-forced convection driven) type domestic refrigerators with evaporator inside the back wall. After the accuracy of the numerical results was verified by comparing with the experimental result, the mixed convection effects were exhaustively investigated on the temperature and flow fields. Also the design parameters which influence the temperature and flow fields were determined through the numerical method. In addition two design studies were carried out according to the obtained knowledge from numerical studies. Based on this study the suitable assumptions were determined for simulations of the static and brewed type domestic refrigerator and it is shown that the numerical method is suitable for the investigation of the temperature and flow fields.

Keywords: Domestic refrigerator, mixed convection, Computational Fluid Dynamics (CFD) with Heat Transfer, numerical method, design parameters of the domestic refrigerator.

BUZDOLAPLARINDA KARIŞIK TAŞINIMIN SAYISAL VE DENEYSEL OLARAK İNCELENMESİ

ÖZ

Bu çalışma, buzdolabı ısıl koşulları için önemli olan sıcaklık ve akış dağılımını deneysel ve sayısal olarak incelemeyi kapsamaktadır. Bu amaçla ilk önce buzdolapları genel hatlarıyla tanıtılmış, sınıflandırılmış ve geliştirme yöntemleri üstünde durulmuştur. Literatürde yapılan çalışmalar doğrultusunda mevcut buzdolaplarında görülen sıcaklık değerlerinin uygunluğundan ve araştırma yöntemlerinden bahsedilmiştir. Sayısal yöntem genel hatlarıyla açıklanarak Hesaplamalı Akışkanlar Dinamiği (HAD) ve Isı Transferi analiz adımlarından, yapılan kabullerden ve uygulanan sınır şartlarından bahsedilmiştir. Daha sonra buharlaştırıcısı arka duvara gömülü statik (doğal taşınım akışlı) ve fanlı statik tip (zorlanmış taşınım akışlı) buzdolapları üstünde deneysel ve sayısal çalışmalar yapılmıştır. Sayısal çalışma sonuçları deneysel çalışma sonuçları ile ispatlandıktan sonra, sayısal çalışmalar ile elde edilen sonuçlar doğrultusunda, karışık taşınımın sıcaklık ve akış dağılımı üstündeki etkisi detaylı bir şekilde araştırılmıştır. Bunun yanında sıcaklık ve akış koşullarını etkileyen tasarım parametreleri sayısal çalışma sonuçlarına göre belirlenmiştir. Ayrıca sayısal çalışmalardan elde edilen bilgiler doğrultusunda iki tasarım çalışması yapılmıştır. Yapılan bu çalışma ile fanlı statik ve statik tip buzdolaplarının sayısal olarak modellenmesi için uygun varsayımlar belirlenmiş ve sayısal yöntemin buzdolabı ısıl koşullarının araştırılması için uygun bir yöntem olduğu elde edilmiştir.

Anahtar Sözcükler: Buzdolabı, karışık taşınım, Hesaplamalı Akışkanlar Dinamiği (HAD) ve Isı Transferi, sayısal yöntem, buzdolabı tasarım parametreleri.

CONTENETS

Page

CHAPTER ONE

INTRODUCTION

1.1 Refrigeration

The basic definition of the refrigeration is “a process of the removal of heat from a substance or from a space” (Anderson, 2004, p. 1). At the end of that process, the temperature of the substance or the space is generally expected much lower than the surrounding temperature. According to that expectation, refrigeration is defined by means of thermodynamics as “… the transfer of heat from a lower temperature region to a higher temperature one” (Çengel & Boles, 2006, p. 607). The lower temperature region represents the substance or space whereas the higher temperature one represents the surrounding temperature.

According to the second law of thermodynamics, the heat doesn’t transfer from the low temperature region to the high temperature one by itself. This problem is accomplished by the work input which is implemented by refrigerator. The refrigerator is a cyclic machine and the working fluids used in the cycle are called refrigerants (Çengel & Boles, 2006, chap. 11).

Cycles that refrigerator operates on are called refrigeration cycles which are thermodynamic cycles. There are three main refrigeration cycles which are the reversed Carnot cycle, the vapor-compression refrigeration cycle and the reversed Brayton cycle (gas refrigeration cycle). Furthermore, there are several refrigeration systems that are occurred by the modifying main refrigeration cycles which are absorption refrigeration, jet ejector refrigeration, cascade refrigeration, multistage compression refrigeration and steam jet refrigeration systems (Çengel & Boles, 2006, chap. 11; Dinçer & Kanoğlu, 2010, chap. 5). Additionally, there are systems which don’t need to refrigerants for complete refrigeration cycle such as thermoelectric, thermoacoustic, magnetic and metal hydride refrigeration systems (Dinçer & Kanoğlu, 2010, chap.5).

Refrigeration applications are used wide range process such as food preservation, control of indoor air quality, gas liquefaction, industrial process control, production of food and drink, computer cooling, condensing vapors and cold storage (Dinçer & Kanoğlu, 2010, chap. 4; International Institue of Refrigeration [IIR], 2003). The desired temperature is large range based on those application types by the end of the refrigeration. Generally, temperature range is 15 C to -60 C or -70 C at industrial and domestic application (Stoecker, 1998, chap. 1). Additionally, required temperature is below -100 C at some applications called cryogenic which is liquefaction of gases (natural gas, nitrogen, oxygen e.t.c.) (Çengel & Boles, 2006, chap. 11).

Therefore, refrigeration applications are indispensable for modern life. Additionally, thermodynamics, heat transfer and fluid mechanics are always encountered in every refrigeration process or application (Dinçer & Kanoğlu, 2010, chap. 1).

1.2 Domestic (Household) Refrigerators

Domestic refrigerator is a cyclic machine that's basic function is foodstuff storage to keep fresh for a long time in the house. In the standard of International Standard Organisation (ISO) 15502, domestic refrigerators are mentioned as "refrigerating appliances" and are defined "factory-assembled insulated cabinet with one or more compartments and of suitable volume and equipment for household use, cooled by natural convection or a frost-free system whereby the cooling is obtained by one or more energy-consuming means" (International Organization of Standardization 15502 [ISO 15502], 2005, p. 2). Based on that definition, fundamental properties of domestic refrigerators have been described following.

1.2.1 Insulated Cabinet

Insulated cabinet keeps thermally the low temperature medium for foodstuffs against surrounding conditions for a long time. Knowing that, heat is transferred from high temperature to low temperature by itself. Since the inner temperature of domestic refrigerator is lower than the outer one, there is continuously heat gain to inside the domestic refrigerator. Hence, insulated cabinet is the most important

components of the domestic refrigerator for accomplishing this heat gain. Furthermore, insulating cabinet is supported to the structure of the domestic refrigerator in terms of the strength. Cabinet design is enough strong for withstanding to weight of shelves, foodstuffs, refrigeration system equipments and the door. In addition dynamic structural loads generated by shipping, daily usage, door opening, thermal stresses and working vibration of refrigeration system are withstood.

Insulated cabinet consist of three layers which are inner plastic, outer shell and insulation material that is filled space between others. The outer shell is usually single fabricated steel structure and inner plastic forms of a single plastic sheet such as High Impact Polystyrene (HIPS) and acrylonitrile butadiene styrene (ABS) (American Society of Heating, Refrigerating and Air-Conditioning Engineers [ASHRAE], 2006, chap. 48). Insulation materials are generally foam of polyurethane, cyclopentane-blown, HFC-134a-blown, HFC-245fa-blown (ASHRAE, 2006, chap. 48). In addition vacuum insulation panels (VIP) have been recently used in cabinet (ASHRAE, 2006, chap. 48).

1.2.2 Compartments

Domestic refrigerators may have different compartments according to types of foodstuffs. Each compartment has to be different environmental conditions that is specified according to storage conditions of foodstuffs that want to store in its. Generally most domestic refrigerators have fresh-food storage (for unfrozen food), frozen-food storage (or freezer), egg and vegetable compartments. In addition there may have the cellar compartment is warmer than the fresh-food compartment and the chill compartment for storage highly perishable foodstuffs is slightly cooler than the fresh-food compartment (ISO 15502, 2005). Furthermore special purpose compartments such as meat storage compartment, special compartment for fish e.t.c. may be in domestic refrigerators (ASHRAE, 2006, chap. 48).

1.2.3 Inner Environment Conditions

Compartments have to be suitable volume in order to retard the growth rate of microorganisms that are responsible for spoilage of foodstuffs. Microorganism

growth in a food item is governed by the combined effects of characteristics of the food (chemical structure, pH level, presence of in inhibitors) and the environmental factors such as temperature which affect strongly and relative humidity (Çengel, 2007, chap. 17). Therefore, environmental conditions of compartments are kept in desirable range.

> The storage life of fresh perishable foods such as meats, fish, vegetables, and fruits can be extended by several days by storing them at temperatures just above freezing, usually between 1 and 4 C. The storage life of foods can be extended by several months by freezing and storing them at subfreezing temperatures, usually between -18 and -35 C, depending on particular food…. The optimum storage temperature of most fruits and vegetables is about 0.5 to 1 C above their freezing points. But this is not the case for some fruits and vegetables such as bananas cucumbers that experience undesirable physiological changes, when exposed to low (but still above freezing) temperatures, usually between 0 and 10 C…. The maintain high quality and product consistency, temperature swings of more than 1 C above or below the desired temperature in the storage room must be avoided (Çengel, 2007, pp. 17-4-5).

Since the various ranges of foodstuffs can be stored in domestic refrigerators, temperature ranges according to compartments are classified by ISO 15502 and shown in Table 1.1. Frozen food compartments are divided three classes according to the maximum storage temperature as shown in Table 1.1. Additionally, shell egg should be stored at 7 to 13 C (Çengel, 2007, chap. 17) in egg compartments and meat compartments have to be maintained at -0.5 C (Çengel & Boles, 2006, pp. 311-315). Furthermore, suitable storage temperature for fish is 0 to 2 C (Çengel, 2007, chap. 17) in fish compartment.

Table 1.1 Temperature range in domestic refrigerators (ISO 15502, 2005)

Fresh-food storage compartment	Frozen food storage compartment			Cellar compartment	Chill compartment
	Food freezer and three-star compartment	Two-star compartment	One-star compartment		
0 C ≤ T ≤ 8 C	≤ -18 C	≤ -12 C	≤ -6 C	8 C≤ T ≤ 14 C	-2 C ≤ T ≤ 3 C

Relative humidity condition in the compartments is as important as temperature one for foodstuffs that is especially leafy vegetables, fresh fruits and eggs. For instance, shell egg should be stored at 75 to 80 percent relative humidity in egg compartments and fish should be stored over 90 percent in fish compartment (Çengel, 2007, chap. 17). Other compartments can be suggested that "Keeping the relative humidity below 60 percent, for example, prevents the growth of all microorganisms on the surfaces" (Çengel, 2007, p. 17-4). Furthermore, vegetable and egg compartments are enough air-tight to seal moisture and protect the drying effect of cool air (Çengel & Boles, 2006, pp. 311-315).

According to the above, the fresh food compartment is suitable for all foodstuffs especially dairy food products, cooked/processed food items and beverages but some perishable foodstuffs such as meats, fish, poultry products and milk can be stored in it for several days. Otherwise, chill, meat or fish compartments are more suitable for these perishable foodstuffs for a long time. In addition the frozen-food compartment is suitable to food storage for more long time (several months) than the others compartments of the domestic refrigerator. It should be noted that increasing the storage temperature causes increasing the growth rate of microorganisms and inherently decreasing the storage time (shelf-life) (Çengel, 2007, chap. 17). For instance shelf life of several food products as a function of temperature are shown in Figure 1.1 and obtained that the shelf life of all product increases as the storage temperature drops (Lorentzen, 1971) cited by (Stoecker, 1998, chap. 1). Furthermore, cellar comportment is suitable for foodstuffs which have higher than 8 C storage temperature such as the butter.

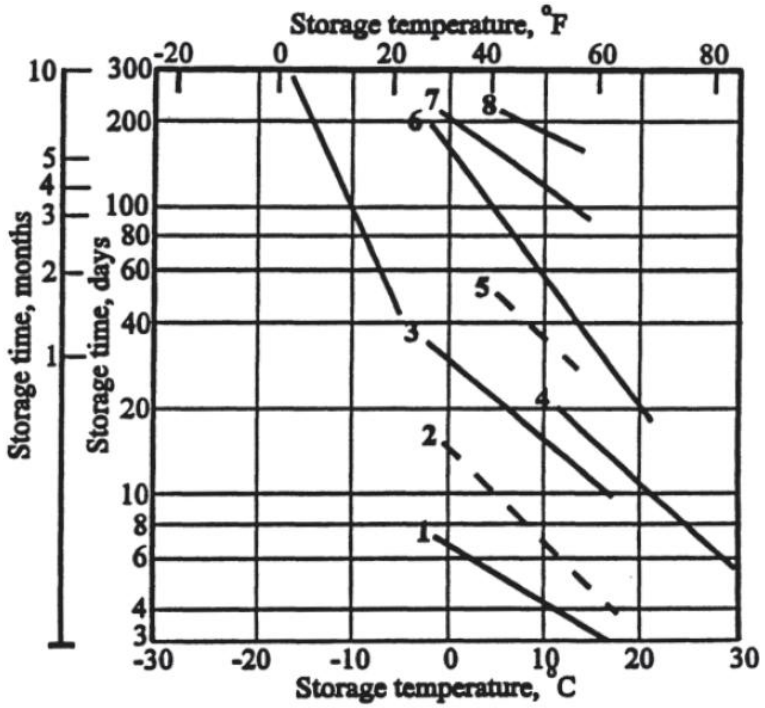

Figure 1.1 Shelf life of several foodstuffs as a function of temperature. (1-chicken, 2-lean fish, 3-beef, 4-bananas, 5-oranges, 6-apples, 7-eggs, 8-apples) (Lorentzen, 1971)

1.2.4 Equipments

Equipments of the domestic refrigerator consist of the refrigeration system equipments (evaporator, condenser, compressor and expansion valve), temperature controller (thermostat), door gasket, defrosting system, fan, external heater and water and ice service maker.

1.2.4.1 Refrigeration System Equipments

Refrigeration system equipments are fundamental components of domestic refrigerator with refrigerant circulated in them and refrigeration process is implemented whereby them. More detailed information has shown in section 1.2.6.

1.2.4.2 Temperature Controller

The temperature controller is the other important component of domestic refrigerator which is ensured maintaining the desired temperature range in the domestic refrigerator conjunction with the refrigeration system. The temperature

controller is started or stopped the refrigeration system with sensed the temperature of evaporator surface or inner air.

1.2.4.3 Door Gasket

The door gasket prevents the heat leakage between the door and the insulated cabinet surfaces. It is generally made of vinyl and a magnetic material is embedded in for door latching (ASHRAE, 2006, chap. 48).

1.2.4.4 Defrosting System

The defrosting system accomplishes accumulation of frost on the evaporator surface. The evaporator in the domestic refrigerator is the most refrigerated surface which transfers heat from the inner air to the refrigerant which flows in it. During this process, the inner air which has warmer temperature comparing with the evaporator surface one contacts at the refrigerated surface. Thus, water vapor in the inner air frosts on the refrigerated surface and an ice layer occurs on it. This ice layer acts as insulation and slows down the heat transfer from the inner air to the refrigerant (Çengel & Boles, 2006, pp. 311-315). Thus, the ice layer on the refrigerated surface impacts the performance of the domestic refrigerator and should be defrosted periodically.

Most domestic refrigerators have defrost system called as no-frost or frost-free system although several ones don't have a defrost system called as manual. The user should turn off the refrigeration system and ice layer is naturally defrosted once every two weeks (Anderson, 2004, chap. 9) in the manual defrosting system. The ice layer is defrosted by electric heater that has 300 W to 1000 W power or by using the hot refrigerant gas in the condenser periodically in the automatic defrosting system (Çengel & Boles, 2006, pp. 311-315).

1.2.4.5 Fan

The fan which generally used propeller type is using some domestic refrigerators for ensuring to the cold airflow all items in compartments. Additionally, some domestic refrigerators have an air duct system with fan which is embedded the

insulated cabinet wall or some ones have a fan box with fan located into compartments.

Additionally, in some domestic refrigerator the fan is mounted on the compressor housing (Anderson, 2004, chap. 11) or condenser for cooling them.

1.2.4.6 External Heater

The external heater prevents the condensation on outer surfaces of insulated cabinet in humid environment (Çengel & Boles, 2006, pp. 311-315). If outer surface temperature of the insulated cabinet is lower than the ambient dew point temperature, water droplets are occurred on the surfaces. This undesirable situation is accomplished to raise the critical outer surface temperature by external heater with located under the outer surface.

Furthermore, external heater may be located under the outer surface that contacts the door gasket. Since this contact surface is cold, the door gasket may be damaged during the door opening. The external heater prevents the damaging of door gasket by increasing the temperature of this surface.

The external heater may consist of routing a loop of condenser tubing or low-wattage wires or ribbon heaters (ASHRAE, 2006, chap. 48).

1.2.4.7 Water and Ice Service Maker

Some domestic refrigerators may have ice or water service maker or both of them. Although manual and automatic ice makers are located in the food-frozen compartment, ice trays are used for manual one, the other requires attachment to a water line (ASHRAE, 2006, chap. 48).

1.2.5 Working Principle and Heat Load

The inner air is firstly cooled by refrigeration systems. Then the cold inner air takes the heat load that comes from both interior and exterior of the domestic refrigerator and gets warm. That warm inner air is again cooled by refrigeration

system. Therefore, that inner air circulation is achieved the desired condition of inside the domestic refrigerator.

The interior heat load is caused by stored foodstuffs, fan motor, light, ice making and defrost and external heaters whereas exterior one is environmental condition through insulated cabinet walls, door gasket region and opening door. “A large portion of the peak heat load may result from door opening, food loading, and ice making, which are variable and unpredictable quantities dependent on customer use” (ASHRAE, 2006, p. 48.3). The others heat load is predictable quantities and relative value of those heat loads are determined by (ASHRAE, 2006, chap. 48) and shown in Figure 1.2.

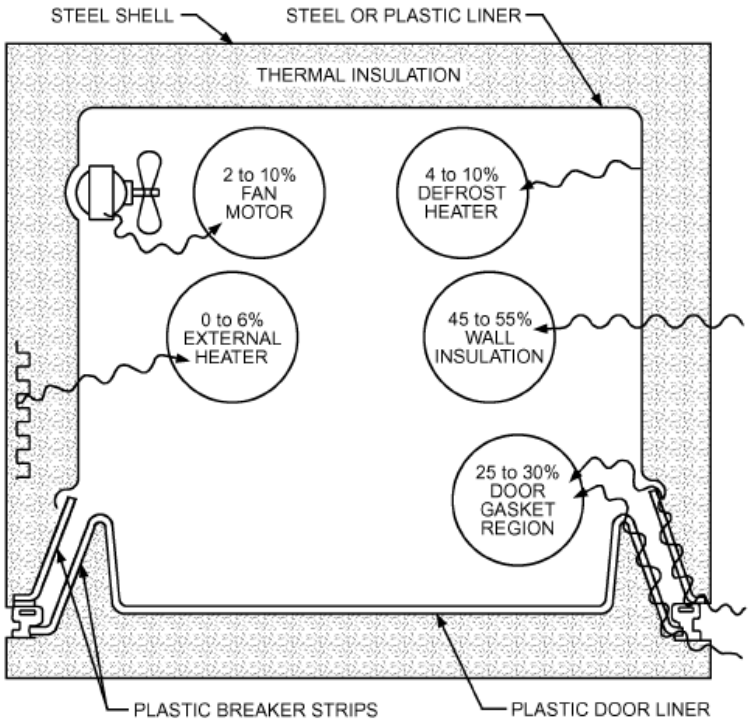

Figure 1.2 Predictable heat loads and relative values. (ASHRAE, 2006, chap. 48)

The inner air circulation is occurred by natural or forced convection driven and has to be circulated all items in the domestic refrigerator. The sufficient cold inner airflow has to be contacted to the surfaces of foodstuffs in order to rapidly refrigerate them. In addition, the warmer inner airflow has to be efficiently transferred its heat to the refrigeration system whereby the evaporator. Thus, good air circulation is vital importance to ensure desired condition for foodstuffs and Anderson (2004) is

described as “If air is restricted from circulating to all parts of the cabinet, food in the lower area will not be refrigerated sufficiently” (p. 313).

1.2.6 Refrigeration System

Refrigeration system is an energy consuming for making refrigeration. There are vapor-compression, absorption and thermoelectric refrigeration systems that use in domestic refrigerator (ASHRAE, 2006, chap. 48). However, vapor-compression system is much efficient than others (Table 1.2) and it is a universally used (ASHRAE, 2006, chap. 48). Hence, only the vapor-compression refrigeration cycle has been specified.

Table 1.2 Coefficient of performance of refrigeration systems usage in domestic refrigerator. (ASHRAE, 2006, chap. 48)

Refrigeration system type	**Approximate coefficient of performance**
Thermoelectric	0.09
Absorption	0.44
Vapor-compression	1.65

1.2.6.1 The Vapor-Compression Refrigeration Cycle

Liquid evaporation and condensation can occur at almost any temperature and pressure combination. The vapor-compression refrigeration cycle is used that principle and consists of compressor, condenser, expansion valve and evaporator as shown schematically in Figure 1.3.a and shown on domestic refrigerator in Figure 1.3.b. The working principle is basically specified by Dinçer & Kanoğlu, 2010 as:

> … A working fluid (called refrigerant) enters the compressor as a vapor and is compressed to the condenser pressure. The high-temperature refrigerant cools in the condenser by rejecting heat to a high-temperature medium (at T_H). The refrigerant enters the expansion valve as liquid. It is expanded in an expansion valve and its pressure and temperature drop. The refrigerant is a mixture of vapor and liquid at the inlet of the evaporator. It absorbs heat from a low-temperature medium (at T_L) as it flows in the evaporator. The cycle is completed when the refrigerant leaves the evaporator as a vapor and enters the compressor… (p. 22).

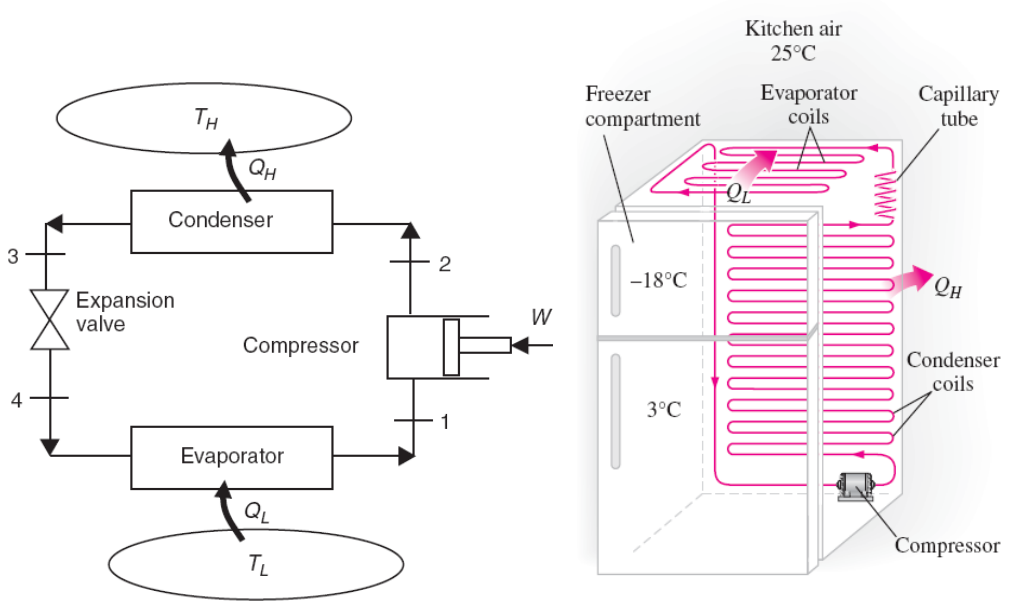

a. **b.**

Figure 1.3 Vapor-compression refrigeration cycle: (a) Schematically shown (Dinçer & Kanoğlu, 2010, p. 23) and (b) Located on domestic refrigerator (Çengel, 2007, p. 611).

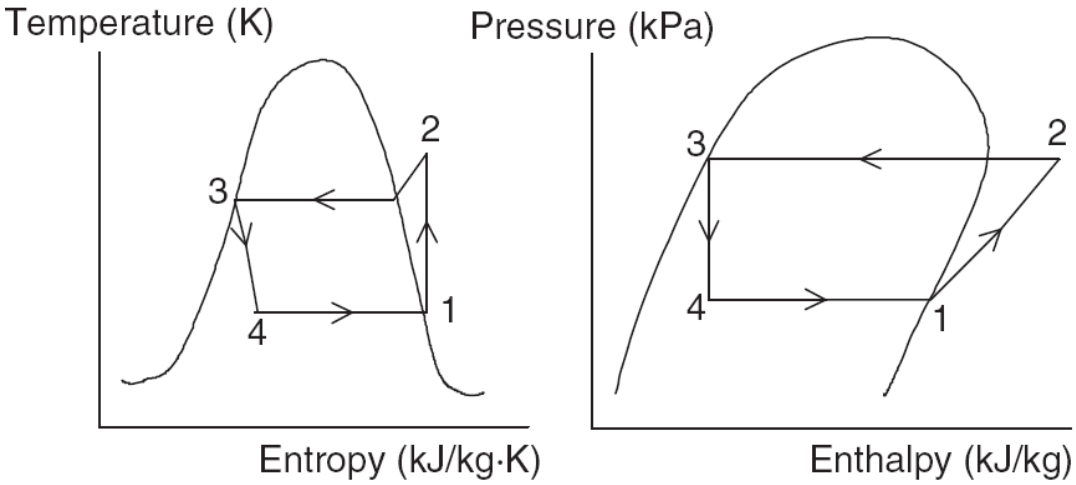

Figure 1.4 The vapor-compression refrigeration cycle diagram a) Temperature-Entropy (T-s), b) Logarithmic pressure-enthalpy (P-h) (Dinçer & Kanoğlu, 2010, p. 156)

In an ideal vapor-compression cycle consists of four processes:

1-2 Isentropic (no heat exchange) compression in a compressor,

2-3 Constant-pressure heat rejection in a condenser (constant-temperature),

3-4 Throttling in an expansion device (no heat exchange)

4-1 Constant-pressure heat absorption in an evaporator (constant-temperature)

In the analysis of vapor-compression refrigeration cycle is used temperature-entropy (T-s) or logarithmic pressure-enthalpy (P-h) diagrams as shown in Figure

1.4. The heat absorbed in the evaporator is represented by the area under or the length of the process curve 4-1 respectively in T-s or P-h diagram. On the other hand, the heat rejection in the condenser is represented by the area under or the length of process curve 2-3 respectively in T-s or P-h diagram.

The performance of refrigerators is expressed in terms of coefficient of performance (COP), defined as (Çengel & Boles, 2006, chap. 11).

$$\mathrm{COP} = \frac{\text{Desired Output}}{\text{Reguired Input}} = \frac{\text{Cooling Effect}}{\text{Work Input}} = \frac{Q_L}{W_{net,in}} = \frac{h_1 - h_4}{h_2 - h_1} \quad (1.1)$$

where “h” represent the enthalpy of the refrigerant. So, the refrigerant is importance for refrigeration system and R-134a or R-600a (isobutene) is generally used in domestic refrigerator. (ASHRAE, 2006, chap. 48)

1.2.6.2 Components of Refrigeration System

The vapor-compression refrigeration cycle has two pressure levels that high and low pressure sides. The high pressure refrigerant flows in the high pressure side which consists of the condenser, expansion valve and compressor. The low pressure refrigerant flows in the low pressure side which consists of the evaporator, accumulator and suction line (Anderson, 2004, chap. 4). All refrigeration system components with refrigerant flow direction shown in Figure 1.5 and with low and high pressure sides shown in Figure 1.6.

1.2.6.2.1 Compressor.

The compressor is supplied with work input in the refrigeration system by electrical power. It has two main functions.

> …One function is to pump the refrigerant vapor from the evaporator so that the desired temperature and pressure can be maintained in the evaporator. The second function is to increase the pressure of the refrigerant vapor through the process of compression, and simultaneously increase the temperature of the refrigerant vapor… (Dinçer & Kanoğlu, 2010, p.109).

Compressor is controlled by temperature controller. If inner temperature is lower than the adjusted temperature range, compressor is stopped and called as off cycle. The opposite situation is called as on cycle.

Compressor used in the domestic refrigerator is positive-displacement compressor and is hermetic type (ASHRAE, 2006, chap. 48; Anderson, 2004, chap. 4). Design of the expectation of the compressor is ease manufacturing, reliability, low cost, quiet operation, and efficiency (ASHRAE, 2006, chap. 48).

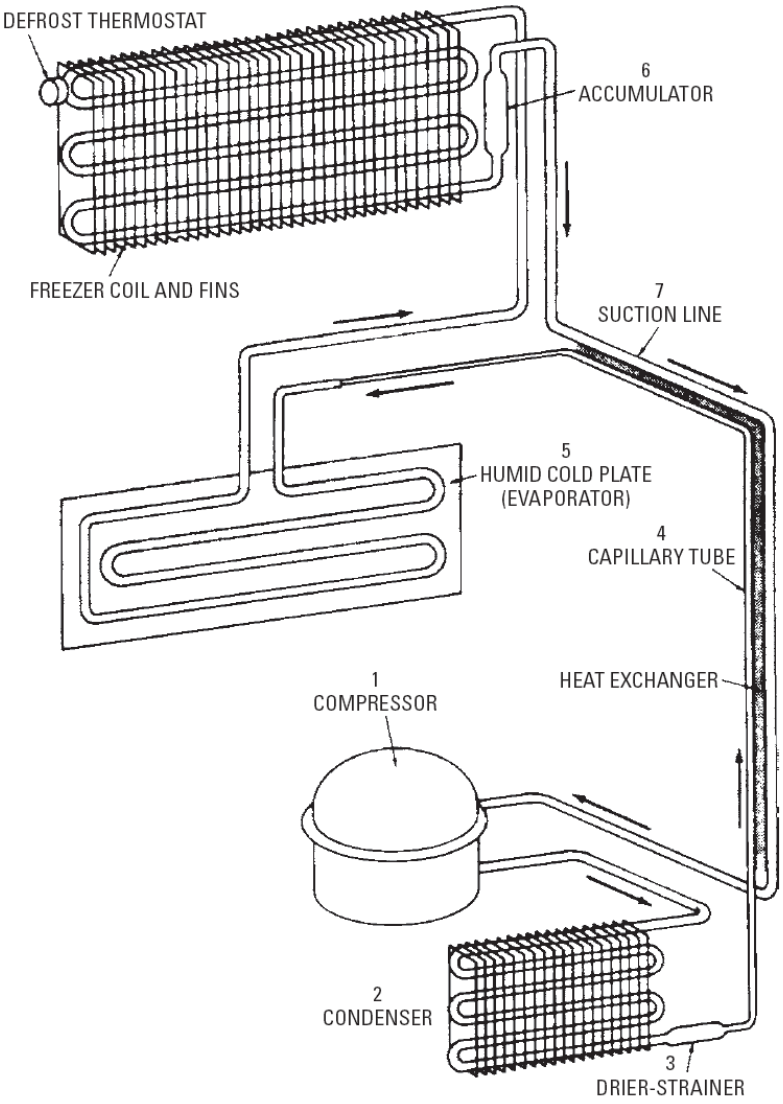

Figure 1.5 Refrigeration system components with refrigerant flow direction (Anderson, 2004, chap. 4)

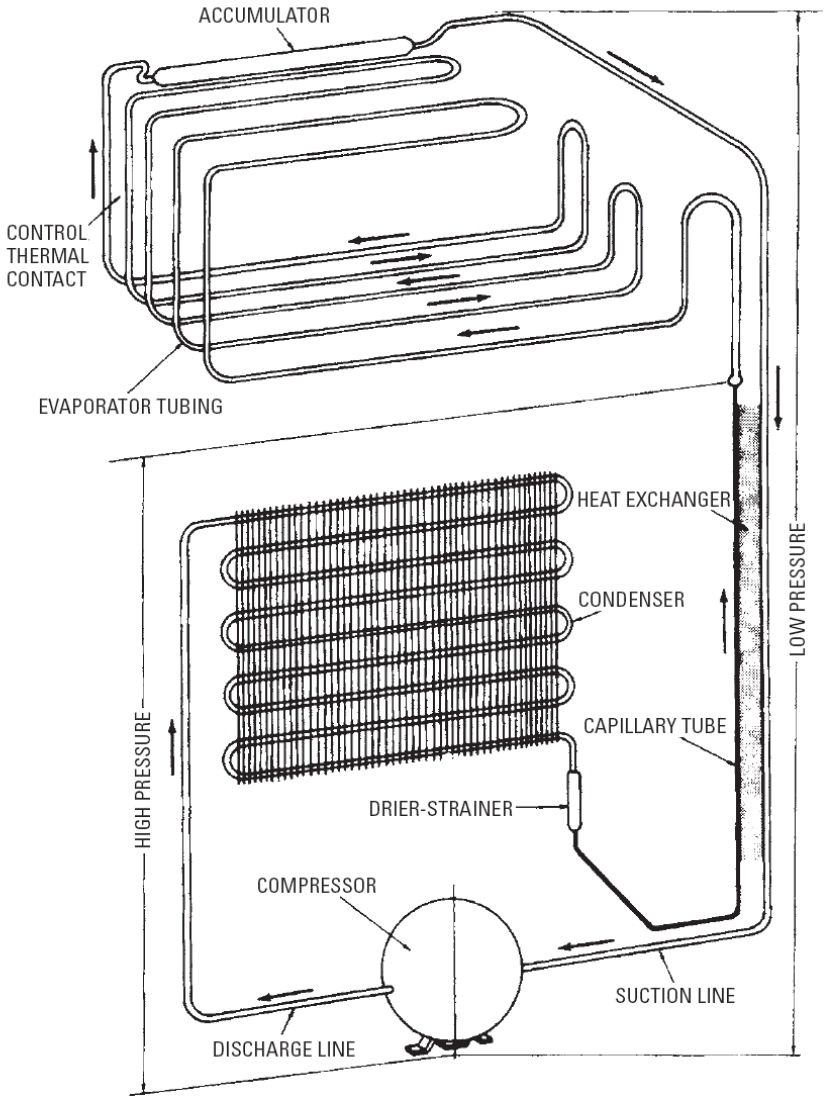

Figure 1.6 Refrigeration system component with high and low pressure sides (Anderson, 2004, chap. 4)

1.2.6.2.2 Condenser.

The condenser is a heat exchanger that function is rejecting the heat of refrigerant that gains from heat load of the domestic refrigerator and compressor working to the outer environment. Thus, refrigerant is changed phase from gas to liquid.

Condenser used in domestic refrigerator is air cooled naturally or forced with fan and is located the outside of the insulated cabinet or under the outer shell. Naturally cooled condenser type is generally of a flat serpentine of steel tubing with steel cross wires (wire on tube) that schematically shown in Figure 1.6 or tube on sheet (ASHRAE, 2006, chap. 48). Forced cooled condenser type is fin-on-tube that

schematically shown in Figure 1.5 or folded banks of tube-and-wire or tube-and-sheet construction (ASHRAE, 2006, chap 48).

Some important design requirements for a condenser include sufficient heat dissipation at peak-load conditions, an external surface that is easily cleaned or designed to avoid dust and lint accumulation (ASHRAE, 2006, chap. 48).

Additionally, for naturally cooled type condenser, it should be noted that the airflow passages on the condenser coils is vital importance and shouldn't be blocked by the consumer in order to ensure the efficiently operating (Çengel & Boles, 2006, pp. 311-315). As shown in Figure 1.7 airflow passages should be ensured with located sufficiently far from the room wall.

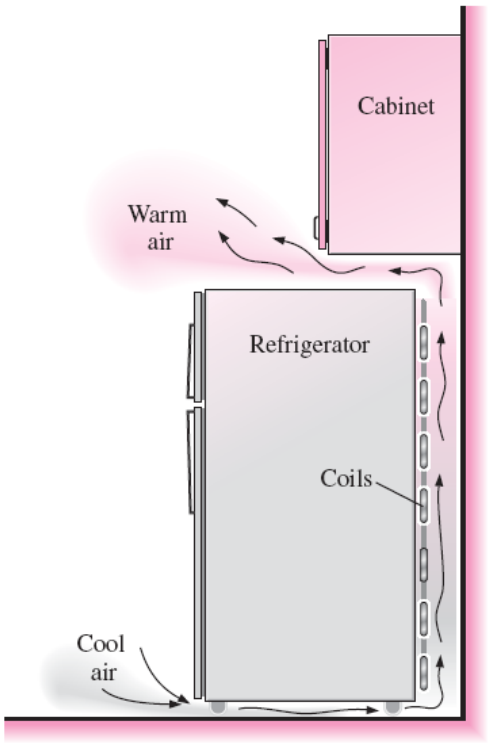

Figure 1.7 Airflow passages on the condenser coils (Çengel & Boles, 2006, pp. 311-315)

1.2.6.2.3 Expansion Valve.

Expansion valve reduces the refrigerant pressure from the condensing pressure (high pressure) to the evaporation one (low pressure) and is placed after the condenser as shown in Figure 1.5. Additionally, it prevents to passing the uncondensed refrigerant gas to the evaporator, equalizing the system pressure during

the off cycle and reduces the starting torque required of the compressor (ASHRAE, 2006, chap. 48).

The most type used in domestic refrigerator is capillary tube. Generally diameter of the capillary tube is very small and its length depends on the condensing unit and the kind of the refrigerant used (Anderson, 2004, chap. 4).

1.2.6.2.4 Evaporator.

Evaporator is a heat exchanger that function is absorbing the heat from warm inner air to the refrigerant which flows in the evaporator. Through this absorbed heat, refrigerant is changed its phase from liquid to gas. In addition, the evaporator is the refrigerated surface which is placed in the insulated cabinet.

Evaporator used in domestic refrigerator cools inner air naturally or forced with fan and is located the under of the inner plastic or in the air duct or is used as a shelf (Figure 1.8) or is wrapped around the frozen-food compartment (Figure 1.9).

Figure 1.8 The wire-on-tube evaporator usage as a shelf

Evaporator coils bond on a sheet metal as called flat plate and shown in Figure 1.5 or around a box as called roll-bonded or box plate type and shown in Figure 1.6 and Figure 1.9. Some evaporator coils weld on steel wires as called wire-on-tube type and this type use as a shelf and is shown in Figure 1.8. Additionally, fin-and-tube type heat exchangers (freezer coil and fin in Figure 1.5) are used as the evaporator and located in the air duct.

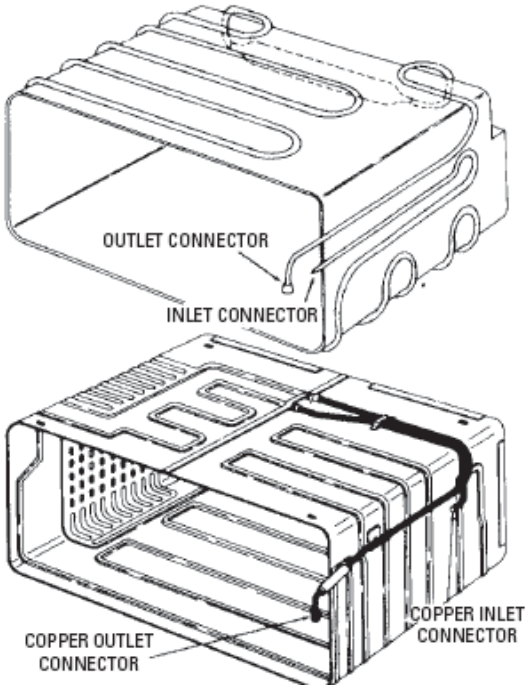

Figure 1.9 Roll-bonded or box plate evaporator (Anderson, 2004), (chap. 4)

1.2.6.2.5 Auxiliary Devices.

Some refrigeration systems have several devices which prevent the system from damages and increase the efficiency of the system.

One device is accumulator (Figure 1.5 and Figure 1.6) which prevents to pass the refrigerant liquid, which may not have changed to gas in the evaporator, to the compressor (Anderson, 2004, chap. 4). It is located the end of the evaporator.

The other device is drier-strainer (Figure 1.5 and Figure 1.6) which is to remove moisture and impurities from the refrigeration system and is usually located ahead of the capillary tube (ASHRAE, 2006, chap. 48; Anderson, 2004, chap. 4).

Generally, a part of the capillary tube is soldered along of the suction line, which is between the evaporator and the compressor, and it is occurred a heat exchanger (Figure 1.5 and Figure 1.6) (Anderson, 2004, chap. 4). Through this heat exchanger, refrigerant flowed in the capillary tube is transferred its heat to refrigerant flowed in the suction line. Thus, much cooled refrigerant flows in the evaporator inherently increasing the efficiently of refrigeration system.

1.2.7 Classification

Fundamentally domestic refrigerators classify as natural convection driven (static) and forced convection driven types accordingly to the occurrence of the inner air circulation.

In static domestic refrigerators inner air circulation is due to variations in air density which result from temperature gradients. Since the density of the hot air is lighter than the cold air, the hot air flows upward and the cold air flow downward. However, inner air circulation is occurred by the effect of the fan in forced convection driven domestic refrigerators.

In the static type the evaporator is directly contact compartments environment and sometimes is called as directly cooled refrigerator and heat is transferred from the inner air to the evaporator by the effect of the natural convection. However in forced convection driven types inner air flows over the evaporator first and then entering compartments (inlet) and heat is transferred from the inner air to the evaporator by the effect of the forced convection. Furthermore, roll-bonded, flat plate and wire-on-tube evaporators are used in static types while fin-and-tube one is used in forced convection driven types. Additionally some forced convection driven types are used fin-and-tube type and flat plate type evaporators together.

Heat is transferred principally natural convection in static types between the inner air and storage foodstuffs and inner walls of the insulated cabinet. On the contrary heat is transferred principally mixed (both natural and forced) convection in forced convection driven types.

A classification was made by Laguerre, Amara, Charrier-Mojtabi, Lartigue, & Flick (2008) as three types which are static, brewed (static with a fan) and no-frost accordingly to available in the market. The brewed type is determined as “is a static refrigerator equipped with a fan” while the no-frost type is determined as the forced convection driven type by Laguerre et al. (2008) (p. 547). Furthermore, the other classification is specified as three types which are ice-box, larder and fridge-freezer refrigerators by S.J. James, Evans, & C. James (2008). The ice box is determined as

"…have a box-plate evaporator within the refrigerator… ", larder and fridge freezer are determined as "Larder refrigerators have a back-plate evaporator, as do fridge-freezer (which can either have one compressor supplying both fridge and freezer, or two separate compressors)" by S.J. James, Evans, & C. James (2008) (p. 6).

Furthermore domestic refrigerator may be classified very different ways such as by the number or type of its compartments or doors. In the literature, there isn't a collective classification of the domestic refrigerators. Otherwise, name of the domestic refrigerators that have been called in the literature a collective classification may be specified as shown in Figure 1.10.

Domestic refrigerators in the Figure 1.10 may be classified accordingly to having a defrosting system such as manual defrost and no-frost or frost-free domestic refrigerators.

If the larder refrigerators have a fan, they are called as brewed type refrigerator. Additionally some vertical and horizontal freezer may have a fan and their type is changed forced convection driven vertical or horizontal freezer.

In the multi-compartment forced convection driven refrigerators have an air duct system and may be has more than one evaporator type. In the double-door refrigerator if the frozen-food compartment is located top of the fresh-food compartment, it is called as top-mount refrigerator. The opposite situation is called as bottom-mount refrigerator. In the side-by-side refrigerator the fresh food and the frozen food compartment is located side by side with double door. The fresh food compartment has double door that placed side by side with on top of the frozen food compartment which is as drawer type door in the French door refrigerator. Some French door models have double drawer type compartment bottom of the fresh food compartment and are called as four doors or two doors plus two drawers (http://www.refrigeratorexpert.com/french-door-refrigerators.html).

Additionally in some multi compartment refrigerator, inner air circulation is occurred by forced convection driven for the frozen food compartment while by natural convection driven for fresh food compartment.

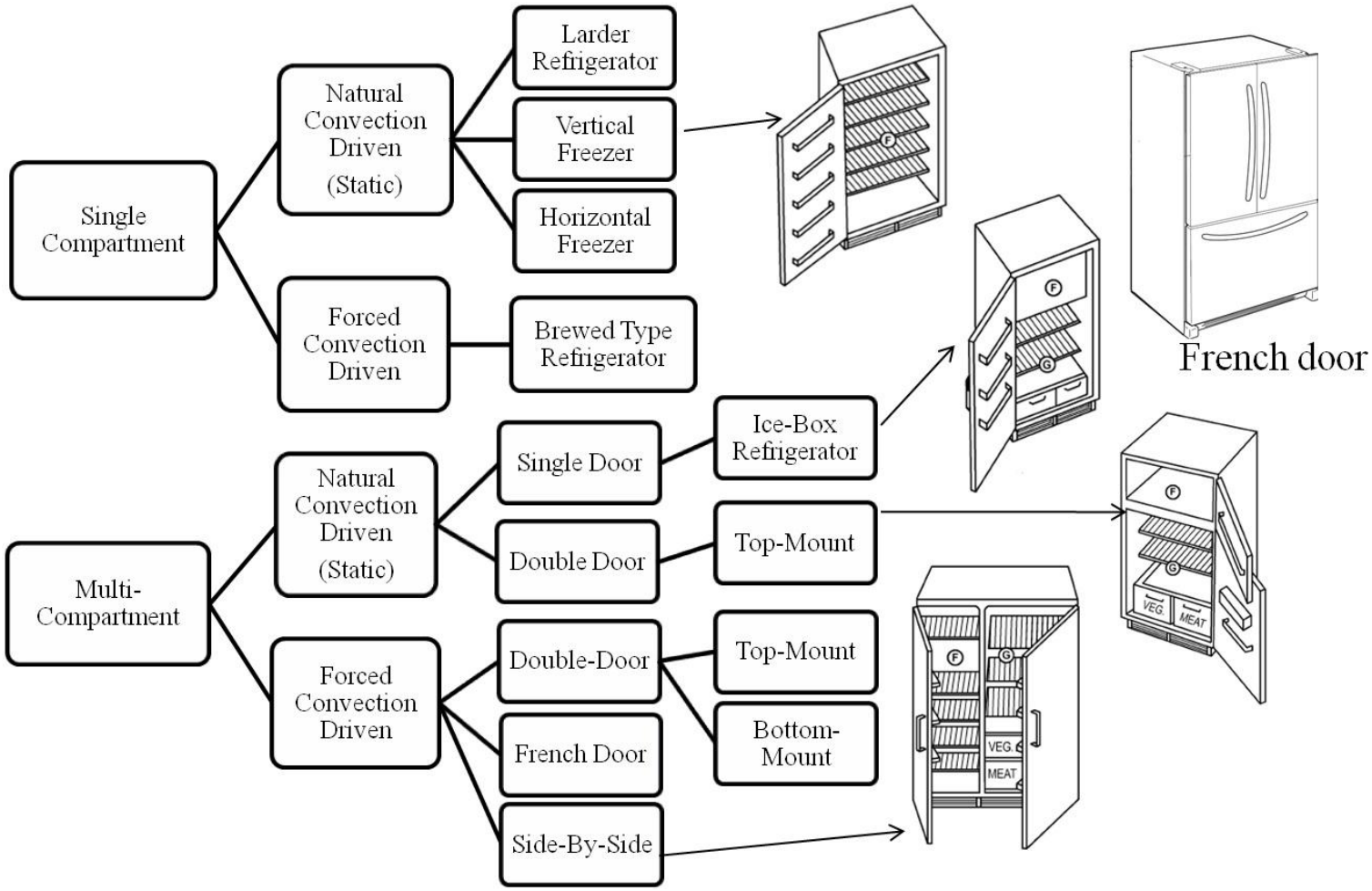

Figure 1.10 Classification of the domestic refrigerators and some schematics (schematic figures by ASHRAE (2006) (chap. 48) except schematic of French door)

1.2.8. Improving Method

The most portion energy consumption in the home appliances is domestic refrigerators as shown in Figure 1.11 according to the BESD (Manufacturers of White Goods Society) cited by Çengel, Akgün, & Arslantaş (2009) in Turkey. Hence improving studies are carried out for reducing the energy consumption.

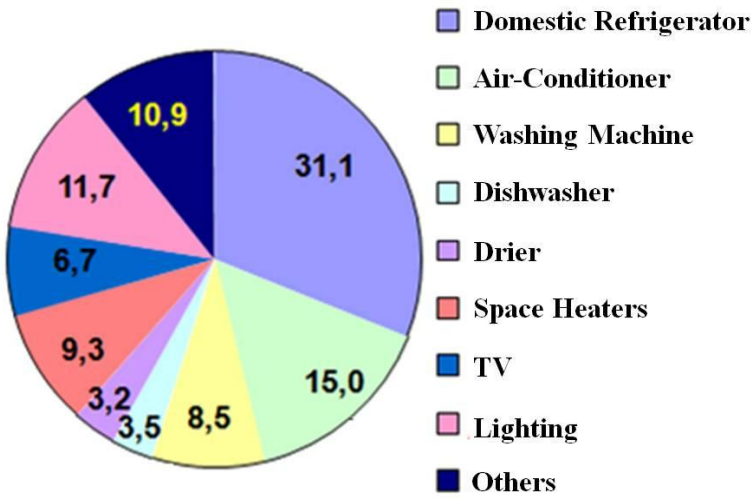

Figure 1.11 Distribution of electric energy consumption on buildings (Çengel, Akgün, & Arslantaş, 2009)

1.2.8.1 Improvement Method of Refrigeration System

Refrigeration system is the most consumed part of the domestic refrigerator compared with other energy usage parts (e.g. fans, defrosting systems, light…). So efficiency of the system may be increased for reducing the energy consuming.

According to COP calculation (Eq. 1.1) one of the improvement method of the efficiency is reducing the required input (work input - $W_{net,in}$) in the same desired output (cooling effect - Q_L). A method is development of the high-efficiency compressor. Since compressors generally operate partial load instead of designed to satisfy maximum load, performance of the refrigeration system is reduced. The last developed compressors which are called as Variable Speed Compressor (VSC) and Variable Capacity Compressor (VCC) were reduced the energy consumption whereby adjusted the work input accordingly to the heat load (Koury, Machado, & İsmail, 2001). For instance; 45% energy saving was attained by replacing the

conventional on/off compressor to VCC but 20% cost increase was obtained by Embraco Company cited by Azzouz, Leducq, & Gobin (2009).

Another reducing work-input method is difference between the evaporation and condensation temperature in the refrigeration system is designed as small as possible (IIR, 2003). Thereby, difference between the evaporation and condensation pressure is reduced and inherently required work-input for compressor is reduced. That situation may be ensured with increasing the air side convective coefficient of the evaporator (Azzouz, Leducq, & Gobin, 2009). Therefore the difference between the evaporator and inner air temperature is reduced and inherently required evaporator temperature is raised and inherently difference between the evaporator and condenser temperature is reduced. Furthermore, effect of the temperature of the evaporator and condenser on COP is specified as "A rule of thumb is that the COP improves by 2 to 4 percent for each C the evaporating temperature is raised or the condensing temperature is lowered" by Çengel & Boles (2006) (p. 611).

The efficiency may be improved by adding the ejector system in the current refrigeration system. Basically the pressure before the compressor input is raised comparing with the conventional system by usage ejector system. Therefore the desired work input of the compressor is reduced and inherently energy consumption is reduced. For instance 12.4% performance improvement is attained by using diffuser pipe combined system by Cao (2009) cited by (Liu, et al., 2011).

The thermodynamic properties (e.g. enthalpy) of the refrigerant directly affected the efficiency of the refrigeration system. So improvement refrigerant studies have been carried out such as refrigerant mixture study (Sekhar, Lal, & Renganarayanan, 2004).

1.2.8.2 Improvement Method of Insulated Cabinet

The interior cabinet is cooled during the compressor on cycle and heats up during the compressor off cycle in the desired temperature range. Since energy is consumed during the compressor on cycle, the compressor off cycle time is as long as possible and on cycle time is as short as possible.

To ensure the long off cycle time may be achieved the better insulation materials and better door seal usage in insulation cabinet design (Çengel & Boles, 2006, pp. 311-315). For instance; usage of gas-filled panel insulating system in the door was reduced as 6.5% (Griffith, Arasteh, & Türler, 1995), usage of five vacuum insulation panel (VIP) with conventional polyurethane foam and pure in the top and left-right walls of insulated cabinet was reduced as respectively 5.7% and 8.53% energy consumption (Tao & Sun, 2001). Furthermore, usage of better insulation material is reduced the thickness of the insulated walls and inherently food storage volume is raised.

To ensure the short on cycle time may be achieved by occurrence better inner air circulation for rapid cooling. The better air circulation may be achieved by modifying the inner cabinet design.

1.3 Motivation and Aim of the Study

During the production, distribution and retailing of foodstuffs the maximum temperature was specified by legislative requirements (James, 2003). However after the purchase of foodstuffs by customers it is outside of any legislative requirements. So the control mechanism of the desired storage temperature for foodstuffs is dependent on the performance of the domestic refrigerator and customer attitudes. Inner air temperature of domestic refrigerators should be desirable range for foodstuffs storage independent the customer attitudes. In the literature, several studies were carried out the investigation of temperature performance of the domestic refrigerator under real or controlled conditions.

James & Evans (1992) were carried out inner air temperature measurements at 22 different points of fresh-food compartments. Four domestic refrigerators which are two box plate types (ice-box refrigerator), two multi compartment type (also called as fridge-freezer) with single and double compressors with located flat plate type evaporator in the back wall of the fresh-food compartment were investigated under controlled conditions. Also influence of door openings and loading warm food product were investigated on the temperature performance. This study was obtained that:

- Box plate type evaporators had much uniform temperature than fridge-freezer in empty condition.
- After the loading of warm (20 C) food products, inner temperature recovery time changes accordingly to the position (top or middle shelves) and is directly relationship the thermostat stage.
- After the door openings, temperature recovery time isn't relationship the position but gets longer with frequent door opening frequency. In addition maximum inner air temperature rises to ambient temperature (20 C) independent of door opening frequency and its position changes according to type.

Furthermore this study was indicated that the inner air temperature is unlikely to be able to food storage for protected against microorganism subjected to frequent door-openings and loading warm food. In addition the maximum temperature position is different from measured position which is specified by standard of ISO.

Laguerre, Derens, & Palagos (2002) were carried out inner temperature measurements at top, middle and bottom of 119 domestic refrigerators under real use condition for a week at France. Its results of statistical analysis of all surveyed refrigerators was obtained 80% one had an average inner temperature above 5 C and 26% one had higher than 8 C without consideration of distinction between the refrigerator characteristics (age or type), door opening frequency, temperature controller settings (thermostat stage) and located near a heat source. In addition this study was obtained that the heterogeneousness of temperature was dependent on type and the most one was found in bottom mounted double door refrigerator types. Furthermore this study was obtained that temperature controller settings and the inner temperature were not directly relationship between each other in some domestic refrigerators.

An under controlled condition investigation of the inner air temperature of domestic refrigerators in China by Shixiong & Jing (1990) cited by Laguerre, Derens, & Palagos (2002) was shown that 2.3% one had <6 C, 34.1% one 8-12 C, 34.1% one 12-14 C, 29.5% one >14 C. An another survey carried out under real use

conditions by Victoria (1993) cited by Laguerre, Derens, & Palagos (2002) was shown that more than 70% domestic refrigerators had over 6 C average inner air temperature at France.

Finally S.J. James, Evans, & C. James (2008) were carried out a review study of surveys which had been investigated the temperature performance of domestic refrigerators around the world in the last 30 years. It was collected all measured data under real conditions in a table that was shown in Table 1.3. An evaluation in the given same results has been carried out following:

- Approximately 69.3% of total 1061 surveyed domestic refrigerators had higher than 4 C average inner air temperature (collected of study no. 9, 13, 15).
- Approximately 64% of total 1632 surveyed domestic refrigerators had higher than 5 C average inner air temperature (collected of study no. 2, 3, 4, 9, 10, 11, 12, 14, 16, 20).
- Approximately 58.6% of total 438 surveyed domestic refrigerators had higher than 6 C average inner air temperature (collected of study no. 5, 17, 18)
- Approximately 27% of total 261 surveyed domestic refrigerators had higher than 9 C average inner air temperature (collected of study no. 6, 8)

This evaluation has implemented without consideration the study year. Therefore this review was indicated that “many refrigerators throughout the world are running at higher than recommended temperatures” (S.J. James, Evans, & C. James, 2008, p. 8).

All above surveys on the temperature performance of domestic refrigerators especially under real use condition were obtained that many of the domestic refrigerator or some locations in the compartments were not suitable for foodstuffs storage healthy for a long time. In other words inner air temperature range isn’t in the desirable range. Other conclusions are the long recovery temperature time (not rapid cooling) after door openings or loading warm foodstuffs and heterogeneous temperature distribution (not uniform). On the other hands importance of the inner

air circulation was indicated by Anderson, (2004) (chap. 12) to refrigeration system efficiency and preservation of food. Therefore, the inner air circulation should be developed to improvement thermal uniformity and rapid cooling (Fukuyo, Tanaami, & Ashida, 2003) and for achieving desirable temperature range to store foodstuffs healthy.

All those results have shown that the inner design is as important as the refrigeration system design in the domestic refrigerator. Even if a perfect refrigeration system is designed in the current technology, desirable condition isn't ensured by an unsuitable inner design. This situation is mentioned as "Knowledge of the air flow patterns inside refrigerated cabinets is essential for the proper design of the household refrigerator…" by Hermes, Marques, Melo, & Negrao (2002) (p. 1). In addition, inner design suitability directly depends on temperature and flow distributions (Ding, Qiao, & Lu, 2004; Gupta, Gopal, & Chakraborty, 2007). Also importance of inner design was specified the last paragraph in section 1.2.8.2 for reducing the on cycle time of compressor inherently improvement the energy efficiency.

In this study temperature and flow distributions have been obtained firstly to understand the air circulation characteristic. Then inner design parameters which affect those distributions have been determined. Finally throughout establishing a relationship between inner design parameters and distributions, improvement methods of inner air circulation have been discussed.

As a summary, the motivation of this study is to have high inner air temperature compare with desirable temperature according to the results of under real use condition surveys and the main goals are to obtain temperature and flow distributions and to determine the important inner design parameters which affect those distributions and to specifying the methods of the inner design.

Table 1.3 Air temperature measured in surveys of domestic refrigerators in real use conditions (James, Evans, & James, 2008)

Study no.	Year	Country	Number of domestic refrigerator	Measurement method	T_{min}	T_{mean}	T_{max}	% in temperature range
1	1987	USA	-	Not known				21% ≥ 10 C
2	1990	UK	75	Not known		< 5		6% > 5 C
3	1991	UK	252	Data logger (3 levels: T, M, B)	0.9	6	11.4	70% > 5 C
4	1992	Northern Ireland	150	Thermometer (3 levels: T, M, B)	0.8	6.5	12.6	71% > 5 C
5*	1993	France	102	Thermometer (3 levels: T, M, B)			14	70% > 6 C
6	1994	The Netherlands	125	Thermometer				30% < 5 C, 42% 5-7 C, 26% 7-9 C, 2% > 9 C
7	1997	New Zealand	50	Thermometer (2 levels: T, B)	0	4.9	11	60% > 4 C
8	1997	Greece	136	Thermometer				50% > 9 C
9	1997	UK	108	Data logger (1 position)	2	5.9	12	50% > 5 C
10	1998	USA	106	Not known				69% > 5 C
11	1998	UK	645	Thermometer	-2	7	13	70% > 5 C
12**	2002	France	119	Data logger (3 levels: T, M, B)	0.9	6.6	11.4	80% > 5 C
13***	2003	UK	901	Not known				69.3% 0-4 C, 27.9% 5-9 C, 2.8% >10 C
								84.2% 0-4 C, 14.8% 5-9 C, 1% >10 C
14	2004	New Zealand	53	Not known				33% > 5 C
15	2003	Greece	110	Data logger (3 levels: T, M, B)				26% < 4 C, 28 4%-6 C, 23% 6-8 C
16	2005	Ireland	100	Data logger (1 level: M)	-7.9	5.4	20.7	59% > 5 C
17	2005	Portugal	86	Digital thermometer				70% > 6 C
18	2005	Greece	250	Data logger	-2	6.3		50% > 6 C, 10% > 10 C
19	2005	The Netherlands	31	Glass thermometer	3.8		11.5	68% > 7 C,
20	2006	UK	24	Glass thermometer in gel		5 (mode)		68% > 5 C

T:Top, M:Middle, B: Bottom, T_{min}: Minimum value of the temperatures, T_{mean}: Average value of the temperatures, T_{max}: Maximum value of the temperatures
* Victoria (1993) cited by Laguerre, Derens, & Palagos (2002)
** Laguerre, Derens, & Palagos (2002)
*** Two measurements

1.4 Literature Reviews

There are three investigation methods which are theoretical, numerical and experimental. Generally basic engineering problems (certain geometry and physic) such as one dimensional, steady state heat conduction problems can be simply investigated by theoretical method. Since the air circulation problem in the domestic refrigerator is combination of heat transfer and fluid mechanics and inner geometry in which air circulated has complex structure, this study has been investigated by numerical and experimental methods. Hence in this section, a literature review has been implemented on numerical or experimental studies which have been investigated temperature and flow distributions in the domestic refrigerator.

1.4.1 Literature Reviews on Numerical Investigation

Several studies were carried out numerical study about inside the domestic refrigerator to several aims which are generally to determination important design parameters or investigation of several design parameters effect or design improvement or attainment optimum design. Among those researches some ones were studied on commercial type refrigerators. The goal of their studies was the same purpose which was obtained temperature and flow distributions inside the refrigerator.

Tao & Sun (2001) were carried out several numerical analyses which used finite element method (FEM) for investigation of some parameters effect that were insulation material and inlet airflow rate and temperature inside a forced convection driven type with double door and top-mounted domestic refrigerator. Also they developed six different designs with different combination of those parameters. A major conclusion of this study is that the higher airflow rate the more uniform temperature but the higher heat load with only modifies the airflow rate.

An inlet airflow rate investigation was carried out with finite volume method to ensure uniform temperature distribution and rapid cooling by Fukuyo, Tanaami, & Ashida (2003). Firstly current state analysis was implemented to identify the problematic region then two new designs were developed for the fresh food

compartment of the domestic refrigerator which owned air supply system. Uniform temperature was achieved whereby inner air was re-circulated without pass over the evaporator with added a blower and three jet slots in the compartment. Finally this study investigated optimum inlet airflow rate and slot dimensions. Also an empirical analysis was occurred to calculation the cooling rate of the new design and they obtained four times higher cooling rate than the current design.

Another uniformity study was carried out by Ding, Qiao, & Lu (2004) on a directly cooled refrigerator (as static) type domestic refrigerator. The gap between main shelves and the back wall in which the evaporator is embedded and the gap between door shelves and the door were investigated to enhance the temperature uniformity. Also the new design with added an axial fan and an air duct on the current model was developed to achieve more uniform temperature distribution. In the new design, this study investigated effect of the inlet airflow direction from the air duct to the compartment on the temperature uniformity. The major conclusion in this study is that the smaller gaps the more temperature uniformity but the weaker heat convection of the air with slow velocity.

Otherwise increasing the gap between the back wall and the main shelf in the freezer compartment was suggested by Gupta, Gopal, & Chakraborty (2007) which implemented numerical study with usage finite volume method on forced convection driven type with top-mounted domestic refrigerator. Additionally increasing the gap between door shelves and main shelves was suggested to utilization of cold air more effectively in the fresh food compartment. That study also emphasized the importance of the inlet airflow rate in the fresh-food compartment for attaining the desired temperature distribution. That study only observed temperature and flow distributions to suggest about improvement ways of the inner design.

The similar study was carried out to only observation of temperature and flow distributions in the fresh food compartment after the experimental study on the static type with double door domestic refrigerator by Afonso & Matos (2006). Experimental study was implemented to specify surfaces on which were placed sheet of aluminum foils as the radiation shield. Aluminum foil was used in order to

minimize the heat gain via radiation by compressor and condenser that own high temperature surfaces.

Different geometric parameters which are air duct design and its location were investigated by Yang, Chang, Chen, & Wang (2010) on forced convection driven type top mounted with three door domestic refrigerator. Firstly current state analysis was implemented and indicated that temperature non-uniformity was related to the velocity non-uniformity. Finally air duct design around the evaporator and location of the inlet slots for the freezer and refrigerating compartment were modified for improving the temperature uniformity.

Another modification study was carried out with usage numerical method by Foster, Madge, & Evans (2005) on commercial type refrigerator to improve air distribution. After the current state analysis, size and location of the evaporator which located in air duct and output width of the air curtain were modified. Also a baffle plate was added in the air duct. By those modifications, energy consumption was reduced from 1.37 to 1.29 kW over a day.

Also air curtain parameters which were velocity or temperature were investigated on commercial type refrigerator to generally reduce air infiltration by Cortella, Manzan, & Comini (2001), Cortella (2002), D'Agaro, Cortella, & Croce (2006), Navaz, Faramarzi, Gharib, Dabiri, & Modarress (2002). In addition cabinet length was investigated by D'Agaro, Cortella, & Croce (2006). Additionally analysis parameters such as dimensional (2D or 3D), flow conditions (laminar, turbulence), analysis type (steady state or transient) were investigated to ensure accurate solution by D'Agaro, Cortella, & Croce (2006).

A numerical study with usage finite volume method was implemented on buoyancy driven flows (as static type) domestic refrigerator by Hermes, Marques, Melo, & Negrao (2002). The evaporator location and inclination were investigated to improve the temperature and flow distribution. Also this study emphasized that numerical method was useful to reduce the real test needed for optimize the system design on domestic refrigerator.

Additionally an optimization study was carried out with numerical method by Saedodin, Torabi, Naserian, & Salehi (2010) on freezer compartment with wire on tube evaporator (as static freezer) in the double door domestic refrigerator. The numbers of evaporator loops in each shelf, the space between vertical walls and shelves and the width and height of freezer were investigated with designed seventeen different models. All analyses were carried out with loaded condition by product.

Another loaded condition analysis was carried out by Laguerre, Amara, Moureh, & Flick (2007) in static type domestic refrigerator. Effects of obstacles which are glass shelves and products were investigated on temperature and flow distributions. They showed that the more obstacles the lower airflow and inherently the higher inner air temperature. Furthermore they indicated that when radiation is not taken into account, temperature which predicted by the numerical study is over estimated in the static type domestic refrigerator.

1.4.2 Literature Reviews on Experimental Investigation

All above review papers on numerical study were also implemented an experimental study in order to validate the numerical study through comparing results or specify boundary conditions which necessary to numerical study.

Generally temperature measurements were implemented with usage the thermocouple. The measured temperature on the outer surfaces, the evaporator surface and inlet air to compartments were generally used as a boundary condition. In the other hand measured temperature of the inner surfaces and inner air were used to validate the numerical study by comparing with the predicted one by numerical study. Otherwise measured temperature of inner surfaces were used as a boundary condition by Afonso & Matos (2006), Ding, Qiao, & Lu (2004), Saedodin, Torabi, Naserian, & Salehi (2010). Additionally numerical studies with loaded condition were measured product temperature on surfaces or centre of the product.

Generally velocity magnitudes were measured at inlet slots to compartments to specify boundary condition by Cortella, Manzan, & Comini (2001), Cortella (2002),

D’Agaro, Cortella, & Croce (2006), Foster, Madge, & Evans (2005), Fukuyo, Tanaami, & Ashida, (2003) and Tao & Sun (2001). A study specified the measurement technique which was a hot-wire anemometer Foster, Madge, & Evans (2005). Additionally this study was used smoke puffers in order to observe the overall airflow pattern. In the other hand several numerical studies used Particle Image Velocimetry (PIV) technique which is simultaneously flow visualization and velocity measurement technique in a certain field in order to validate numerical study and/or specify boundary condition (Amara, Laguerre, Charrier-Mojtabi, Lartigue, & Flick, 2008; Navaz, Faramarzi, Gharib, Dabiri, & Modarress, 2002). .

Furthermore several papers carried out only experimental study in order to observed temperature and flow distributions. Lacerda, Melo, Barbosa Jr, & Duarte (2005) were implemented temperature measurement with thermocouples and velocity field measurement with PIV technique in the freezer compartment on forced convection driven type domestic refrigerator. Due to the necessity of the PIV technique several modifications were implemented for instance constructed transparent glass window and the covered black opaque paint inside freezer surfaces. The end of the observed flow field at different time during the compressor on-cycle they obtained that after the jet slots, airflow direction get vertically down along the transient. They emphasized that this treatment causes reducing the rate of chilled air that reaches the upper region of the freezer compartment and an undesirable temperature region was occurred.

Laguerre, Amara, & Flick (2005) and Laguerre, Amara, Charrier-Mojtabi, Lartigue, & Flick (2008) were carried out serial comprehensive experimental studies in order to investigation of the effects of temperature and surface area of the evaporator and obstacles respectively on temperature and flow distribution. They designed a basic static type prototype domestic refrigerator with evaporator located in the back wall as a rectangular closed cavity. In order to the same type domestic refrigerator has been investigated in our study, detailed information about those studies has been indicated follow.

Both of two studies, evaporator temperature was set to 0 and -10 C and area of the evaporator surface was set to whole back wall area and upper half back wall area in

order to investigation of their effects. Also they investigated the effect of the obstacles through filled 4 blocks of hollow spheres.

In temperature measurement study (Laguerre, Amara, & Flick, 2005) in order to specify thermal boundary layer, equipment was designed with nine thermocouples attached at 5 mm intervals. Additionally five rods on which have totally thirty five thermocouples attached were located inner air. This study has been obtained that the knowing situation which is that the warm zone at the top region and the cold zone at the bottom region in this type (as static type) enclosure which has a cooled vertical surface. A conclusion was indicated that the surface area of the evaporator was no effect temperature of the top zone but was noticeable effect at the bottom zone. An interesting conclusion in this study is that inner air temperature with obstacles is lower than the without one. This result was explained that "The obstacles enhance channeling near the wall and the convective exchanged is thus improved" (p. 536). But the following should be taken account that the obstacles were located without prevention the air circulation in this study. Also they emphasized that the presence of obstacles increase the maximum air temperature at the top of the refrigerator. After the air temperature data analyses, this study made a prediction of possible airflow scheme and shown in Figure 1.12.a

In the other hand airflow measurement (Laguerre, Amara, Charrier-Mojtabi, Lartigue, & Flick, 2008) were implemented with PIV technique. First airflow fields were measured at small areas and then obtained all small airflow fields were combined in order to attained whole airflow field. This study indicated that the temperature of the evaporator was more effective than the area of the evaporator surface on the velocity field and the lower evaporator temperature the higher air velocity. Also this study observed that an air flow downward along the evaporator surface and the maximum air velocity is obtained at the bottom of the evaporator. The more homogeneous air velocity field was obtained with the presence of obstacles with the lower velocity compared with no obstacles case. The main conclusions of this study are: observation of non-stationary air recirculation at the bottom corner and the stagnant air region at the top of the refrigerator. Also this study emphasized that results of the current experimental study on airflow and their

previous experimental study (Laguerre, Amara, & Flick, 2005) on temperature are complemented each other. For instance stagnant air region and high temperature region which is resulted by stagnant air was found at the top of the refrigerator. The observed airflow field by PIV has been shown in Figure 1.12.b.

Additionally Amara, Laguerre, Charrier-Mojtabi, Lartigue, & Flick (2008) carried out a numerical study on the same refrigerator model used in Laguerre, Amara, Charrier-Mojtabi, Lartigue, & Flick (2008) to compare airflow results with it. Through this comparison they have shown that the numerical studies were good agreement with PIV results. Predicted airflow field with numerical study by (Amara, Laguerre, Charrier-Mojtabi, Lartigue, & Flick (2008) has been shown in Figure 1.12.c.

Airflow field in the closed cavity with one vertical wall as cold wall and the other one as warm wall and insulated horizontal walls as static type domestic refrigerator was observed by Tian & Karayiannis (2000) cited by Laguerre, Amara, Charrier-Mojtabi, Lartigue, & Flick (2008) and shown in Figure 1.12.d. When comparing airflow fields in Figure 1.12, relatively similar airflow profiles is observed. The main air circulation throughout the walls and small air circulations at the corners is occurred. In order to airflow characteristic is specified in the static domestic refrigerator which has been investigated in this study. Results to be shown in Figure 1.12 have been compared with results of this study to validation.

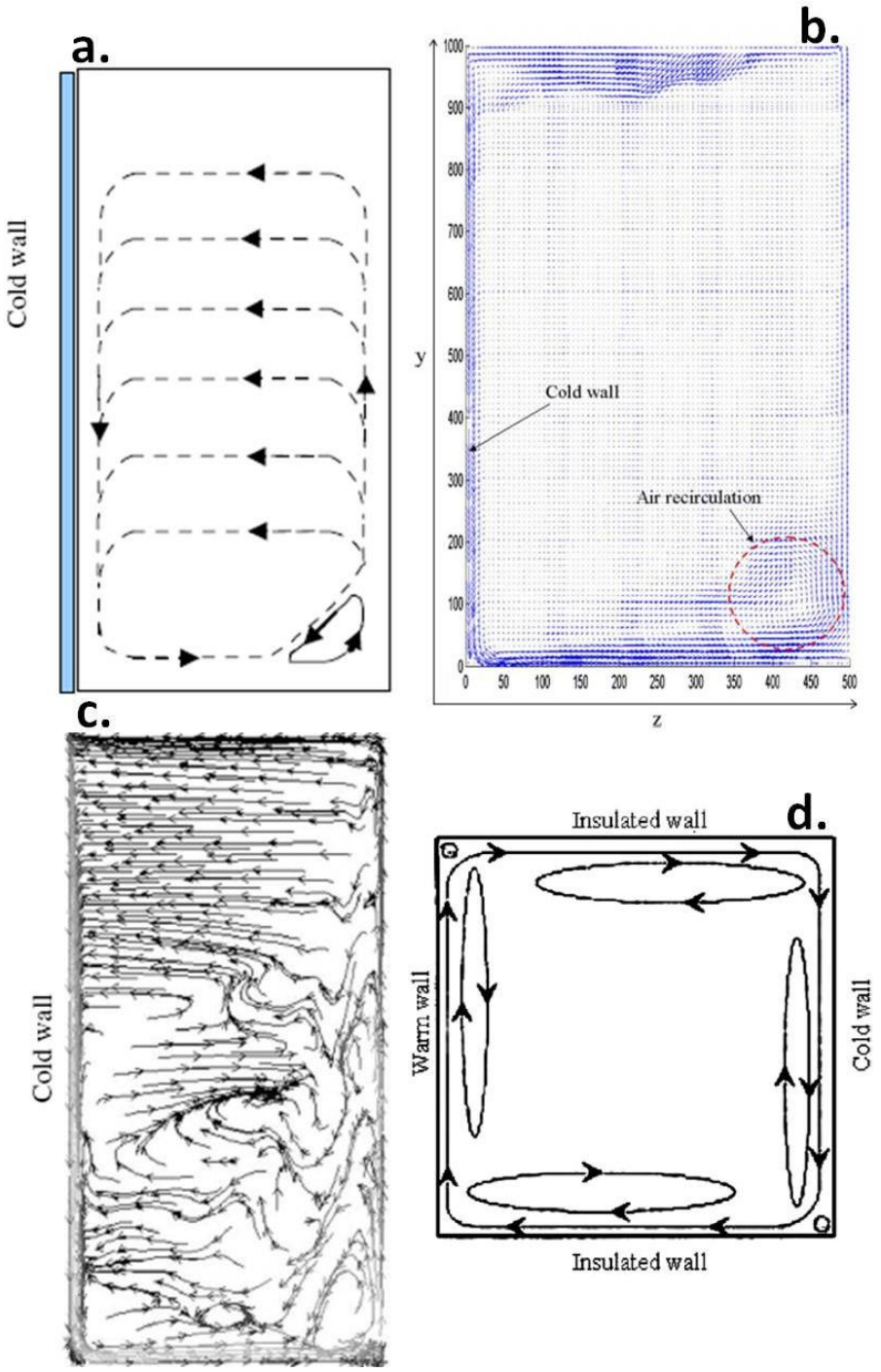

Figure 1.12Airflow field in the static domestic refrigerator a)Prediction by measured temperature by (Laguerre, Amara, & Flick, 2005), b) Observation by PIV measured by (Laguerre, Amara, Charrier-Mojtabi, Lartigue, & Flick, 2008), c) Prediction by numerical study by (Amara, Laguerre, Charrier-Mojtabi, Lartigue, & Flick, 2008), d) Prediction by two dimensional case study by (Tian & Karayiannis, 2000)

1.4.3 Summary

All above review studies on domestic refrigerator have shown in Table 1.4. Inlet airflow rate and temperature were the most investigated design parameter on forced convection driven type domestic refrigerator. In the other hand design parameters related to the evaporator such as its location, temperature, loop number were much to investigate on static type domestic refrigerator. Several gaps which situated inside the domestic refrigerator were investigated both of two types.

According to Table 1.4 most of these studies (8 studies) were investigated by numerical method. Also this conclusion has shown that numerical method is suitable to investigation of the design parameter on the temperature and flow distributions inside the domestic refrigerators.

Table 1.4 Some properties of studies about on domestic refrigerator

Study No	Study Name	Type	Determinate or investigated design parameters	Investigation method
1	Tao & Sun, 2001	forced convection driven	insulation material inlet airflow rates inlet airflow temperatures	numerical
2	Hermes, Marques, Melo, & Negrao, 2002	static	evaporator location and inclination	
3	Fukuyo, Tanaami, & Ashida, 2003	forced convection driven	inlet airflow rates height of the inlet slots	
4	Ding, Qiao, & Lu, 2004	static	gap between main shelves and the back wall gap between door shelves and the door	
		brewed	inlet airflow direction-(fan box shape)	
5	Gupta, Gopal, & Chakraborty, 2007	forced convection driven	gap between the back wall and main shelves gap between door shelves and main shelves inlet airflow rate	
6	Laguerre, Amara, Moureh, & Flick, 2007	static	presence of glass shelves presence of products (loaded condition)	
7	Yang, Chang, Chen, & Wang, 2010	forced convection driven	air duct design inlet airflow direction - (location of the inlet slot)	
8	Saedodin, Torabi, Naserian, & Salehi, 2010	static	numbers of evaporator loop gap between vertical walls and shelves freezer width and height	
9	Laguerre, Amara, & Flick, 2005	static	evaporator temperature evaporator area presence of obstacles (loaded condition)	experimental
10	Laguerre, Amara, Charrier-Mojtabi, Lartigue, & Flick, 2008	static		

CHAPTER TWO

NUMERICAL METHOD

2.1 Governing Equations

Generally the aim of the fluid mechanics and heat transfer problems is finding the six unknowns which are the pressure (p), temperature (T), velocity components (u, v, w) and density (ρ). All governing equations which are the mass, momentum (x, y, z), energy conservation equations and equations of state are interconnected to each other throughout those unknowns. Also those unknowns are functions of the space (x, y, z) and time (t).

The governing equations of fluid flow represent mathematical statements of the conservation laws of physics.

- The mass of a fluid is conserved.
- The rate of change of momentum equals the sum of the forces on a fluid particle (Newton's second law)
- The rate of change of energy is equal to the sum of the rate of heat addition to and the rate of work done on a fluid particle (first law of thermodynamics). (Versteeg & Malalasekera, 1995, p. 10).

Although the system (the closed system) approach used to be worked in thermodynamics and solid mechanics, the control volume (the open system) one used to be worked in fluid mechanics problems (Çengel & Cimbala, 2006, chap. 4). For development of the governing equations, the smallest element of the fluid is considered as a control volume (Figure 2.1). Also unknowns (or properties) of this fluid element are considered constant and the fluid is regarded as a continuum.

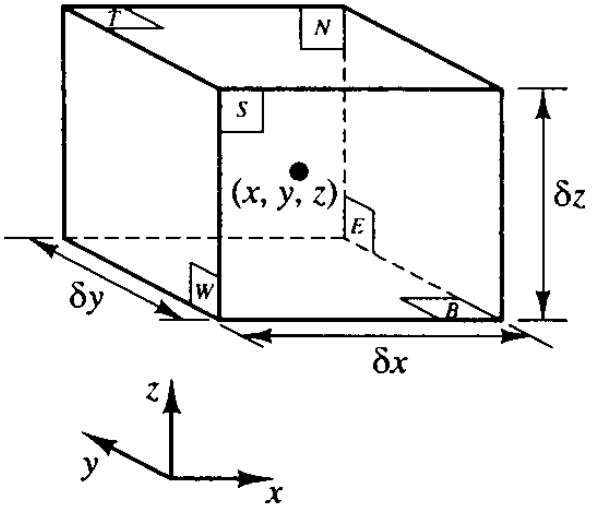

Figure 2.1 Fluid element as control volume (Versteeg & Malalasekera, 1995)

The centre of the element is located at position (x, y, z). A systematic account of changes in the mass, momentum and energy of the fluid element due to fluid flow across its boundaries and, where appropriate, due to the action of sources inside the element, leads to the fluid flow equation… The element under consideration is so small that fluid properties at the faces can be expressed accurately enough by means of the first two terms of a Taylor series expansion. So, for example, the pressure at the E and W faces, which are both a distance of 1/2δx from the element centre, can be expressed as $p-\frac{\delta p}{\delta x}\frac{1}{2}\delta x$ and $p+\frac{\delta p}{\delta x}\frac{1}{2}\delta x$ (Versteeg & Malalasekera, 1995, p. 11).

2.1.1 Mass Conservation Equation

This equation represents that rate of increase of mass in fluid element is equal to the net rate of flow of mass into fluid element. The rate of increase of mass in the fluid element is written as (Versteeg & Malalasekera, 1995):

$$\frac{\partial}{\partial t}(\rho\delta x\delta y\delta z)=\frac{\partial \rho}{\partial t}(\delta x\delta y\delta z) \tag{2.1}$$

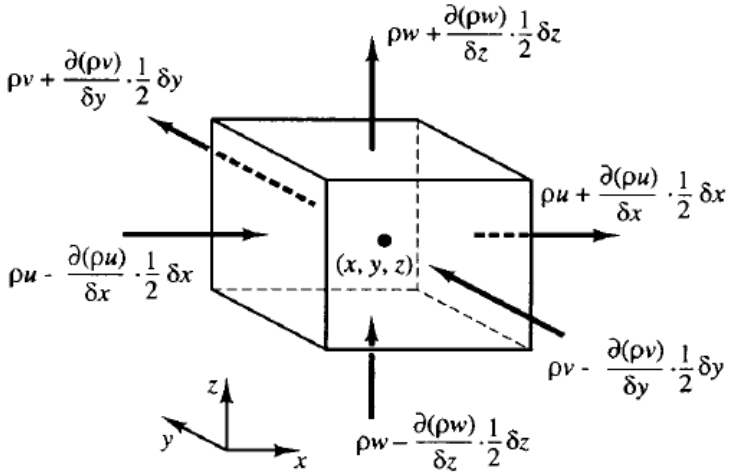

Figure 2.2 Mass flow in and out of fluid element (Versteeg & Malalasekera, 1995)

The net rate of flow of mass into the element is shown in Figure 2.2 across boundaries and is written as (Versteeg & Malalasekera, 1995):

$$\left(\rho u - \frac{\partial(\rho u)}{\partial x}\frac{1}{2}\delta x\right)\delta y\delta z - \left(\rho u + \frac{\partial(\rho u)}{\partial x}\frac{1}{2}\delta x\right)\delta y\delta z + \left(\rho v - \frac{\partial(\rho v)}{\partial y}\frac{1}{2}\delta y\right)\delta x\delta z - \left(\rho v + \frac{\partial(\rho v)}{\partial y}\frac{1}{2}\delta y\right)\delta x\delta z + \left(\rho w - \frac{\partial(\rho w)}{\partial z}\frac{1}{2}\delta z\right)\delta x\delta y - \left(\rho w + \frac{\partial(\rho w)}{\partial z}\frac{1}{2}\delta z\right)\delta x\delta y \quad (2.2)$$

The mass flow rate across a face of the element in equation (2.2) is accounted by product of density, area and the velocity component normal to the face. If equation (2.1) is equated equation (2.2) and the expression is divided by the element volume ($\delta x\delta y\delta z$), the mass conservation equation (2.3) is yielded.

$$\frac{\partial \rho}{\partial t} + \frac{\partial(\rho u)}{\partial x} + \frac{\partial(\rho v)}{\partial y} + \frac{\partial(\rho w)}{\partial z} = 0 \text{ or } \frac{\partial \rho}{\partial t} + \text{div}(\rho u) = 0 \quad (2.3)$$

In the mass conservation equation (Eq. 2.3) "the first term on the left hand side is the rate of change in time of the density (mass per unit volume)" and the other terms "describe the net flow of mass out of the element across its boundaries and is called convective term" (Versteeg & Malalasekera, 1995, pp. 12-13). It is should be noted that the mass conservation equation (Eq. 2.3) is written for the unit volume.

2.1.2 Reynolds Transport Theorem (RTT)

The momentum and energy conservation equations represent "…the changes of properties of a fluid particle" (Versteeg & Malalasekera, 1995, p. 13). Since a fluid particle follows a flow, its position (x, y, z) changes with time (t). The following fluid particle may be thought of moving in a system (the closed system) approach. The other hand the considered fluid element (the control volume) is stationary in space. So there is a need to relate the changes in a fluid element (control volume) to the changes in a following fluid particle (in the system or the closed system) (Çengel & Cimbala, 2006, chap. 4). "The relationship between the time rates of change of an extensive property for a system and for a control volume is expressed by the Reynolds transport theorem (RTT), which provides the link between the system and control volume approaches" (Çengel & Cimbala, 2006, p. 149). The extensive property represents the fluid particle property such as density or velocity or pressure or temperature.

….The value of a property per unit mass is denoted by ϕ. The total or substantive derivative of ϕ with respect to time following a fluid particle, written as Dϕ/Dt, is

$$\frac{\mathrm{D}\phi}{\mathrm{Dt}} = \frac{\partial\phi}{\partial \mathrm{t}} + \frac{\partial\phi}{\partial \mathrm{x}}\frac{\mathrm{dx}}{\mathrm{dt}} + \frac{\partial\phi}{\partial \mathrm{y}}\frac{\mathrm{dy}}{\mathrm{dt}} + \frac{\partial\phi}{\partial \mathrm{z}}\frac{\mathrm{dz}}{\mathrm{dt}} \tag{2.4}$$

A fluid particle follows the flow, so dx/dt = u, dy/dt = v and dz/dt = w. Hence the substantive derivative of ϕ is given by

$$\frac{\mathrm{D}\phi}{\mathrm{Dt}} = \frac{\partial\phi}{\partial \mathrm{t}} + \mathrm{u}\frac{\partial\phi}{\partial \mathrm{x}} + \mathrm{v}\frac{\partial\phi}{\partial \mathrm{y}} + \mathrm{w}\frac{\partial\phi}{\partial \mathrm{z}} + \mathrm{u}.\,\mathrm{grad}\,\phi \tag{2.5}$$

Dϕ/Dt defines the rate of change of property ϕ per unit mass….The rate of change of property ϕ per unit volume for a fluid particle is given by the product of Dϕ/Dt and density ρ, hence

$$\rho\frac{\mathrm{D}\phi}{\mathrm{Dt}} = \rho\left(\frac{\partial\phi}{\partial \mathrm{t}} + \mathbf{u}.\,\mathrm{grad}\,\phi\right) \tag{2.6}$$

…. The relationship between the substantive derivative of ϕ, which follows a fluid particle and rate of change of ϕ for a fluid element is now developed.

The mass conservation equation contains the mass per unit volume (i.e. the density ρ) as the conserved quantity. The sum of the rate of change of density and the convective term in the mass conservation equation for a fluid element is described in equation (2.3).

The generalization of these terms for an arbitrary conserved property is

$$\frac{\partial(\rho\phi)}{\partial t} + \text{div}\,(\rho\phi\mathbf{u}) \tag{2.7}$$

… expressed the rate of change of ϕ per unit volume plus the net flow of ϕ out of the fluid element per unit volume. It is now re-written to illustrate its relationship with the substantive derivative of ϕ:

$$\frac{\partial(\rho\phi)}{\partial t} + \text{div}\,(\rho\phi\mathbf{u}) = \rho\left[\frac{\partial\phi}{\partial t} + \mathbf{u}\,.\,\text{grad}\,\phi\right] + \phi\left[\frac{\partial\rho}{\partial t} + \text{div}(\rho\mathbf{u})\right] = \rho\frac{\mathrm{D}\phi}{\mathrm{D}t} \tag{2.8}$$

The term $\phi[\partial\rho/\partial t + div(\rho\boldsymbol{u})]$ is equal to zero by virtue of mass conservation. In words, relationship states

$$\begin{bmatrix}\text{Rate of increase}\\ \text{of } \phi \text{ of}\\ \text{fluid element}\end{bmatrix} + \begin{bmatrix}\text{Net rate of flow}\\ \text{of } \phi \text{ out of}\\ \text{fluid element}\end{bmatrix} = \begin{bmatrix}\text{Rate of increase}\\ \text{of } \phi \text{ for a}\\ \text{fluid particle}\end{bmatrix}$$

(Versteeg & Malalasekera, 1995, pp. 13-14).

In the other words equation (2.8) was described as "…states that the time rate of change of the property B of the system is equal to the time rate of change of B of the control volume plus the net flux of B out of the control volume by mass crossing the control surface" by (Çengel & Cimbala, 2006, p. 150). The B represents the property of following fluid particle such as mass or energy or momentum. The three components of momentum equation and the energy equation the relevant entries for ϕ and their rates of change per unit volume as defined by Versteeg & Malalasekera (1995) and shown in Table 2.1.

Table 2.1 Relations the changes of properties in a fluid element (control volume) to the changes in a following fluid particle (Versteeg & Malalasekera, 1995)

Equation	**Fluid Property**	**Rate of increase for a fluid particle**	**Rate of increase of fluid element + Net rate of flow out of fluid element**
x-momentum	U	$\rho\frac{Du}{Dt}$	$\frac{\partial(\rho u)}{\partial t} + div(\rho u\boldsymbol{u})$
y-momentum	V	$\rho\frac{Dv}{Dt}$	$\frac{\partial(\rho v)}{\partial t} + div(\rho v\boldsymbol{u})$
z-momentum	W	$\rho\frac{Dw}{Dt}$	$\frac{\partial(\rho w)}{\partial t} + div(\rho w\boldsymbol{u})$
Energy	E	$\rho\frac{DE}{Dt}$	$\frac{\partial(\rho E)}{\partial t} + div(\rho E\boldsymbol{u})$

2.1.3 Momentum Equations

The momentum equations derived from the Newton's second law and represent "…the rate of change of momentum of a fluid particle equals the sum of the forces on the particle" (Versteeg & Malalasekera, 1995, p. 14). The rate of change of x, y and z momentum per unit volume has shown in Table 2.1.

There are two types of forces which are surface forces and body forces on fluid particle. The surface forces are based on the static pressure and viscous stresses and also are the results of the interaction of between neighboring fluid elements. The static pressure acts normal direction of the surface and always into the control volume, so normal stress is occurred. The viscous stresses have three components that x, y and z direction and shown in Figure 2.3. The viscous stress components which are act to the normal direction of the surface are occurred normal stresses although the other ones are occurred shear stresses. (Incropera, DeWitt, Bergman, & Lavine, 2007; Versteeg & Malalasekera, 1995)

The body forces are based on gravity, centrifugal, coriolis and electromagnetic effects (Versteeg & Malalasekera, 1995, chap. 1). Those forces include as source terms (S) in the momentum equations.

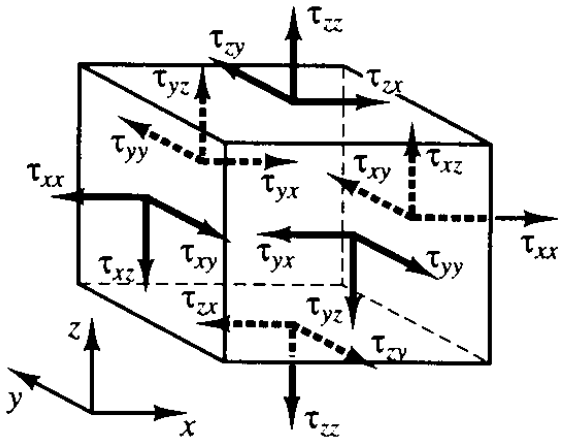

Figure 2.3 Stress components on boundaries of fluid element (Versteeg & Malalasekera, 1995)

The x components of surface stresses have shown in Figure 2.4. The surface forces that act x direction is the product of stress and area on the surface of fluid element. The net force in x-direction is yielded through the sum of those forces. The total force per unit volume in x-direction is yielded through the total forces are divided by the volume (δxδyδz). Therefore the x-momentum equation (Eq. 2.9) is yielded through plus the net force per unit volume in x-direction and source terms in x-direction (S_{Mx}) (Versteeg & Malalasekera, 1995).

$$\rho \frac{Du}{Dt} = \frac{\partial(-\rho+\tau_{xx})}{\partial x} + \frac{\partial \tau_{yx}}{\partial y} + \frac{\partial \tau_{zx}}{\partial z} + S_{Mx} \tag{2.9}$$

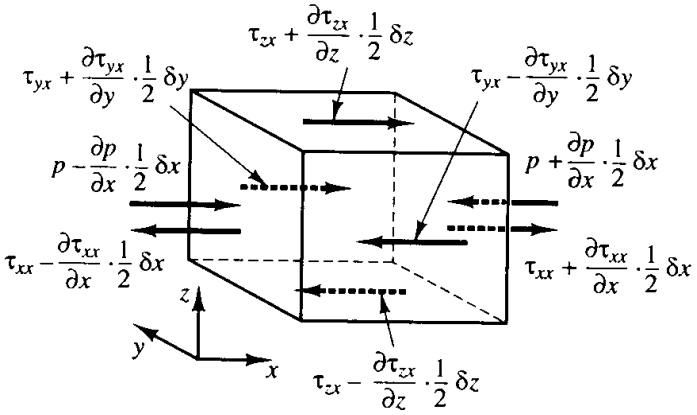

Figure 2.4 Stress components in the x-direction (Versteeg & Malalasekera, 1995)

The left hand side term represent the rate of change of x-momentum of the fluid particle and shown in Table 2.1. The y and z momentum equations are found to the same way and written by Versteeg & Malalasekera (1995)

$$\rho\frac{\mathrm{Dv}}{\mathrm{Dt}} = \frac{\partial\tau_{xy}}{\partial x} + \frac{\partial(-\rho+\tau_{yy})}{\partial y} + \frac{\partial\tau_{zy}}{\partial z} + S_{My} \tag{2.10}$$

$$\rho\frac{\mathrm{Dw}}{\mathrm{Dt}} = \frac{\partial\tau_{xz}}{\partial x} + \frac{\partial\tau_{yz}}{\partial y} + \frac{\partial(-\rho+\tau_{zz})}{\partial z} + S_{Mz} \tag{2.11}$$

The source terms S_{Mx}, S_{My} and S_{Mz} include contributions due to body forces only. For example, the body force due to the gravity would be modeled by $S_{Mx} = 0$, $S_{My} = 0$ and $S_{Mz} = -\rho g$.

2.1.4 Energy Equation

The energy equation is derived from the first law of thermodynamics which states that the rate of change of energy of a fluid particle is equal to the rate of heat addition to the fluid particle plus the rate of work done on particle (Versteeg & Malalasekera, 1995, p. 17).

The rate of increase of energy for a fluid particle has given in Table 2.1.

The net work done on the fluid particle is based on surface forces and found through product of the force and velocity component in the direction of the force. The net work done per unit volume is written as by Versteeg & Malalasekera (1995).

$$-\frac{\partial(\mathrm{up})}{\partial x} - \frac{\partial(\mathrm{vp})}{\partial y} - \frac{\partial(\mathrm{wp})}{\partial z} = -div(\rho\boldsymbol{u})$$

or

$$[-\mathrm{div}(\rho\mathbf{u})] + \left[\frac{\partial(u\tau_{xx})}{\partial x} + \frac{\partial(u\tau_{yx})}{\partial y} + \frac{\partial(u\tau_{zx})}{\partial z} + \frac{\partial(v\tau_{xy})}{\partial x} + \frac{\partial(v\tau_{yy})}{\partial y} + \frac{\partial(v\tau_{zy})}{\partial z} + \frac{\partial(w\tau_{xz})}{\partial x} + \frac{\partial(w\tau_{yz})}{\partial y} + \frac{\partial(w\tau_{zz})}{\partial z}\right] \tag{2.12}$$

The rate of heat addition across boundaries of fluid element is based on heat conduction. The Fourier's law of heat conduction relates the heat flux (Figure 2.5) to the local temperature gradient. Also heat transfer is calculated by the product of the

heat flux and its related area on the fluid element surfaces. Therefore, the net rate of heat added to the fluid particle per unit volume due to the heat flow across its boundaries is yielded by the sum of the heat flows divided by the volume (δxδyδz) (Versteeg & Malalasekera, 1995).

$$-\frac{\partial \mathrm{q_x}}{\partial \mathrm{x}}-\frac{\partial \mathrm{q_y}}{\partial \mathrm{y}}-\frac{\partial \mathrm{q_z}}{\partial \mathrm{z}}=-\mathrm{div}\,\mathbf{q} \qquad (2.13)$$

Where;

$$\mathrm{q_x}=-\mathrm{k}\,\frac{\partial \mathrm{T}}{\partial \mathrm{x}},\ \mathrm{q_y}=-\mathrm{k}\,\frac{\partial \mathrm{T}}{\partial \mathrm{y}},\ \mathrm{q_z}=-\mathrm{k}\,\frac{\partial \mathrm{T}}{\partial \mathrm{z}},$$

$$\mathbf{q}=-\mathrm{k}\,\mathrm{grad}\,\mathrm{T}\ \mathrm{so}-\mathrm{div}\,\mathbf{q}=\mathrm{div}(\mathrm{k}\,\mathrm{grad}\,\mathrm{T})$$

"The energy of fluid (E) is defined as the sum of internal (thermal) energy *i*, kinetic energy $(1/2(\ u\text{^}2+v\text{^}2+w\text{^}2))$ and gravitational potential energy" (Versteeg & Malalasekera, 1995, p. 19).

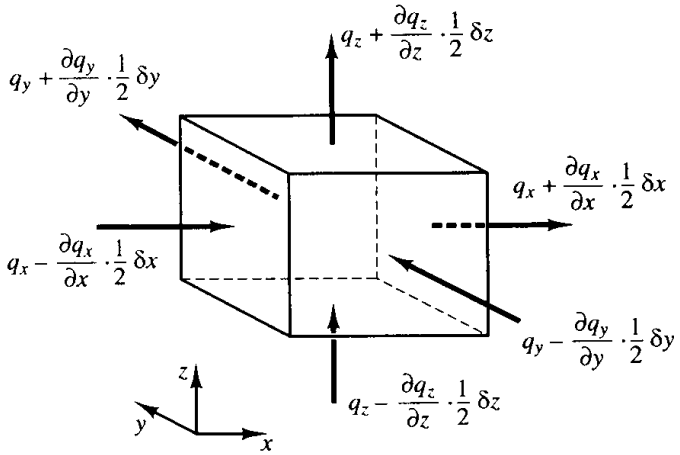

Figure 2.5 Components of heat flux vector (Versteeg & Malalasekera, 1995)

The effects of potential energy changes include as a source term (S_E) in energy equation. Therefore the energy equation is obtained by the sum of the net rate of work done and the net rate of heat addition and the rate of increase of energy due to sources and written as

$$\rho\frac{DE}{Dt} = -\text{div}(\rho\mathbf{u}) + \left[\frac{\partial(u\tau_{xx})}{\partial x} + \frac{\partial(u\tau_{yx})}{\partial y} + \frac{\partial(u\tau_{zx})}{\partial z} + \frac{\partial(v\tau_{xy})}{\partial x} + \frac{\partial(v\tau_{yy})}{\partial y} + \frac{\partial(v\tau_{zy})}{\partial z} + \frac{\partial(w\tau_{xz})}{\partial x} + \frac{\partial(w\tau_{yz})}{\partial y} + \frac{\partial(w\tau_{zz})}{\partial z}\right] + \text{div}(k\,\text{grad}\,T) + S_E \quad (2.14)$$

In equation (2.14), "E" is the sum of the internal energy (i) and the kinetic energy $(1/2(u\text{^}2 + v\text{^}2 + w\text{^}2))$.

Although equation (2.14) is a perfectly adequate energy equation it is common practice to extract the changes of the (mechanical) kinetic energy to obtain an equation for internal energy i or temperature T. The part of the energy equation attributable to the kinetic energy can be found by multiplying the x-momentum equation by velocity component u, the y- momentum equation by v and the z-momentum equation by w and adding the results together. It can be shown that this yields the following conservation equation for the kinetic energy:

$$\rho\frac{D\left[\frac{1}{2}(u^2+v^2+w^2)\right]}{Dt} = -\mathbf{u}.\,\text{grad}\,p + u\left(\frac{\partial\tau_{xx}}{\partial x} + \frac{\partial\tau_{yx}}{\partial y} + \frac{\partial\tau_{zx}}{\partial z}\right) + v\left(\frac{\partial\tau_{xy}}{\partial x} + \frac{\partial\tau_{yy}}{\partial y} + \frac{\partial\tau_{zy}}{\partial z}\right) + w\left(\frac{\partial\tau_{xz}}{\partial x} + \frac{\partial\tau_{yz}}{\partial y} + \frac{\partial\tau_{zz}}{\partial z}\right)\mathbf{u}.\,\mathbf{S}_M \quad (2.15)$$

Subtracting (2.15) from (2.14) and defining a new source term as $S_i = S_E - \mathbf{u}.\mathbf{S}_M$ yields the internal energy equation (Versteeg & Malalasekera, 1995, p. 19).

$$\rho\frac{Di}{Dt} = -p\,\text{div}\,\mathbf{u} + \text{div}(k\,\text{grad}\,T) + \tau_{xx}\frac{\partial u}{\partial x} + \tau_{yx}\frac{\partial u}{\partial y} + \tau_{zx}\frac{\partial u}{\partial z} + \tau_{xy}\frac{\partial v}{\partial x} + \tau_{yy}\frac{\partial v}{\partial y} + \tau_{zy}\frac{\partial v}{\partial z} + \tau_{xz}\frac{\partial w}{\partial x} + \tau_{yz}\frac{\partial w}{\partial y} + \tau_{zz}\frac{\partial w}{\partial z} S_i \quad (2.16)$$

2.1.5 Equation of State

All above five differential equations which are mass conservation equation, x- y- and z- momentum equations and energy equation may be solved together to find unknowns. Furthermore in some cases a linkage between the five differential equations is needed. Equation of state is provided that linkage.

Among the unknowns are four thermodynamic variables: density (ρ), pressure (p), internal energy (i) and temperature (T). Relationship between the thermodynamic

variables can be obtained through the assumption of thermodynamic equilibrium…. the fluid can thermodynamically adjust itself to new conditions so quickly that the changes are effectively instantaneous. Thus the fluid always remains in thermodynamic equilibrium…. If we use ρ and T as state variables we have equations for pressure (p) and specific internal energy (i):

$$p = p(\rho, T) \text{ and } i = i(\rho, T)$$

For a perfect gas the following, well-known, equations of state are useful:

$$p = \rho RT \text{ and } i = C_v T$$

The assumption of thermodynamics equilibrium eliminates all but the two thermodynamic state variables. In the flow compressible fluids the equations of state provide the linkage between the energy equation on the one hand and mass conservation and momentum equations on the other. This linkage arises through the possibility of density variations as a result of pressure and temperature variations in the flow field.

Liquid and gases flowing at low speeds behave as incompressible fluids. Without density variations there is no linkage between the energy equation and the mass conservation and momentum equations. The flow field can often be solved by considering mass conservation and momentum equations only. The energy equation only needs to be solved alongside the others if the problem involves heat transfer (Versteeg & Malalasekera, 1995, p. 21).

2.1.6 Navier-Stokes Equations

As mentioned before, generally there are six unknowns (ρ, p, u, v, w and T) to desire finding. Otherwise in the governing equations (mass conservation, three momentum conservations, energy conservation and equation of state) there are six unknown viscous stress terms (τ_{ij}) besides those six unknowns. Due to the presence of six equations and twelve unknowns, this equation system is mathematically unsolvable. Therefore a relationship between the viscous stress terms and the other variables is needed.

In many fluid flows the viscous stresses can be expressed as functions of the local deformation rate (or strain rate). In three dimensional flows the local rate of deformation is composed of the linear deformation rate and the volumetric deformation rate (Versteeg & Malalasekera, 1995, p. 21).

The fluids assumes isotropic and the linear deformation denotes e_{ij}. There are three linear elongating deformation components (Versteeg & Malalasekera, 1995):

$$e_{xx} = \frac{\partial u}{\partial x}, \; e_{yy} = \frac{\partial v}{\partial x}, \; e_{zz} = \frac{\partial w}{\partial x} \tag{2.17}$$

There are also six shearing linear deformation components (Versteeg & Malalasekera, 1995):

$$e_{xy} = e_{yx} = \frac{1}{2}\left(\frac{\partial u}{\partial y} + \frac{\partial v}{\partial x}\right), \; e_{xz} = e_{zx} = \frac{1}{2}\left(\frac{\partial u}{\partial z} + \frac{\partial w}{\partial x}\right), \; e_{yz} = e_{zy} = \frac{1}{2}\left(\frac{\partial v}{\partial z} + \frac{\partial w}{\partial v}\right) \tag{2.18}$$

The volumetric deformation is given by (Versteeg & Malalasekera, 1995):

$$\frac{\partial u}{\partial x} + \frac{\partial v}{\partial y} + \frac{\partial w}{\partial z} = \text{div } \mathbf{u} \tag{2.19}$$

In a Newtonian fluid flow the viscous stresses are proportional to the rates of deformation. The three-dimensional form of Newton's law of viscosity for compressible flows involves two constant of proportionally: the (first) dynamic viscosity, μ, to relate stresses to linear deformations, and the second viscosity, λ, to relate stresses to the volumetric deformation. The nine viscous components, of which six are independent, are:

$$\tau_{xx} = 2\mu\frac{\partial u}{\partial x} + \lambda \text{ div } \mathbf{u}, \; \tau_{yy} = 2\mu\frac{\partial v}{\partial y} + \lambda \text{ div } \mathbf{u}, \; \tau_{zz} = 2\mu\frac{\partial w}{\partial z} + \lambda \text{ div } \mathbf{u}$$

$$\tau_{xy} = \tau_{yx} = \mu\left(\frac{\partial u}{\partial y} + \frac{\partial v}{\partial x}\right), \; \tau_{xz} = \tau_{zx} = \mu\left(\frac{\partial u}{\partial z} + \frac{\partial w}{\partial x}\right)$$

$$\tau_{yz} = \tau_{zy} = \mu\left(\frac{\partial v}{\partial z} + \frac{\partial w}{\partial y}\right) \tag{2.20}$$

…. Substitution of the above shear stresses into momentum equation yields the so called Navier-Stokes equations…. (Versteeg & Malalasekera, 1995, p. 22).

Re-arranged Navier-Stokes equations have shown as (Versteeg & Malalasekera, 1995):

$$\rho \frac{\mathrm{Du}}{\mathrm{Dt}} = -\frac{\partial \mathrm{p}}{\partial \mathrm{x}} + \mathrm{div}(\mu\ \mathrm{grad\ u}) + \mathrm{S_{Mx}} \tag{2.21}$$

$$\rho \frac{\mathrm{Dv}}{\mathrm{Dt}} = -\frac{\partial \mathrm{p}}{\partial \mathrm{y}} + \mathrm{div}(\mu\ \mathrm{grad\ v}) + \mathrm{S_{My}} \tag{2.22}$$

$$\rho \frac{\mathrm{Dw}}{\mathrm{Dt}} = -\frac{\partial \mathrm{p}}{\partial \mathrm{z}} + \mathrm{div}(\mu\ \mathrm{grad\ w}) + \mathrm{S_{Mz}} \tag{2.23}$$

If the Newtonian model viscous stresses are substituted in the (internal) energy conservation equation, the new re-arranged energy conservation equation is yielded (Versteeg & Malalasekera, 1995).

$$\rho \frac{\mathrm{Di}}{\mathrm{Dt}} = -\mathrm{p}\ \mathrm{div}\ \mathbf{u} + \mathrm{div}(\mathrm{k\ grad\ T}) + \Phi + \mathrm{S_i} \tag{2.24}$$

Φ represents the dissipation function which describes all the effects due to the viscous stresses in this internal energy and can be shown to be equal to (Versteeg & Malalasekera, 1995):

$$\Phi = \mu\left\{2\left[\left(\frac{\partial u}{\partial x}\right)^2 + \left(\frac{\partial v}{\partial y}\right)^2 + \left(\frac{\partial w}{\partial z}\right)^2\right] + \left(\frac{\partial u}{\partial y} + \frac{\partial v}{\partial x}\right)^2 + \left(\frac{\partial u}{\partial z} + \frac{\partial w}{\partial x}\right)^2 + \left(\frac{\partial v}{\partial z} + \frac{\partial w}{\partial y}\right)^2\right\}$$

$$+\lambda(div\ \boldsymbol{u})^2 \tag{2.25}$$

Therefore the unknown viscous stresses terms are defined with the function of the properties of fluid (μ and λ) and the velocity gradient for the Newtonian fluids. So the number of unknowns is equal to the number of equations. It is should be noted that μ and λ is a measurable properties of fluid and generally λ is equal to -2/3 of μ (Versteeg & Malalasekera, 1995). So these properties of fluid aren't the unknown.

2.1.7 Conservation Form of the Governing Equation for Incompressible Newtonian Fluid Flow

In this study, since the speed magnitude is low (~0-5 m/s), fluid (inner air of the domestic refrigerator) is assumed an incompressible fluid.

For an incompressible fluid, Versteeg & Malalasekera (1995) emphasized that "… the density (ρ) is constant…" (p. 13).

So mass conservation equation (Eq. 2.3) converts to:

$$\frac{\partial u}{\partial x}+\frac{\partial v}{\partial y}+\frac{\partial w}{\partial z}=0 \tag{2.26}$$

For an incompressible fluid Versteeg & Malalasekera (1995) emphasized that "… the viscous stresses are just twice the local rate of linear deformation times the dynamic viscosity" (p. 22). Also dynamic viscosity is constant. Through considering that attention and equation (2.26) the x-, y-, and z- momentum equations (Eq. 2.21-22-23) convert to

$$\rho\left(\frac{\partial u}{\partial t}+u\frac{\partial u}{\partial x}+v\frac{\partial u}{\partial y}+w\frac{\partial u}{\partial z}\right)=-\frac{\partial p}{\partial x}+\mu\left(\frac{\partial^2 u}{\partial x^2}+\frac{\partial^2 u}{\partial y^2}+\frac{\partial^2 u}{\partial z^2}\right)+S_{Mx} \tag{2.27}$$

$$\rho\left(\frac{\partial v}{\partial t}+u\frac{\partial v}{\partial x}+v\frac{\partial v}{\partial y}+w\frac{\partial v}{\partial z}\right)=-\frac{\partial p}{\partial y}+\mu\left(\frac{\partial^2 v}{\partial x^2}+\frac{\partial^2 v}{\partial y^2}+\frac{\partial^2 v}{\partial z^2}\right)+S_{My} \tag{2.28}$$

$$\rho\left(\frac{\partial w}{\partial t}+u\frac{\partial w}{\partial x}+v\frac{\partial w}{\partial y}+w\frac{\partial w}{\partial z}\right)=-\frac{\partial p}{\partial z}+\mu\left(\frac{\partial^2 w}{\partial x^2}+\frac{\partial^2 w}{\partial y^2}+\frac{\partial^2 w}{\partial z^2}\right)+S_{Mxz} \tag{2.29}$$

For an incompressible fluid Versteeg & Malalasekera (1995) emphasized that "…i = cT, where c is the specific heat…" (p. 20). So energy equation (Eq. 2.24) converts to:

$$\rho c\left(\frac{\partial T}{\partial t}+u\frac{\partial T}{\partial x}+v\frac{\partial T}{\partial y}+w\frac{\partial T}{\partial z}\right)=\frac{\partial}{\partial x}\left(k\frac{\partial T}{\partial x}\right)+\frac{\partial}{\partial y}\left(k\frac{\partial T}{\partial y}\right)+\frac{\partial}{\partial z}\left(k\frac{\partial T}{\partial z}\right)+\left(u\frac{\partial p}{\partial x}+v\frac{\partial p}{\partial y}+w\frac{\partial p}{\partial z}\right)+\Phi \tag{2.30}$$

Through the incompressible assumption the density is converted a known term like a dynamic viscosity. So the equations of state don't need to be for solving the governing equations.

2.2 Computational Fluid Dynamics (CFD)

All governing equations which are mass, three component of momentum and energy conservation equations are partial differential equations and have no known

general analytical solution but can be solved numerically. Also since some problems may be complex geometry and physics, solution of the governing equations to get difficult. CFD accomplishes those difficulties through computer based analysis systems. So CFD are numerically solved fluid mechanics and heat transfer problems with usage special form of the governing equations.

There are three numerical method which are finite difference method, finite element method and spectral methods (Versteeg & Malalasekera, 1995 ,chap. 1). Also there is a method called as the finite volume method which is developed special finite difference formulation and that method is most common method to usage in CFD. The finite volume method is described basically following.

…. The numerical algorithm consists of the following steps:

- Formal integration of the governing equations of fluid flow over all the (finite) control volumes of the solution domain.
- Discretisation involves the substitution of a variety of finite-difference-type approximations for the terms in the integrated equation representing flow processes such as convection, diffusion and sources. This converts the integral equations into a system of algebraic equations.
- Solution of the algebraic equations by an iterative method.

…. The conservation of a general flow variable ϕ, for example a velocity component or enthalpy, within a finite control volume can be expressed as a balance between the various processes tending to increase or decrease it. In words we have;

$$\begin{bmatrix} Rate\ of\ change\ of\ \phi \\ in\ the\ control\ volume\ with \\ respect\ to\ time \end{bmatrix} = \begin{bmatrix} Net\ flux\ of\ \phi\ due\ to \\ convection\ into\ the \\ control\ volume \end{bmatrix} +$$

$$\begin{bmatrix} Net\ flux\ of\ \phi\ due\ to \\ diffusion\ into\ the \\ control\ volume \end{bmatrix} + \begin{bmatrix} Net\ flux\ rate\ of\ creation\ of\ \phi \\ inside\ the \\ control\ volume \end{bmatrix}$$

CFD codes contain discretisation techniques suitable for the treatment of the key transport phenomena, convection (transport due to fluid flow) and diffusion (transport due to variations of ϕ from point to point) as well as for the source terms (associated with the creation or destruction of ϕ) and the rate of change with respect to time. The underlying physical phenomena are complex and non-linear so an iterative solution approach is required (Versteeg & Malalasekera, 1995, pp. 4-5).

As a summary that "…. In this technique, the region of interest is divided into small sub-regions, called control volumes. The equations are discredited and solved iteratively for each control volume…." (Analysis Systems [ANSYS] CFX, Release 12.1, 2009).

2.2.1 Steps of the CFD

All CFD simulation studies consist of three steps (Versteeg & Malalasekera, 1995, chap. 1):

1. Pre-Processor
2. Solver
3. Post processor

2.2.1.1 Pre-Processor

The pre-processor consist of geometry and mesh creating process and defining the physics process. This step involves (Versteeg & Malalasekera, 1995, chap. 1):

- Definition of the geometry of the region of interest: the computational domain.
- Grid generation-the sub-division of the domain into a number of smaller, non-overlapping sub-domains: a grid (or mesh) of cells (or control volumes or elements).
- Selection of the physical and chemical phenomena that need to be modeled.
- Definition of fluid properties.

- Specification of appropriate boundary conditions at cells which coincide with or touch the domain boundary.

All geometries in the fluid field may not need to be modeled. For instance solid parts inside or around the fluid field may not need to be modeled, those solid surfaces are the boundaries of the problem. Also geometry of the computational domain may not match the original geometry for simplifying the CFD problem. For instance modeling small radius, small inclines for occurring mold, small holes or edges comparing with the whole geometry sizes causes the redundant cell number in the mesh. It is should be attained that implemented simplification for the computational domain doesn't have to be influenced the results of the problem.

In addition mesh density (the number of element of the mesh) should be good enough for the solution. For instance the mesh density is higher near the boundary of the computational domain comparing with the centre of the computational domain for calculated the boundary layer properties.

The selection of the physical phenomena such as natural convection or radiation or flow condition (laminar or turbulent) or analysis type (steady-state or transient) is huge importance step for the accuracy of the solution because assumptions for the physics of the computational domain are influenced of the results. Also selections or assumptions are should be based on the appropriate principles of the fluid mechanics and/or heat transfer.

Specification of the fluid properties such as density, dynamic viscosity, thermal conductivity or specific heat capacity are used for solution the governing equations. So specified values of those properties are very important. Those properties may sometimes be assumed constant and sometimes may be expressed by the function of the temperature or pressure.

Boundary conditions are required for the CFD problems. Those conditions may be specified with experimental study or appropriate assumptions.

2.2.1.2 Solver

Created mathematical model in the pre-processor is solved by the solver with usage one of the numerical methods. Solver is performed following steps (ANSYS CFX, Release 12.1, 2009):

- The partial differential equations are integrated over all the control volumes in the region of interest. This is equivalent to applying a basic conservation law (for example, for mass or momentum) to each control volume.
- These integral equations are converted to a system of algebraic equations by generating a set of approximations for the terms in the integral equations.
- The algebraic equations are solved iteratively.

An iterative approach is required because of the non-linear nature of the equations, and as the solution approaches the exact solution, it is said to converge. For each iteration, an error, or residual is reported as a measure of the overall conservation of the flow properties.

How close the final solution is to the exact solution depends on a number of factors, including the size and shape of the control volumes and the size of the final residuals. Complex physical processes, such as combustion and turbulence, are often modeled using empirical relationships. The approximations inherent in these models also contribute to differences between the CFD solution and the real flow (ANSYS CFX, Release 12.1, 2009).

Besides the residual the other importance factor is imbalance percent for understanding the accuracy of the solution. Basically this factor is implemented the conservation laws on the boundary surfaces and is given the how the fluid properties are conserved by the solver. For instance in energy imbalance is calculated by the sum of the heat fluxes all boundary surfaces in the no energy generation problems and if energy imbalance percent value is 0% or near the 0%, solver has made adequately iterations and calculation has been completed by the means of the

imbalance. So the accuracy of the solution is understood by residual and imbalance values. Generally residual values in this study should be near the 10^{-4} and imbalance ones should be near the ±5% for good results.

In the other hand the accuracy of the CFD solution has to be validated by experimental result. If validation is implemented for a problem, validation may not be required for the other same problems.

2.2.1.3 Post-Processor

CFD results are observed with several visualizing method or calculated several variables with specification the expression between results variables such as velocity components or temperature or pressure. Examples of some investigation techniques of post-processor are (ANSYS CFX, Release 12.1, 2009):

- Vector plots showing the direction and magnitude of the flow
- 2D or 3D stream lines showing
- Visualization of the variation of scalar variables (variables which have only magnitude, not direction, such as temperature, pressure and speed) through the domain (contour plots)
- Quantitative numerical calculations
- Animation
- Charts showing graphical plots of variables.

It should be attained that the scale of variables which are visualization has to be given with results. Otherwise given visualization results will not be meant anything.

2.3 Assumptions

2.3.1The CFD Domain

Domains are regions of space in which the equations of fluid flow or heat transfer are solved. Geometry of the domains may be two or three dimensional. Also they may consist of more than one body in three dimensional geometry or face in two dimensional geometry.

Two dimensional assumption decreases the solution time in the some cases which are change of the properties of fluid flow in two directions. If the case is opposite of this situation, the domain geometry has to be three dimensional.

In addition some CFD problems consist of more than one domain. Those domains may be different types that are fluid and solid or the same types that are fluid and fluid depend on the problem definitions. Those separate domains connect each other via domain interface. Also in some cases region of interest geometry may be divided two or more suitable domains for generating suitable mesh.

In this study the geometry of the domestic refrigerator domain is three dimensional. In some numerical simulations domain is unique fluid region. In some simulations this unique fluid region divided two parts, so two fluid domains were created for attaining the suitable mesh. Also in some simulations besides those fluid domains, solid domains were added.

2.3.2 Analysis Type

Analysis type represents the steady-state or transient assumptions. Basically steady-state analyses are used in fluid flow properties that do not change over time, while transient analyses are used in opposite situation.

In the transient analyses the time step factor which is affected the accuracy of the solution. The time step is specified according to the velocity and length scale of the problem. In natural convection problems the maximum time step (Δt_{max}) should be calculated follow equation by (ANSYS CFX, Release 12.1, 2009).

$$\nabla t_{max} \approx \sqrt{\frac{dl}{\beta g \Delta T}} \tag{2.31}$$

Where, “dl” is length of the vertical temperature gradient, “β” is thermal expansion coefficient of the fluid, “g” is the gravitational acceleration and “ΔT” is the temperature variation in the fluid. The setting time step value shouldn’t be greater than the calculated one via the equation (2.32) in natural convection dominated flows.

On the other hand for forced convection dominated flows, the time step (Δt) should be calculated follow equation by (ANSYS CFX, Release 12.1, 2009).

$$\nabla t \approx \frac{L}{U} \tag{2.32}$$

Where; "L" is the characteristic length and "U" is the velocity magnitude. For instance characteristic length may be height of the evaporator or domestic refrigerator and the velocity may be the mean of the velocity in whole fluid domain.

In addition the initialization properties values such as temperature or velocity are determined for the transient analyses. The best way of the determination the initialization is that firstly steady-state assumption is used and then the results of the steady-state simulation are used as initialization values.

In this study, first steady-state assumption has been implemented and then transient analysis has been carried out for comparing each other. Actually the domestic refrigerator is a transient problem because of the compressor on-off cycles. That cycle causes the fluctuations of the temperatures inside the domestic refrigerator. Since those fluctuations represent the equilibrium conditions inside the domestic refrigerator, the steady-state assumption may be suitable through using average fluid properties in the equilibrium conditions.

2.3.3 Incompressible Assumption

Incompressible flow is an approximation depends on the rate of change of the density value. That assumption is embedded by Çengel & Cimbala (2006) "… a flow is said to be incompressible if the density remains nearly constant" (p. 10). Also Çengel & Cimbala (2006) is determined that:

> The densities of liquids are essentially constant, and thus the flow of liquids is typically incompressible…. Gases, on the other hand, are highly compressible.
>
> …. the flow speed is often expressed in terms of the dimensionless **Mach number** defined as

$$\mathrm{Ma} = \frac{\mathrm{V}}{\mathrm{c}} = \frac{\text{Speed of flow}}{\text{Speed of sound}} \tag{2.33}$$

where *c* is the **speed of sound** whose value is 346 m/s in air at room temperature at sea level.

…. the level of variation in density in gas flows and the consequent level of approximation made when modeling gas flows as incompressible depends on the Mach number. Gas flows can often be approximated as incompressible if the density changes are under about 5 percent, which is usually the case when Ma<0.3. Therefore, the compressibility effects of air can be neglected at speeds under about 100 m/s (p. 10).

According the above conditions inner air flow for the domestic refrigerator assumes an incompressible flow because the inner air flow speed is never at 100 m/s. Therefore the density of the inner air may be considered a constant fluid property.

2.3.4 Natural (Free) Convection Modeling

Physical fundamental of the natural convection is defined as:

In free convection fluid motion is due to buoyancy forces within the fluid… Buoyancy is due to the combined presence of a fluid density gradient and a body force that is proportional to density. In practice, the body force is usually gravitational… There are also several ways in which a mass density gradient may arise in a fluid, but for the most common situation it is due to the presence of a temperature gradient. We know that the density of gases and liquids depends on temperature, generally decreasing (due to fluid expansion) with increasing temperature… (Incropera, DeWitt, Bergman, & Lavine, 2007, p. 560).

Since the density gradient is due to a temperature gradient and the body force is gravitational in the domestic refrigerator which investigated in this study, natural convection effect has been considered in numerical studies. Also some simulations in this study forced convection effect due to the fan has been added so both natural and forced convection effects that called as mixed convection effect has been investigated.

There are two assumptions which are Boussinesq and Full Buoyancy model for modeling natural convection effects. Both of two assumptions a source term is added to the momentum equations as follows for buoyancy calculations (ANSYS CFX, Release 12.1, 2009).

$$S_{M,buoy} = (\rho - \rho_{ref})g \tag{2.34}$$

Where "ρ" is the density of the fluid, "ρ_{ref}" is the reference density that is an approximate average value of the expected domain density, "g" is the gravity acceleration.

In "Full Buoyancy Model" fluid having density set as a function of pressure, temperature, or other field variables. Therefore density variation (ρ - ρ_{ref}) is evaluated directly. If variable variation such as pressure variation or temperature variation is more in the domain that assumption should be used.

In "Boussinesq Model", fluid density is assumed constant whole domain. So density variations (ρ - ρ_{ref}) calculated as follows.

$$\rho - \rho_{ref} = -\rho_{ref}\beta(T - T_{ref}) \tag{2.35}$$

Where "β" is the thermal expansion coefficient, "T" is the calculated temperature and "T_{ref}" is the buoyancy reference temperature that is an approximate average value of the expected domain temperature. That model should be used if the density variation is driven only by small temperature variations.

In this study Boussinesq model assumption has been used for numerical studies because the temperature variation is approximately expected 7 - 8 C in whole domain.

2.3.5 Flow Condition

Flow condition represents the laminar or turbulent flow. Generally flow condition is specified by Rayleigh and Reynolds numbers respectively for natural and force convection driven problems. Rayleigh number calculates as follow equation (Incropera, DeWitt, Bergman, & Lavine, 2007).

$$Ra = \frac{g\beta\Delta TL^3}{\nu\alpha} \tag{2.36}$$

Where "ν" is the kinematic viscosity of the fluid and "α" is the thermal diffusivity of the fluid. On the other hand the Reynolds number calculates as follow equation (Incropera, DeWitt, Bergman, & Lavine, 2007).

$$Re = \frac{UL}{\nu} \tag{2.37}$$

The critical values of those dimensionless numbers are determined for several situations. For example the critical Rayleigh number is equal to 10^9 for flow over a vertical plate although the critical Reynolds number is equal to $5x10^5$ for parallel flow over a flat plate (Incropera, DeWitt, Bergman, & Lavine, 2007). If calculated dimensionless number is less than the critic value the flow assumes laminar flow. The opposite cases flow assumes turbulent flow.

The Navier-Stokes equations is described both laminar and turbulent flows (Çengel & Cimbala, 2006, chap. 15). However since turbulence causes three dimensional, unsteady flow field the mesh has to be fine enough to resolve the flow properties. Therefore the solution of the turbulent flows requires computational power due to the prohibitively fine mesh. Instead of this, several turbulence model approximations which can be solved with applicable mesh have been developed for turbulent flows. Those assumptions generate additional equations which have to be solved along with Navier-Stokes equations. Also it should be noted that since most turbulence models are statistical approximation, those models cannot be suitable for each CFD problem.

In this study some numerical simulations, the turbulent flow has occurred. For these simulations, suitable turbulence model was specified by the trial. Then result of the trial model was comparing with experimental results. Thus the most suitable turbulence model assumption has been selected for the domestic refrigerators.

2.3.6 Radiation Modeling

In some CFD problems, radiation is a significant. Not considered radiant heat transfer causes the erroneous results in these situations. Hence several radiation models have been developed for solving the radiant heat transfer in CFD problems.

Thermal radiation is associated that "… the rate at which energy is emitted by matter as a result of its finite temperature" by Incropera, DeWitt, Bergman, & Lavine (2007) (p. 724). Also it emphasized that although thermal radiation is a volumetric phenomena, it may be considered a surface phenomena in most situation. In addition it described that the emitted thermal radiation on a surface is a function of the wavelength (spectral model) and directionality.

Radiant heat transfer should be considered if there is a temperature difference between the surfaces which are looked each other. This heat transfer depends on surface geometries, its orientations, temperatures and radiation properties which are emission, absorption, reflection and transmission (Incropera, DeWitt, Bergman, & Lavine, 2007, chap. 12-13).

A source term which is called as radiation transport equation is required to be added in the energy equation to solve radiant heat transfer. The radiation transport equation includes ray tracing terms. Those terms represent the directional distribution of the radiation with specification the path. Since the generation of the ray path requires more computational time and power it is a complicated process and inherently calculation process of the thermal radiation is too. Otherwise thermal radiation models which accomplish that complicated are good approximation. The most used thermal radiation models are "Discrete Transfer" and "Monte Carlo".

In this study since the temperature difference between the inner walls of the domestic refrigerator expected above 10 C the radiant heat transfer is taken into account. For that purpose "Discrete Transfer" model was used for directional approximation and "Gray Surface" assumption was made for spectral approximation. Also volumetric emission, absorption and reflection were neglected so the radiation

transfers only surface to surface. Also the walls where are the domain boundary assumed opaque which represents only the emission and absorption.

2.4 Boundary Conditions

Boundary conditions which apply on the all boundary surfaces of the computational domain, require for the defining the flow problem. Solution of the CFD problems depends on the applied boundary condition. If a fluid domain boundary interacts with a fluid, the inlet, outlet or opening type boundary conditions may be used. If the fluid or solid domain boundary interacts with a solid, the wall boundary conditions which are includes several types may be used. For instance in Figure 2.6 has been shown some boundary conditions which is used for a fluid domain boundary surfaces. Basically the inlet represents the fluid flow into the domain, the outlet is fluid flow outside the domain, the opening is fluid flow the both into and outside the domain and the wall is the stationary or sliding and adiabatic or transferred heat.

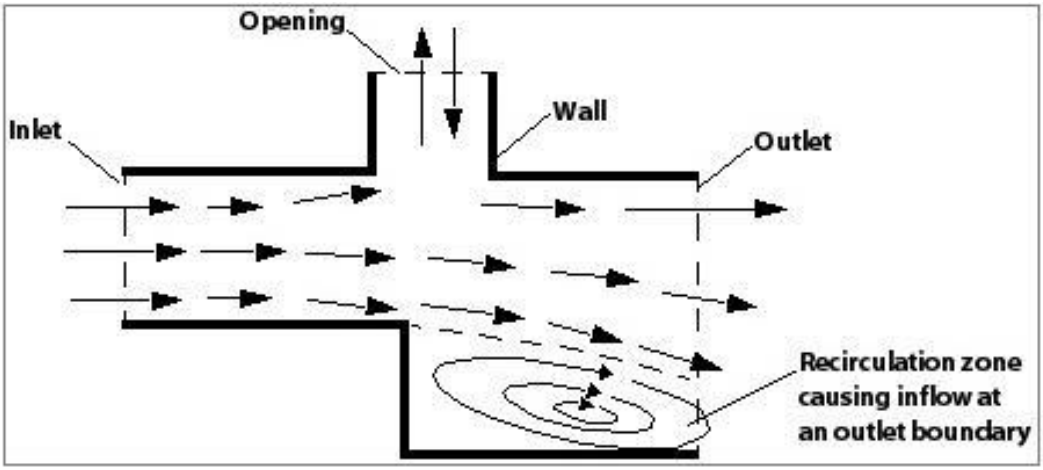

Figure 2.6 Boundary conditions for fluid domain (ANSYS CFX, Release 12.1, 2009)

In this section some boundary conditions which have been used in this study has been described follow.

2.4.1 The Wall

Walls are solid boundaries of fluid flow. This boundary condition allows to modeling heat transfer via solid conduction. For that purposes the “Fixed

Temperature", "Heat Transfer Coefficient" and "Adiabatic" types are used for modeling heat transfer.

Also it allows to moving the boundary surface. For that purposes several slip condition types are included. In this study all wall boundary condition is stationary so the wall velocity is zero which is called as no-slip wall.

2.4.1.1Fixed Temperature

The boundary surface temperature assumes constant at as specified temperature during the analysis in the fixed temperature boundary conditions. The heat flux into the domain is calculated from the temperature gradient at the wall with usage fixed temperature. Further specified temperature may be a single value or the distribution of the values.

In this study the fixed boundary condition was used to modeling the evaporator surface in investigated domestic refrigerator. The specified temperature was determined by the experimental study. So the heat transfer between the inner air and the evaporator was calculated.

2.4.1.2 Heat Transfer Coefficient

"Heat Transfer Coefficient" is the modeling the heat transfer via solid conduction by the help of the thermal resistance. The solid conduction is modeled with specifying "heat transfer coefficient" outside the computational domain and "outside temperature". Therefore solid domains are not required the added CFD problems. For instance the solid domain in the Figure 2.7 is represented by the specifying the heat transfer coefficient (h_c) and outside temperature (T_o). In the Figure 2.7 "q_w" represents the heat flux via solid domain, "T_w" is the calculated wall boundary temperature, "q_{cond}" is occurred heat transfer via fluid conduction in the fluid domain and "q_{rad}" is occurred heat transfer via radiation in the fluid domain.

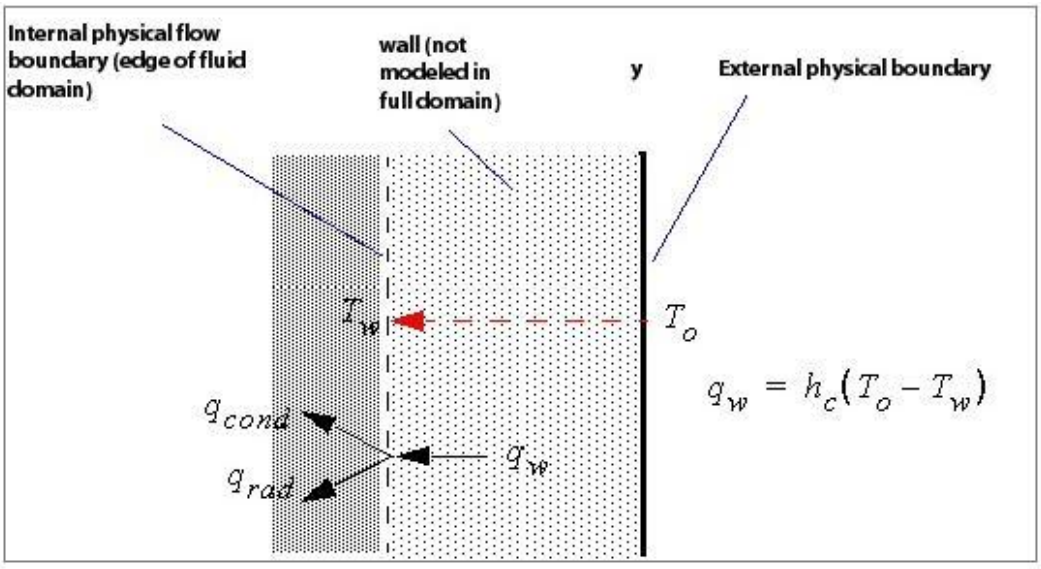

Figure 2.7 Heat transfer coefficient boundary conditions (ANSYS CFX, Release 12.1, 2009)

In this study occurred heat transfer via insulated cabinet was modeled by the help of this boundary condition. For that purposed thermal solid resistance ($R_{t,cond}$) was calculated for specified the heat transfer coefficient by the follow equation (Incropera, DeWitt, Bergman, & Lavine, 2007, chap. 3).

$$R_{t,cond} = \frac{L}{kA} \tag{2.38}$$

Where "L" is the cabinet layer thickness, "k" is the cabinet layer thermal conductivity and "A" is the area of the cabinet wall. Then the heat transfer coefficient was calculated by the follow equation (Incropera, DeWitt, Bergman, & Lavine, 2007, chap. 3).

$$U = \frac{1}{R_{t,tot}} \tag{2.39}$$

Where "U" is the heat transfer coefficient and "$R_{t,tot}$" is the total thermal resistance. The total thermal resistance is calculated by the help of the convection resistance terms, radiation resistance terms and conduction resistance terms. However in this study radiation heat transfer between the outer surface of the cabinet wall and environment wall was neglected because of the small temperature difference between each other. Also the convection heat transfer between the outer surface of the cabinet

wall and the environment air was not accounted because of the known outer surface temperature of the cabinet wall.

Therefore the total thermal resistance was equaled to the total conduction resistance which is calculated by the insulated cabinet layers thermal resistances. However since the thickness of the sheet metal (0.5 mm) and the inner plastic (1.5 mm) is too small comparing with the insulation material thickness (40 - 80 mm) only the thermal resistance of the insulation material was calculated. So the total conduction resistance was equaled to insulation material thermal resistance. Since the thicknesses of the insulation material were various depend on the insulated cabinet wall direction in investigated domestic refrigerator, various heat transfer coefficient was calculated. The calculated heat transfer coefficients with polyurethane foam have shown in Table 2.2.

Table 2.2 The heat transfer coefficient for investigated domestic refrigerator

Insulated Cabinet Wall Position	**Heat Transfer Coefficient [W/m^2 K]**
Top Wall	353.745x10^{-3}
Back Wall	331.210 x10^{-3}
Horizontal Wall Near the Compressor Cavity	416 x10^{-3}
Vertical Inclined Wall Near the Compressor Cavity	327.044 x10^{-3}
Bottom Wall	419.355 x10^{-3}
The Door	619.0476 x10^{-3}
Side (Left and Right) Walls	465.95 x10^{-3}

The outside temperature represents the outer surface temperature of the insulated cabinet in this study. The outer surface temperatures were specified by the experimental study (see sec. 3.2.1).

2.4.1.3 Adiabatic

The “Adiabatic” boundary condition represents that the heat flux is zero across the wall boundary. That mean is insulated wall. This boundary condition is used at the boundary which is the heat transfer is too small to negligible comparing with the other wall boundaries.

In this study adiabatic wall was used on the outer surfaces which have small area comparing with the whole wall.

2.4.2 Inlet and Outlet

Inlet boundary condition is used where the fluid is flowed dominantly into domain from boundary. Fluid flow direction on the boundary may be specified several ways which are normal to boundary or depend on the cartesian components or depend on the cylindrical components. Further the inlet velocity value may be specified as speed or mass flow rate. Also velocity value may be specified as a function of the any other variables. In addition pressure magnitude may be specified too for calculation the velocity.

Furthermore in heat transfer problems, the inlet fluid flow temperature has to be specified.

Outlet boundary condition is used where the fluid is flowed dominantly out to the domain from boundary. Generally outlet boundary condition is used with inlet boundary condition to ensure the mass conservation. As inlet boundary condition velocity value and direction are specified at the outlet boundary. In contrast to the inlet boundary condition any specified value relation to the heat transfer don’t need to be determination.

In this study inlet and outlet boundary conditions has been used for modeling the fan effects inherently mixed convection effects. For that purpose inlet velocity speed which has been determined by experimental study (see sec. 3.2.3) has been specified normal to the boundary. The inlet temperature has been specified as the average temperature at the outlet boundary. And the outlet boundary condition has been specified pressure value which is zero relative pressure and which may be called as free out flow.

CHAPTER THREE

EXPERIMENTAL STUDY

The aims of the experimental studies were the specification of the boundary conditions and the validation of the numerical studies. For those purposes five experiments were implemented. These experiments are:

1. Inner and outer surface temperature measurements.
2. The inner plastic emissivity measurement.
3. Velocity measurement at the fan box grilles.
4. Inner air temperature measurements for low thermostat stage.
5. Inner air temperature measurements for high thermostat stage.

Experiments number one, two and three were carried out for the specification of the boundary conditions, while the experiments four and five were for the validation of the numerical studies.

All the experimental studies were implemented on the same domestic refrigerator model which called as “Model 395” and is manufactured by the “VESTEL White Good Company”.

In addition, all experiments were carried out in a controlled room which was made by the “Angelantoni Industrie”. The accuracy of the controlled room for the temperature and relative humidity setting are ±0.1 C and 0.5%, respectively. The controlled room conditions were set to the same temperature (25 C) and the relative humidity (50%) for the all experiments.

3.1 Materials

3.1.1 Domestic Refrigerator (Model 395)

The Model 395 is a single compartment - forced convection driven - brewed type (static with fan) domestic refrigerator. Its inner dimensions are 1.7m x 0.48m x 0.45m (Height x Width x Depth). The net inside volume is 350 l. The evaporator is a

flat plate type and located under the back wall and its area is 44.5 x 91cm^2 (W x H). The condenser is a wire-on-tube type and is located on the outer surface of the back wall. The isometric transparent view of the domestic refrigerator is shown in Figure 3.1.a.

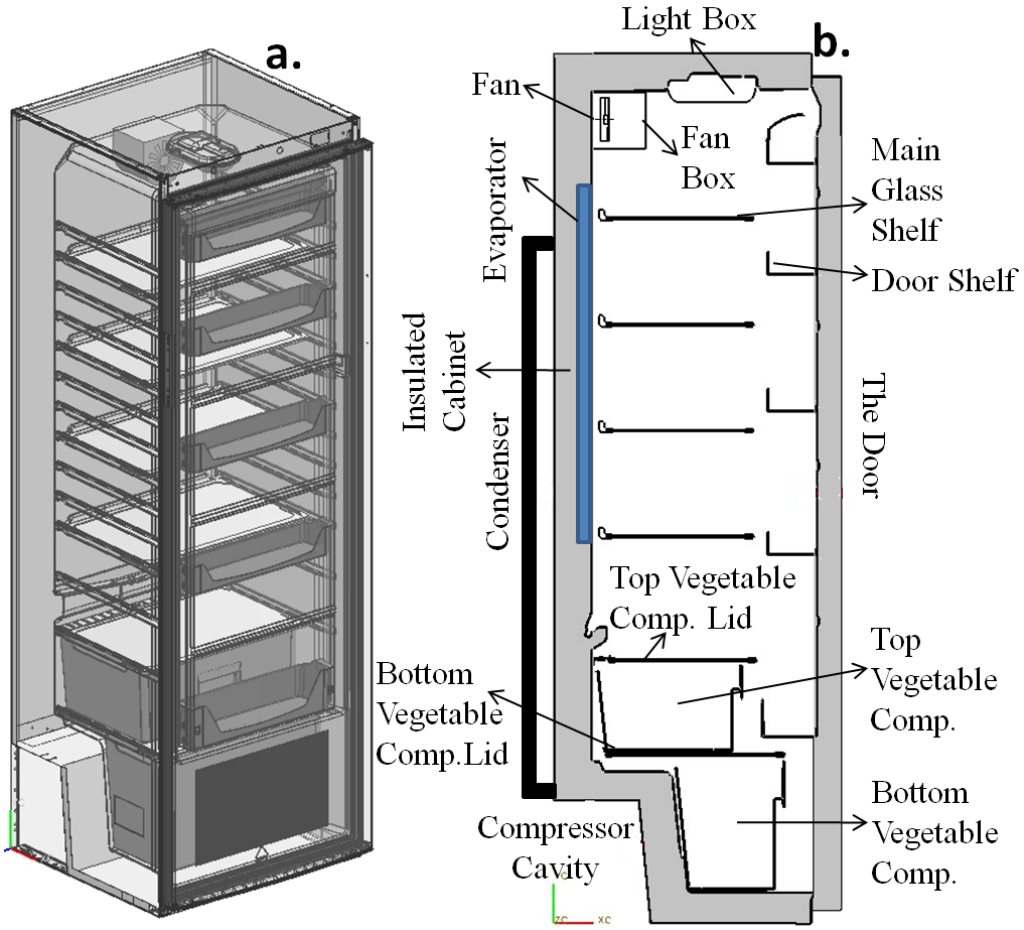

Figure 3.1 The investigated domestic refrigerator (Model 395) a. Isometric View b. Cross section view

The insulated cabinet consists of 1.5 mm inner plastic which is High Impact Polystyrene (HIPS), various thickness insulation materials that is Polyurethane foam and 0.5 mm sheet metal from inside to outside.

The domestic refrigerator has a single door with only a fresh-food compartment. Also it consists of four main glass shelves, five door shelves, two vegetable compartment baskets and their glass lids, a fan box and a propeller fan and a light box. The main glass shelves arrangement that is adjustable by the customers and the

other parts arrangement that is not adjustable are schematically shown in Figure 3.1.b.

In the literature reviews, some inner design parameters were determined which are the gap between the main shelves and the back wall (t_b), the gap between the main shelves and the door shelves (t_f). Dimensions of those parameters and also the gaps between the main shelves (t_s and t_{s-1}) and the fan location parameter (t_{fan}) have been specified in Table 3.1 and shown in Figure 3.2.

Table 3.1 Values of the inner design parameters

Parameter	t_b [mm]	t_f [mm]	t_s [mm]	t_{s-1} [mm]	t_{fan} [mm]
Value	15	32	218	256	239

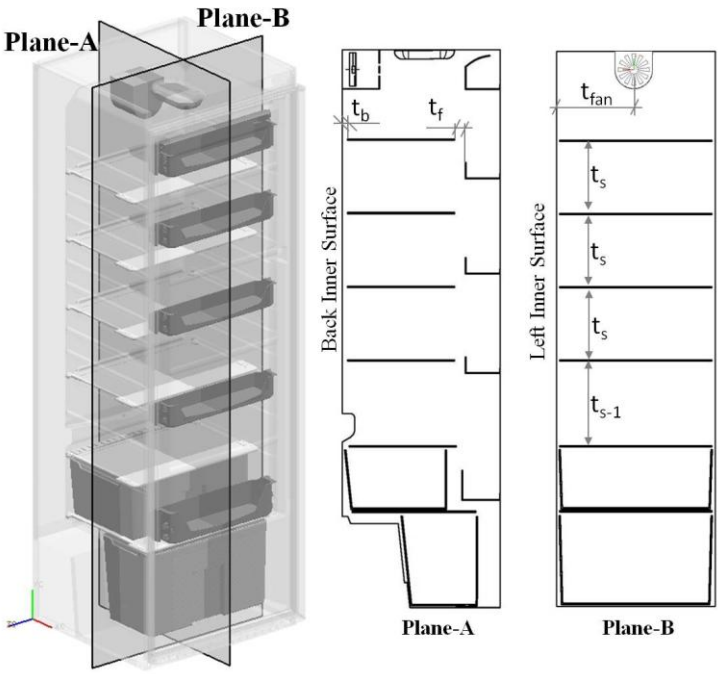

Figure 3.2 Inner design parameters

3.1.2 Experiment Devices

3.1.2.1 Thermocouple and Auxiliary Devices

T and K type thermocouples were used for measuring the temperature. The control of the instrumentation problems was tested by usage a cup of water. All calibrated thermocouples were placed in the cup and controlled by reading the temperatures in terms of the observation of the same values.

Copper support rods (Figure 3.13 and Figure 3.14) were used for placing the thermocouples for measuring the air temperature at the desired locations inside the domestic refrigerator. On the other hand the strong tape was used on the surfaces to fix the thermocouples. Also the taped thermocouples were wrapped with the thermal paste to ensure proper reading of the surface temperatures. Furthermore, thermal paste was used for covering the gaps at the surface of the door junction which were caused by the outgoing thermocouple wires to the data logger.

3.1.2.2 Thermo-Anemometer

In the velocity measurement experiment, Ahlborn FVA935-TH4 model thermo-anemometer was used for measuring the inlet velocities from discharge grilles at the bottom of the fan box. That device is a hot-wire type (Figure 3.3) and measures the air velocity by the following principle:

> An electrical current is increasing the temperature of a resistor on the substrate. The flowing air causes a reduction of this temperature. The cooling effect is directly proportional to the mass flow and consequently to the air velocity and inversely proportional to the air temperature. At equilibrium, the temperature of the sensor's surface is the measure for mass flow (ALMEMO Manual, 2009, chap.3.5.2).

Figure 3.3 Ahlborn FVA935-TH4 hot-wire anemometer

3.1.2.3 Thermal Camera and Auxiliary Devices

In the emissivity measurement experiments, Flir SC325 model thermal camera was used for determination the emissivity of the inner plastic. Also Omega KHR-3/10 model flexible heater was used for ensuring the fixed temperature on the surface of interest which is the thermal view area. And also a variable autotransformer

(variac) was used to attain the desired temperature through the flexible heater by the help of adjusting the voltage.

3.1.2.4 Data Acquisition Systems

In the experiments which are the inner and outer surface temperature measurements, velocity measurements and inner air measurements for low thermostat stage "ALMEMO 5690-2M" which includes two data acquisition module and a total of eighteen channels was used as the data acquisition system. Also the "AMR-Control" software was used for the data analysis.

In the inner air temperature measurements for high thermostat stage experiment, controlled room data acquisition system which includes thirty one channels for thermocouple connection was used as the data acquisition system. Also the "LabVIEW 8.5.1" software was used for the data analysis.

All thorough these experiments both two data analysis software were set to the recording the data at 1 s. interval. In the other hand, in the emissivity measurement experiment, "FlirSystem ThermaCAM Researcher Pro 2.9" software was used to record and analyze the thermal view.

3.2 Experiments for Determining the Boundary Conditions

3.2.1 Inner and Outer Surface Temperature Measurements

Twelve T and K type thermocouples were used in this experiment. Six thermocouples were placed around the middle points of the inner and outer surfaces of the left wall, top wall and the door. One thermocouple was placed at the middle point of the outer surface of the back wall (near the condenser). One thermocouple was placed on the vertical inclined outer surface which is located near the compressor cavity. Three thermocouples were placed on the symmetry line of the evaporator surface. Arrangement of those thermocouples has been schematically shown in Figure 3.4. Additionally, one thermocouple was placed around the middle point of the inner volume.

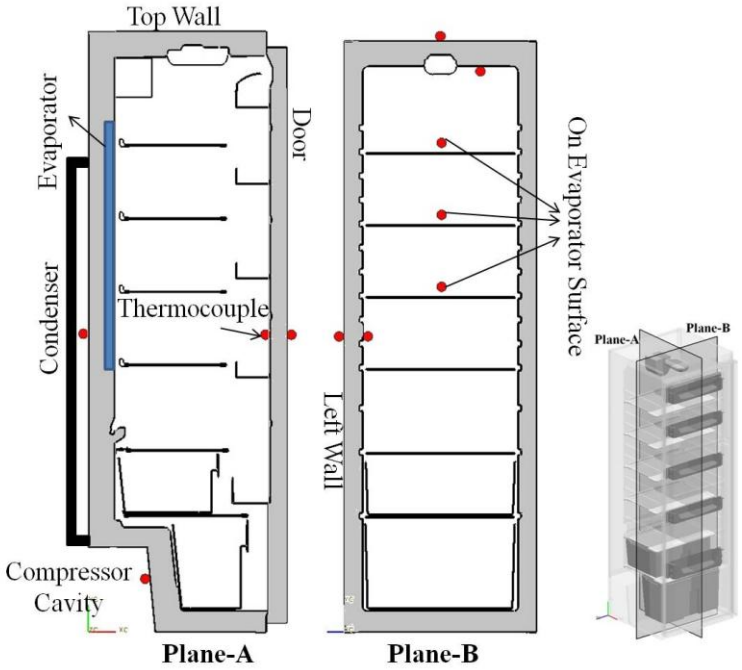

Figure 3.4 Arrangement of thermocouples on the inner and outer surfaces

The experiment was started when the inner and outer air were thermal equilibrium. And also all recorded temperatures were obtained for fourth thermostat stage. It should be noted that there are five thermostat stages and the higher the stage the lower the temperatures. In addition the propeller fan was taken out from the domestic refrigerator so the experiment was carried out without fan.

An example of the recorded data is shown in Figure 3.5. This figure shows the temperature - time curves for the thermocouples on the evaporator surface. The x-axis represents the date and time. Initially the recorded temperatures were at 25 C and then the recorded temperatures decreased. After a certain time the temperatures began to fluctuate in the range of -18 C and 8 C depending on the compressor's on-off cycle. This fluctuation was observed at all measured temperatures in different temperature ranges.

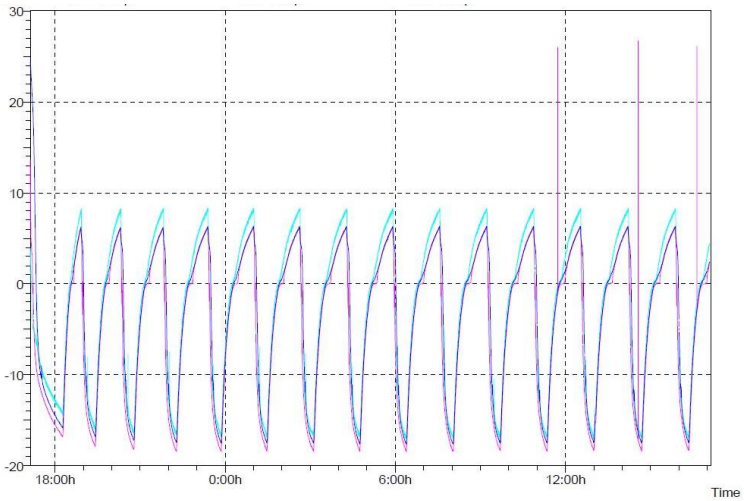

Figure 3.5 Recorded evaporator surface temperatures with respect to time

This fluctuation represents that the equilibrium state is reached for the domestic refrigerator. The data which were recorded over the 24 h at the equilibrium state were considered. The time averaged values of the recorded data for each thermocouple were used to determine boundary conditions.

The calculated time averaged temperatures of each thermocouple on the outer surfaces are considered as representing the corresponding outer wall surface temperature. Measured temperature on the outer left wall is assumed to represent both left and right outer surface temperatures. Temperature on the vertical inclined outer surface which is located near the compressor cavity represented the whole outer surface temperature around the compressor cavity. Also time and arithmetic averaged temperature of the three thermocouples on the evaporator surface is considered as the evaporator temperature. All above average temperatures have been used as boundary conditions and shown in Table 3.2 and Table 3.3

Table 3.2 Measured temperatures on the outer surfaces

Thermocouple Position	**Representation Surfaces**	**Time Average Temperature [C]**
Top Wall	Top Wall	25.09
Left Wall	Left and Right Wall	24.9
The Door	The Door	24.82
Back Wall	Back Wall	25.47
Vertical Inclined Wall Near the Compressor Cavity	Around the Compressor Cavity	26.01

Table 3.2 shows that the outer surface temperatures are close to 25 C which is the set temperature of the controlled room. Also the maximum temperature is observed on the inclined vertical surface of the compressor cavity. That situation is due to the presence of the compressor and the cavity.

Table 3.3 Measured evaporator surface temperature at fourth thermostat stage without fan experiment

Thermocouple Position	**Time Average Temperature [C]**	**Arithmetic Average Temperature [C]**
Top	-2.46	-3.16
Middle	-4.02	
Bottom	-3.02	

Table 3.3 shows that the evaporator average temperature is -3.16 C which has been used as boundary conditions in the numerical studies. Also in the numerical studies, this evaporator temperature is represented at the fourth thermostat stage.

In addition the measured temperature from the thermocouple which is placed at the middle point of the inner volume was used for specifying the thermo-physical properties of the inner air. The time averaged temperature and thermo-physical properties of the inner air are shown in Table 3.4.

Table 3.4 Measured temperature and thermo-physical properties of the inner air

Time Average Temperature [C]	**Density [kg/m^3]**	**Specific Heat [J/kgK]**	**Dynamic Viscosity [Ns/m^2]**	**Thermal Conductivity [W/mK]**	**Thermal Expansion Coefficient [1/K]**
3.768	1.269	1006.538	1.73×10^{-5}	24.453×10^{-3}	361.117×10^{-5}

Furthermore measured temperatures of the inner surfaces have been used for the validation of the numerical studies. Those average temperatures are shown in Table 3.5.

Table 3.5 Measured temperatures on the inner surfaces at fourth thermostat stage without fan case

Thermocouple Position	**Time Average Temperature [C]**
Top Wall	10.99
Left Wall	5.89
The Door	5.92

3.2.2 Inner Plastic Emissivity Measurement

Emissivity is a surface radiative property and defined as "… the ratio of the radiation emitted by the surface to the radiation emitted by a blackbody at the same temperature" by Incropera, DeWitt, Bergman, & Lavine (2007) (p. 744). Therefore the emissivity is the most important parameter for radiation modeling in the numerical studies.

Generally the emissivity depends on the material, surface temperature and surface characteristic such as coat, paint or method of fabrication. Since the emissivity depends on several factors, the emissivity measurement was implemented for the accuracy of the numerical studies.

For the determination of the emissivity of the inner plastic surface, a thermal camera was used. Thermal camera senses the emitted infrared radiation from an object. The dependent parameters for the radiation measurements were embedded that "… radiation is a function of object surface temperature makes it possible for the camera to calculate and display this temperature… also is a function of the emissivity" by Flir Systems (2010) (p. 55). So the emissivity is used for calculating the object temperature from the measured radiation energy. Therefore to find the emissivity, the following steps which were suggested by Flir Systems (2010) were carried out. The experimental set up has been schematically shown in Figure 3.6.

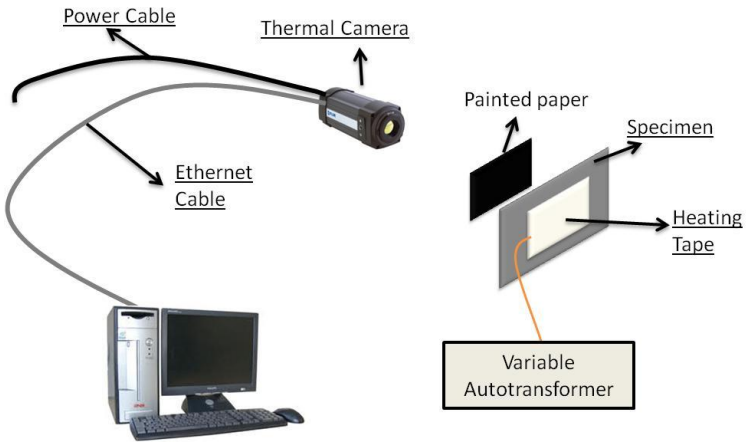

Figure 3.6 Set-up of emissivity measurement

1. A specimen is coated with a known high emissivity material. For that purpose a paper was coated with oil-black flat paint. The emissivity of oil-black flat paint was specified as 0.94 by Paljak & Peterson (1972) cited by Flir Systems (2010). Then the painted paper was put on the one side of the specimen of the inner plastic (Figure 3.7.b). This step's aim is to obtain a radiation emission for the surface as closer as a black body emission. Thus, emitted radiation is measured by the camera with a slight influence from the reflected radiation due to the presence of the other objects and emitted radiation due to the other objects.
2. The specimen should be heated at least 20̊ above from the room temperature. For that purpose Omega KHR-3/10 model flexible heater was put on the other side of the specimen (Figure 3.7.a). Then the temperature was set through adjusting the voltage of the heater via variable autotransformer. The aim of this step is to reduce the reflected radiation effect on the specimen surface due to the other object.
3. The thermal view of the specimen is taken by the thermal camera. Then temperature of the specimen surface is calculated via adjust emissivity. For that purposes FlirSystem ThermaCAM Researcher Pro 2.9 software was used. First the thermal view of the painted paper side of the specimen was taken and then the temperature of the surface was calculated with oil-black flat emissivity (0.94). Then the average temperature was calculated as 59.2 C in a circular area on the thermal view (Figure 3.8.a).
4. The step-3 is repeated without painted paper (Figure 3.7.c). Then the emissivity changes until the same temperature is calculated with calculated temperature from step-3. For that purpose the painted paper was put off and then thermal view was taken without change the camera view field (Figure 3.8.b). Then the same circular area in the step-3 was created and the same average temperature was calculated via the emissivity change way. Therefore the emissivity of the specimen of the inner plastic was found as 0.971.

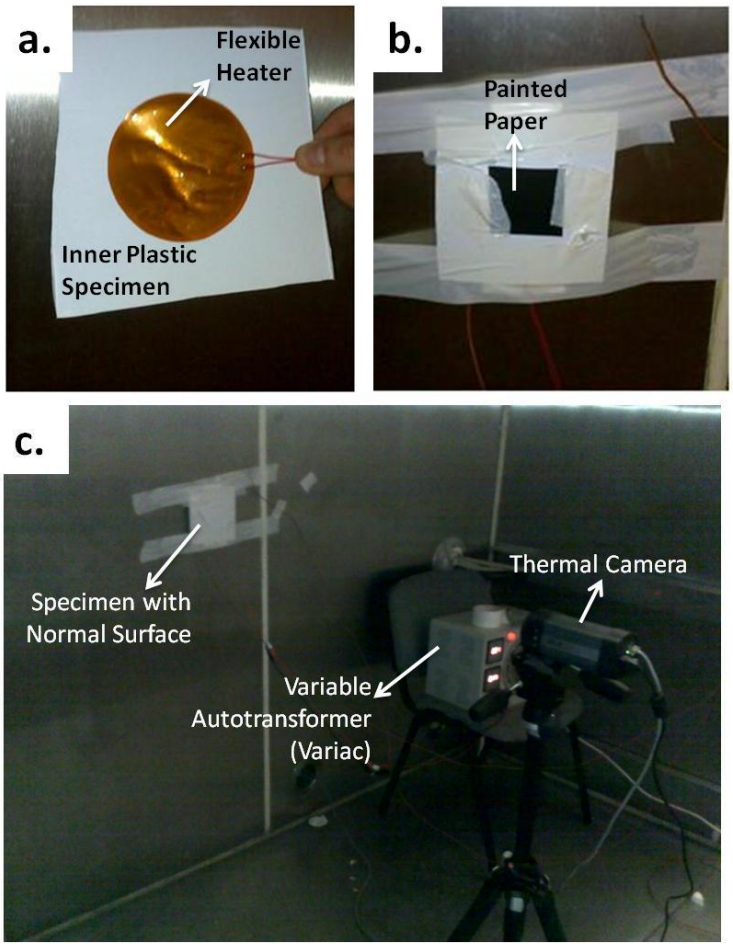

Figure 3.7 Steps of emissivity measurement set-up: (a) Placement the flexible heater, (b) Placement the painted paper, (c) Taking the thermal view

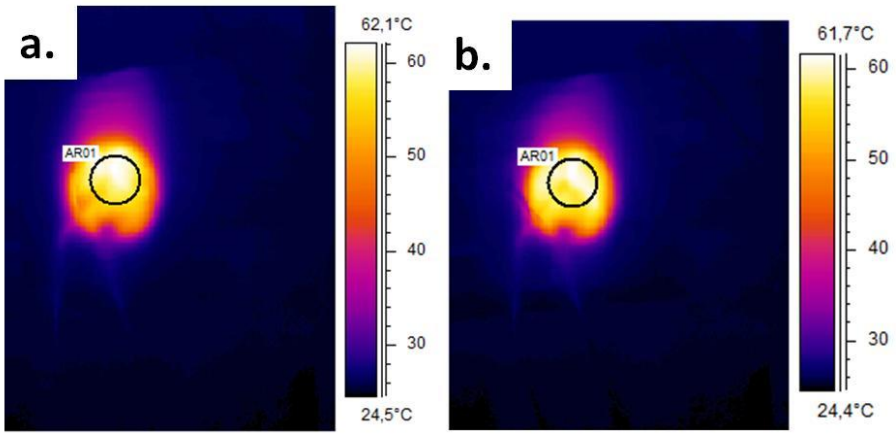

Figure 3.8 Thermal camera views: (a) Specimen with painted paper surface (b) Specimen with normal surface

The calculated minimum, maximum and average temperatures in the circular area have shown in Table 3.6. Table shows that the maximum temperature difference was observed between the minimum temperatures of the circular area. Maybe that situation caused by slightly change view field. Otherwise the other temperatures are in good agreement.

Table 3.6 Calculated temperature and emissivity by thermal camera

Surface Type	**Emissivity**	**Minimum Temperature [C]**	**Maximum Temperature [C]**	**Average Temperature [C]**
Painted	0.94	54.3	62.3	59.2
Normal	0.971	56.1	62	59.2

3.2.3 Velocity Measurement

Velocity measurement was implemented for modeling the fan effects in the numerical simulation. For that purpose an anemometer which is hot-wire or hot film type was used at discharge grilles where is at bottom of the fan box and shown in Figure 3.9. The fan box, propeller fan and grilles have shown in Figure 3.10.a. The fan is pulled the air from the suction grilles and blew from the discharge grilles on the evaporator surface (Figure 3.10.b).

It should be noted that air flow has to be parallel to the sensor surface for measure correctly. For ensure that note the sensor was circulated around the each grilles and then the recorded maximum data were used as boundary conditions and shown in Table 3.7.

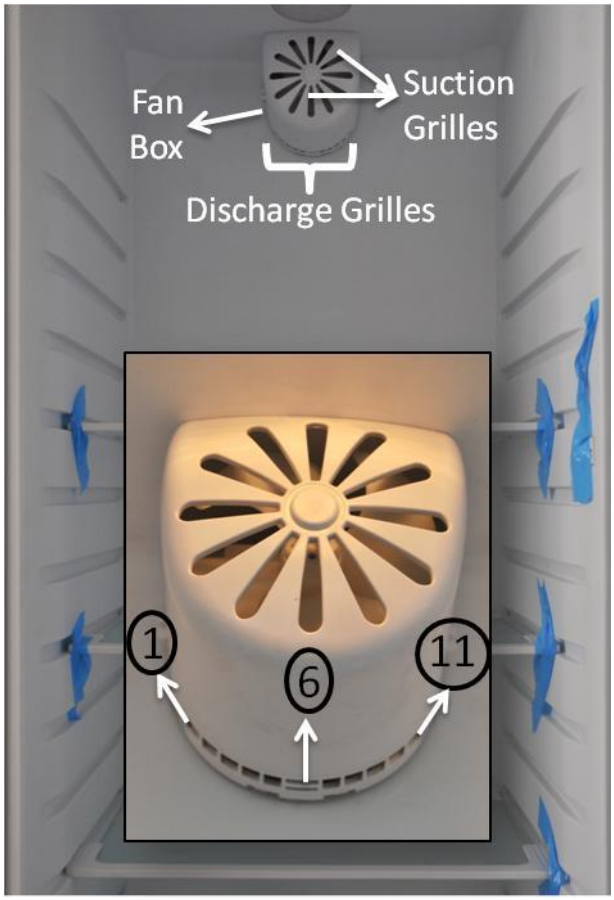

Figure 3.9 The fan box and its grilles positions

Table 3.7 The measured velocity at the each discharge grilles

Discharge Grille No	**Velocity [m/s]**
The Left Port - 1	4,35
2	4,6
3	4,68
4	4,35
5	4
The Middle Port - 6	3
7	3,47
8	3,58
9	3,2
10	2,84
The Right Port - 11	2,8

Discharge grilles were numbered 1 to 11 from left to right (Figure 3.9). Also Table 3.7 shows that the velocity gets slower from the left to right grille. Therefore the non-uniform inlet airflow was observed from discharge grilles.

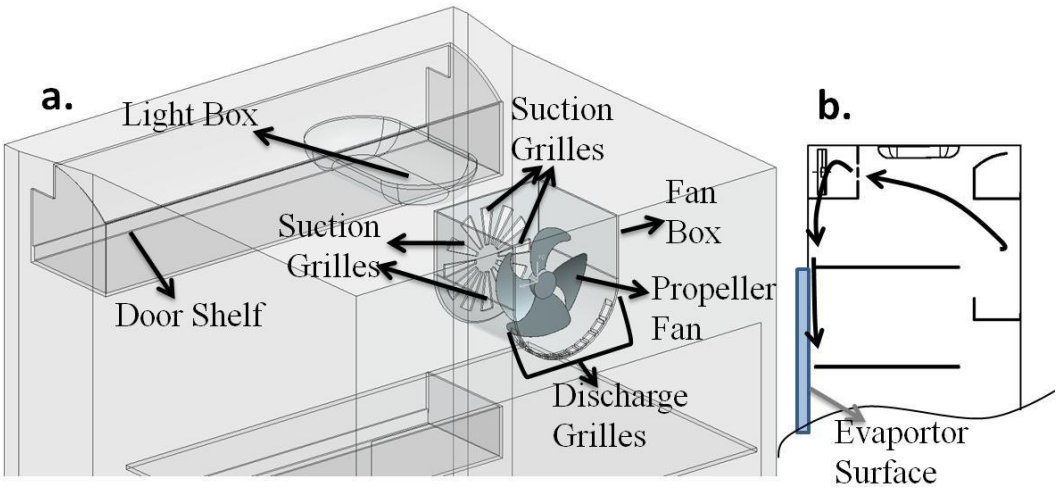

Figure 3.10 (a) The fan and fan box location, (b) Flow principle of the fan

3.3 Experiments for the Validation of the Numerical Results

3.3.1 Inner Air Temperature Measurements for Low Thermostat Stage

That experimental study's aim is the obtainment of inner air temperatures to validate the numerical studies. For that purposes two different experiments were implemented to investigation of mixed convection effects. The difference of the experiments is the presence of the fan. The propeller fan was included in the one experiment (with fan) while the other one was not (without fan). The all other conditions were the same both two experiments. Also the thermostat setting was adjusted the fourth stage so the average evaporator temperature is -3.16 C (see sec. 3.2.1).

In both experiments twelve thermocouples were used. Arrangement of those thermocouples is shown in Figure 3.11. The abbreviations in Figure 3.11 are explained in Table 3.8. Some thermocouples were attached on the support rod. Five thermocouples were placed on the middle point of the each shelf (170 mm away from the back wall) and 110 mm above from the each shelf on the Plane-A and numbered as "0". Other five thermocouples were placed on plane which situated at

125 mm right side from the Plane-A and numbered as “1”. Also a thermocouple was placed around the middle points of each vegetable compartment.

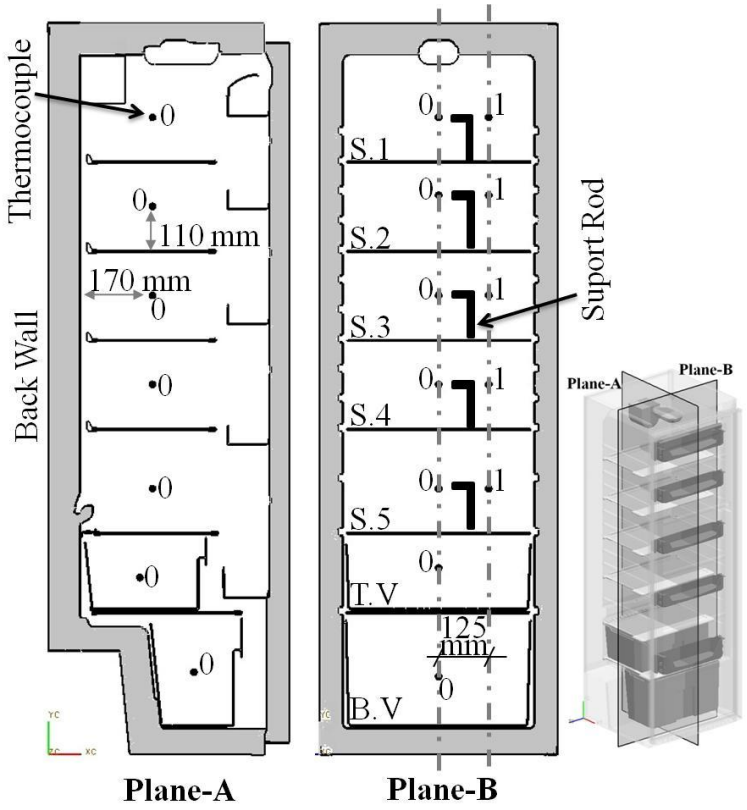

Figure 3.11 Arrangement of thermocouples at fourth thermostat stage experiments

As emphasized in section 3.2.1 that the data which were recorded over the 24 h at the equilibrium state were considered. The time average temperatures of each thermocouple have shown in Table 3.8 both with fan and without fan experiments.

Table 3.8 shows that the following results:

- Temperatures at the same shelf such as temperatures of the S.1-0 and S.1-1 are almost same value at both two experiments. This situation shows that there are uniform temperatures at each shelf.
- Also the maximum air temperature was observed at the bottom vegetable compartment and the top vegetable compartment temperature was lower than the bottom vegetable compartment both two experiments. Also temperatures of the vegetable compartments were not affected with the presence of the fan.

Table 3.8 Measured inner air temperatures at fourth thermostat stage experiments

Thermocouple Position		Time Average Temperature [C]	
		Without Fan	**With Fan**
Shelf-1 (S.1)	S.1-0	9.21	5.42
	S.1-1	9.31	5.59
Shelf-2 (S.2)	S.2-0	5.99	3.5
	S.2-1	5.76	3.3
Shelf-3 (S.3)	S.3-0	4.51	2.39
	S.3-1	4.62	2.54
Shelf-4 (S.4)	S.4-0	4.32	2.66
	S.4-1	4.31	2.74
Shelf-5 (S.5)	S.5-0	4.43	3.73
	S.5-1	4.45	3.86
Top Vegetable Compartment (T.V-0)		6.864	6.427
Bottom Vegetable Compartment (B.V-0)		9.4	8.81

- Fan affected the above of the vegetable compartments which is the fresh-food cabinet. Temperatures especially at the shelf-1 were decreased with fan. The maximum temperature decreasing is ~4 C at the top section. That situation is showed the improvement effect of the fan inherently mixed convection. Also the fan effect gets reducing from top to bottom region. Also it is showed that the top region of the domestic refrigerator is the most affected region from the fan inherently mixed convection.
- The uniformity at the fresh-food cabinet was improved with fan. The temperature difference between the top (S.1-0) and bottom (S.5-0) thermocouples decreased from 4.68 to 1.69 with fan. That situation shows that the thermal uniformity is improved by mixed convection effects.

3.3.2 Inner Air Temperature Measurements for High Thermostat Stage

This experimental study's aim is the same as the previous experimental study (see sec. 3.3.1). The differences of this experiment are the number of thermocouples (thirty one thermocouples) and the thermostat stage (fifth stage). As the previous experimental study, two experiments which were without and with fan cases were carried out in this experimental study too.

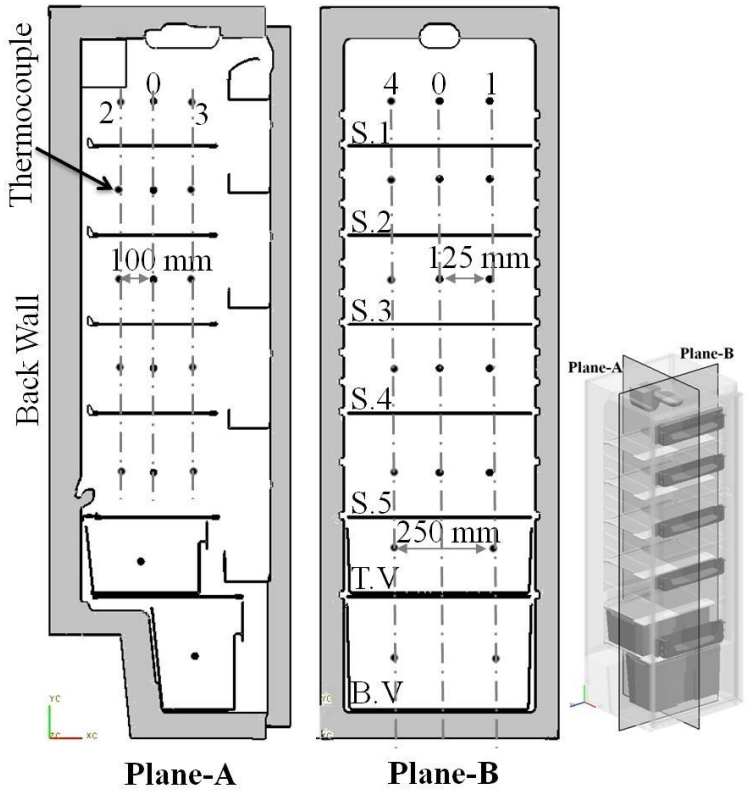

Figure 3.12 Arrangements of thermocouples at fifth thermostat stage experiments

Twenty nine thermocouples were used for measurement the inner air temperature. Arrangement of them has shown in Figure 3.12. Five thermocouples that attached on the support rod (Figure 3.13) were placed each five shelves (Figure 3.15). One thermocouple was placed on the middle point of the shelf (170 mm away from the back wall) on the Plane-A and it numbered as “0”. Two thermocouples were placed at 100 mm back and front side from “thermocouple no 0” on the Plane-A and they numbered as “2” and “3” respectively. The other two thermocouples were placed at 125 mm right and left side from “thermocouple no 0” on the Plane-B and they numbered as “1” and “4” respectively. Also two thermocouples that attached support rod (Figure 3.14) were placed at 125 mm right and left side from the middle point of the each vegetable compartment and they respectively numbered as “1” and “4”. All above thermocouples were placed 110 mm above from the each shelf and each vegetable compartment floor.

Also two thermocouples were placed on the evaporator surface (Figure 3.15). One of them was placed near the shelf-2 (S.2), the other one was near the shelf-3 (S.3).

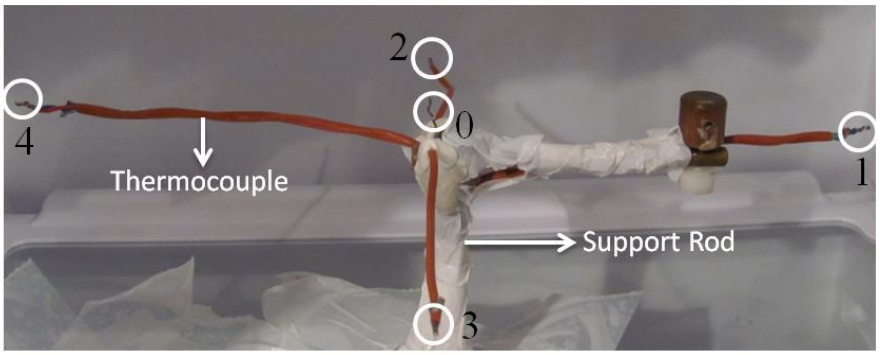

Figure 3.13 Thermocouples with support rod to placed each shelf

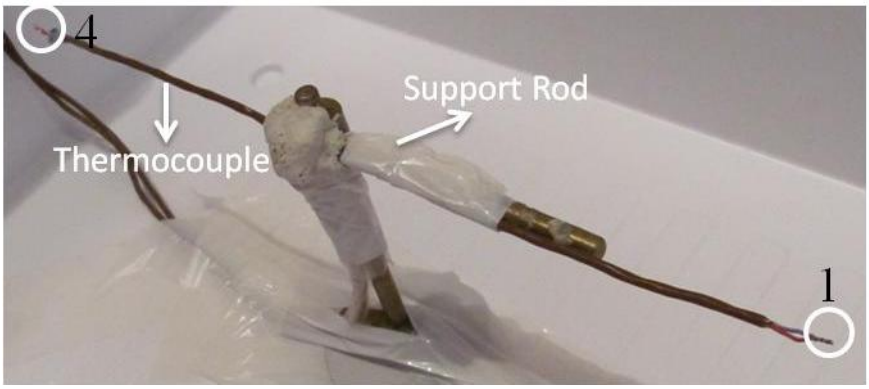

Figure 3.14 Thermocouples with support rod to place each vegetable compartment

As emphasized in section 3.2.1 that the data which were recorded over the 24 h at the equilibrium state were considered. The time average temperatures of thermocouples which measured inner air have shown in Table 3.9 for both with fan and without fan experiments.

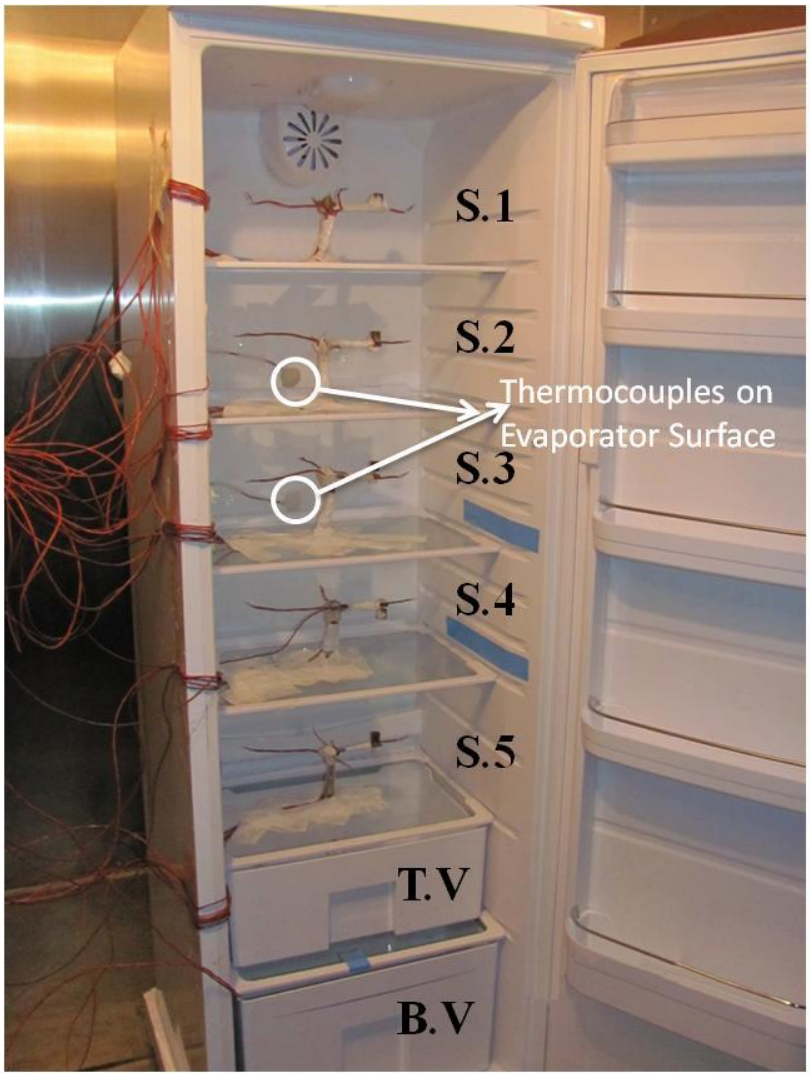

Figure 3.15 Arrangement of thermocouples at fifth thermostat stage experiments

Table 3.9 shows that the following results:

- Temperatures of the left and right thermocouples such as S.1-1 and S.1-4 are almost same value at both two experiments except the S.5 positions. That situation shows that there are uniform temperatures at each shelf between right and left side.
- However temperature difference of the back and front thermocouples such as between S.1-2 and S.1-3 is 0.641 C is relatively great comparing with between left and right thermocouples such as between S.1-1 and S.1-4 is 0.2 C in without fan experiment. This situation shows that thermal uniformity in each shelf is not good between back and front side of the shelves compare with the right and left sides of the shelves.

Table 3.9 Measured inner air temperatures at fifth thermostat stage experiments

Thermocouple Position		**Time Average Temperature [C]**	
		Without Fan	**With Fan**
Shelf-1 (S.1)	S.1-0	7.748	3.775
	S.1-1	8.043	4.2
	S.1-2	7.799	3.937
	S.1-3	8.44	4.158
	S.1-4	8.271	4.27
Shelf-2 (S.2)	S.2-0	3.912	1.613
	S.2-1	3.994	1.768
	S.2-2	4.213	1.906
	S.2-3	4.557	1.918
	S.2-4	4.247	1.95
Shelf-3 (S.3)	S.3-0	2.792	0.772
	S.3-1	2.981	0.848
	S.3-2	2.960	0.962
	S.3-3	3.601	1.438
	S.3-4	2.961	0.84
Shelf-4 (S.4)	S.4-0	2.46	1.026
	S.4-1	2.722	1.165
	S.4-2	2.484	1.026
	S.4-3	2.62	1.021
	S.4-4	2.416	0.884
Shelf-5 (S.5)	S.5-0	3.809	3.462
	S.5-1	3.085	2.737
	S.5-2	3.221	2.723
	S.5-3	2.885	2.489
	S.5-4	2.653	2.277
Top Vegetable Compartment (T.V)	T.V-1	6.719	6.455
	T.V-4	6.217	5.936
Bottom Vegetable Compartment (B.V)	B.V-1	8.278	7.947
	B.V-4	8.319	7.968

- Also in the both two experiments the temperature differences were great between the thermocouples on the S.5 positions. This situation shows that there is an air circulation that was observed in the literature too on the bottom of the domestic refrigerator.
- The same results observed with the previous experimental result by means of the vegetable compartments temperature.
- The temperature decreasing were ~4 C at the S.1, ~2 C at the S.2-3, ~1 C at the S.4 and ~0.5 C at the S.5 with presence of the fan. This situation shows that the same conclusion with previous experimental study by means of mixed convection effect on the temperature improvement.

- The temperature difference between the top (S.1-0) and bottom (S.5-0) thermocouples decreased from 3.939 to 0.313 with fan. This situation shows that the same conclusion with previous experimental study by means of mixed convection effect on the thermal uniformity.

In addition the time and arithmetic average temperatures on the thermocouples which are on the evaporator surface have shown in Table 3.10.

Table 3.10 Measured evaporator surface temperature at fifth thermostat stage experiments

Thermocouple Position	**Time Average Temperature [C]**		**Arithmetic Average Temperature [C]**	
	Without Fan	With Fan	Without Fan	With Fan
Top	-6.982	-6.570	-6.727	-6.466
Bottom	-6.471	-6.362		

Table 3.10 shows that the evaporator average temperature is -6.727 C without fan and is -6.466 C with fan which have been used as boundary conditions in the numerical studies. Also in the numerical studies this average evaporator temperature is represented the fifth thermostat stage.

3.4 Comparisons

3.4.1 Comparison of the Effects of the Evaporator Surface Temperature

To investigation the evaporator surface temperature, experiments were carried out with different thermostat stages. Figure 3.16 illustrated the average temperature each shelf and vegetable compartment with different experimental conditions. Term “T.S-4” is represented the fourth thermostat stage while the term “T.S-5” is represented the fifth thermostat stage. It can be seen that the evaporator temperature affects the above of the vegetable compartments. Approximately inner air temperature on those shelf regions is decreased at ~2 C by the increasing the thermostat stage with independent the presence of the fan.

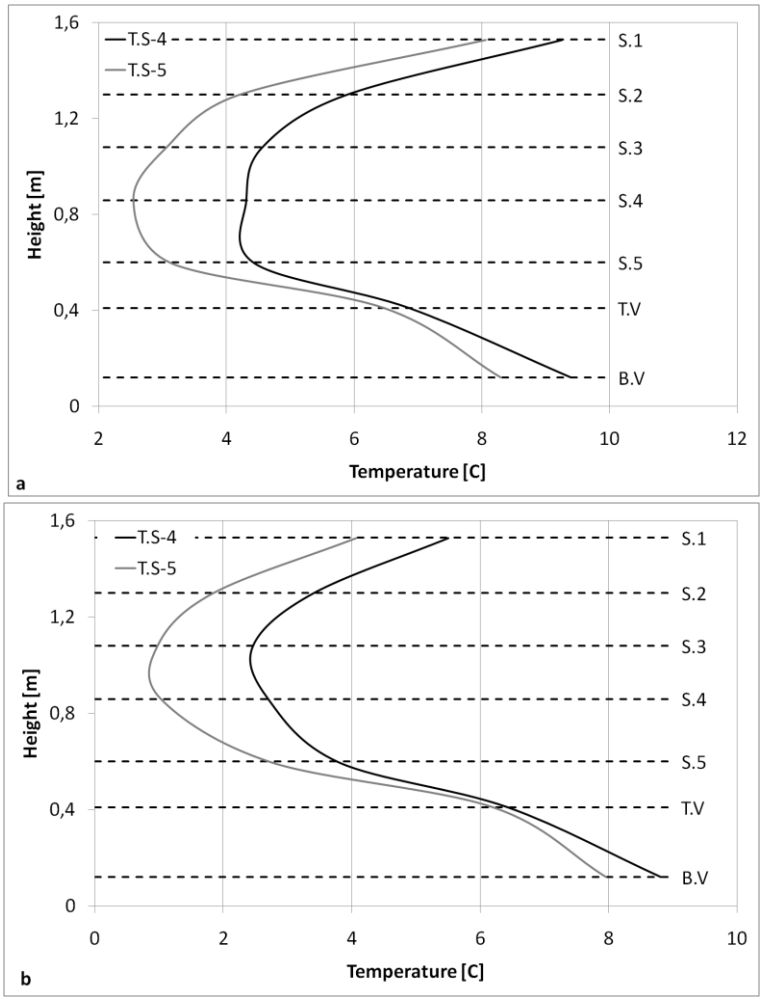

Figure 3.16 The effect of the evaporator surface temperature on the average inner air temperatures (a) Without fan experiments, (b) With fan experiments

Also the average evaporator surface temperature decreased from -3.16 C to ~ -6.5 C with increasing the thermostat stage. In addition the minimum measured temperatures were observed at ~ -18 C in all experiments. Otherwise the maximum one was decreased from 8 C to 4 C with increasing the thermostat stage. Therefore the thermostat stage is indirectly adjusted the compressor on-off cycle times in the same conditions. In addition it shows that the calculated average temperature of the evaporator surface depends on the minimum and maximum points of the fluctuations.

3.4.2 Comparison of the Effects of the Fan

To investigation the effects of the mixed convection, experiments were carried out with fan and without fan. With fan experiments represent the mixed convection conditions. Mixed convection effect has shown in Figure 3.17 in the experiments with fifth thermostat stage. It can be seen that the most affected region is the top of the domestic refrigerator. Those effects have been emphasized in section 3.3.2. Also it shows that vegetable compartments were not affected with fan so mixed convection effects.

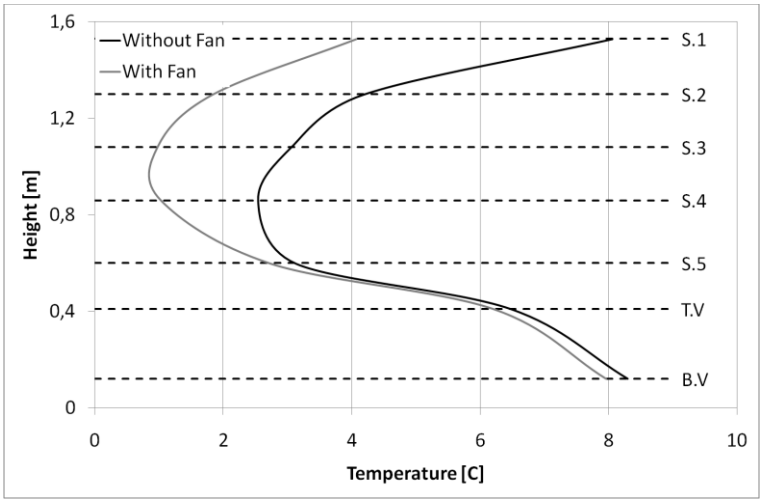

Figure 3.17 The effect of the mixed convection on the inner air temperature in experiments with fifth thermostat stage

3.5 Summary

Experimental results which are explained in section 3.3 have been used as boundary conditions while in section 3.4 have been used for validation.

The results in Table 3.2 have been used for the heat transfer coefficient boundary conditions, in Table 3.4 for specification the fluid material properties and in Table 3.6 for emissivity (0.971) on inner plastic surfaces in all numerical simulations.

Also for fixed temperature boundary conditions which are represented the evaporator surface temperatures, results in Table 3.3 and Table 3.10 have been used for numerical simulations with respectively fourth and fifth thermostat stage cases.

Also results in Table 3.7 have been used for inlet boundary conditions for numerical simulations with fan.

In the velocity measurement study (see sec. 3.2.3) the non-uniform inlet airflow has been emphasized according to airflow speed at the each discharge grilles (Table 3.7). This result shows that the fan box location is an important inner design parameter. As the inner design suggestion can be made that the fan box should be placed closer the right side of the domestic refrigerator. This suggestion will be investigated with numerical study.

CHAPTER FOUR

NUMERICAL STUDY

4.1 CFD Domain Geometry

The CFD domain includes the inner air geometry which is filled inside the insulated cabinet of the investigated domestic refrigerator which has specified in section 3.1.1. The inner surfaces of the inner plastic and the door are boundary surfaces of the CFD domain (Figure 4.1).

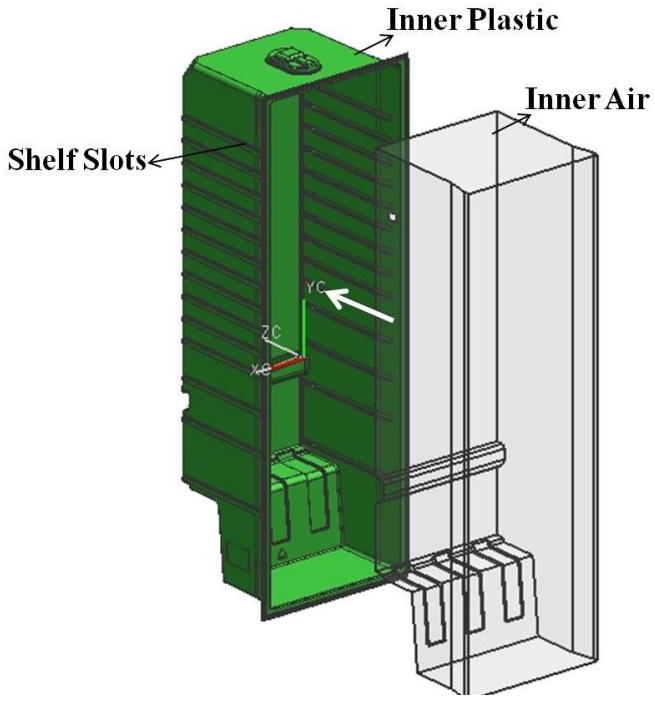

Figure 4.1 Inner air geometry

The CFD domain has been simplified according to the information in section 2.2.1.1. A simplification has shown in Figure 4.1 that the shelf slots were not created because of the small size comparing with the height or width of the domestic refrigerator and believed to have no influence on the flow and heat transfer. Also two simplification regions have been shown in Figure 4.2. Those simplifications have given as example. Besides those, some simplifications were made similar way.

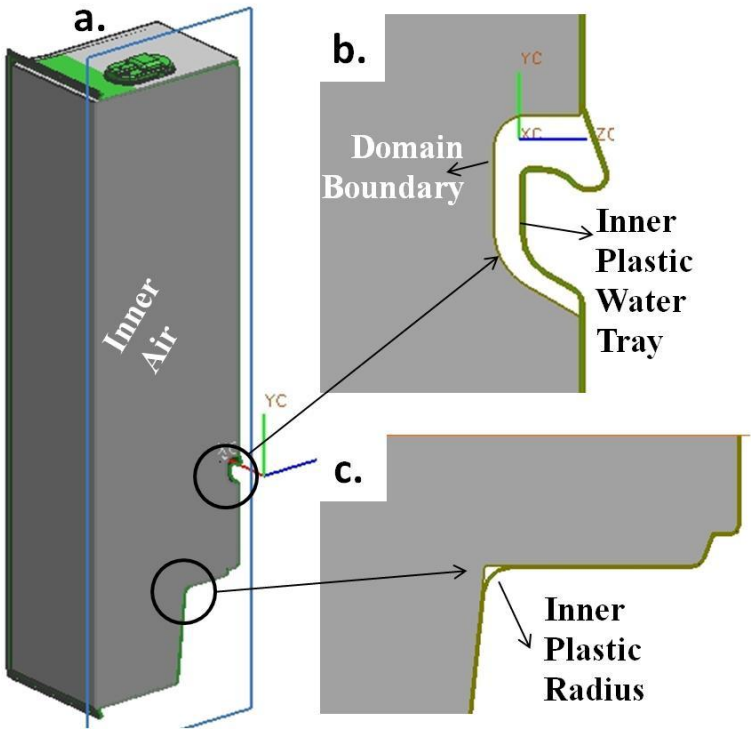

Figure 4.2 (a) Cross section of the inner air and plastic, (b, c) Simplification region examples

The solid part bodies which are main glass shelves (4 mm thickness), vegetable compartments lids (4 mm thickness), door shelves (2.5mm thickness) and vegetable compartment baskets (2.5 mm thickness) have been subtracted from the inner air body. Formed internal surfaces are occurred inner boundaries. Also some numerical simulations the solid bodies have been added as solid domains in this study.

Also surfaces of the fan box and light box assumed the boundaries of the domain. So the bodies which fill in the fan box and in the light box have been subtracted from the inner air body.

Finally the evaporator surface has been created as imprint face on the back wall.

The created CFD domain according to above information has been shown in Figure 4.3. This fluid domain has been used in the numerical simulations without fan and named as “Domain Without Fan”. On the other hand the suction and discharge grilles’ surfaces have been created as imprint face on the fan box

boundary for numerical simulations with fan. So created fluid domain by this way has been used for investigation the mixed convection effects and named as “Domain With Fan”. Only the discharge and suction grilles boundary has been shown in Figure 4.4 because the other region is the same in Figure 4.3.

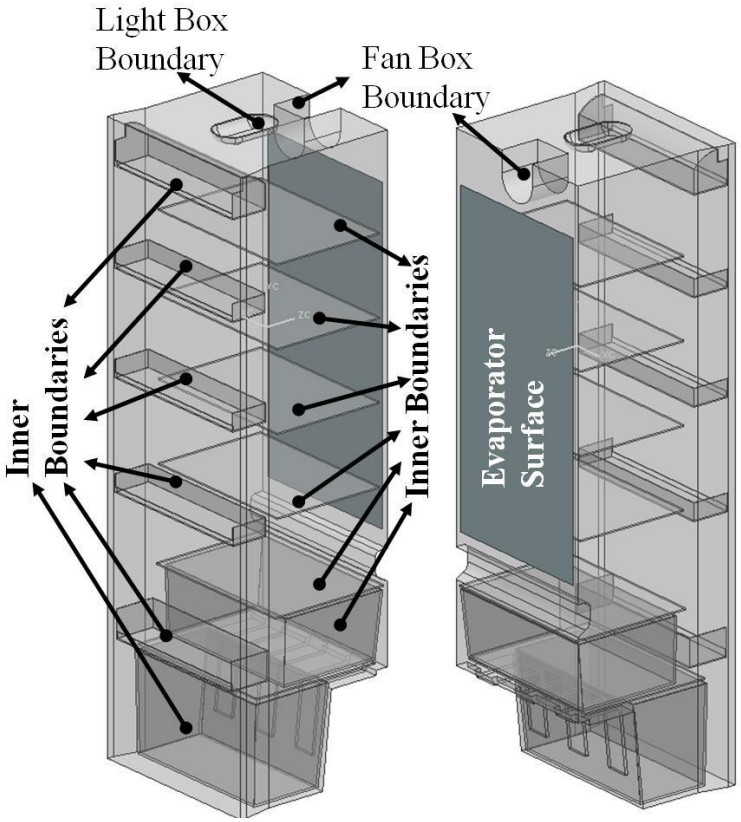

Figure 4.3 CFD domain without fan

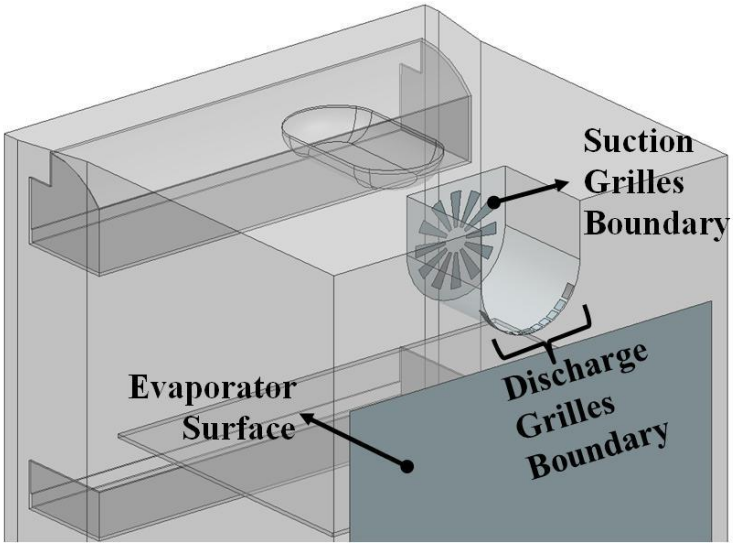

Figure 4.4 Detailed view of the CFD domain with fan

Also for the loaded condition simulations, the test packages were created as solid domains. The dimensions of the test packages are specified by standard of ISO 15502 (2005). In addition the loaded (storage) plan which are applied during the energy tests of the freezers or the food-freezer compartments of the domestic refrigerator was implemented according to ISO 15502 (2005). It should be noted that although the loaded plain was not described for this investigated type domestic refrigerators in the standard of ISO (2005), this plan implemented for accomplishing the uncertainty of the loaded plan for investigated type domestic refrigerators. The created bodies of the test packages were subtracted from the fluid domain body. Based on this processes, the loaded domains with fan and without fan were created and shown in Figure 4.5. The dimensions which are in the color boxes are represented the test packages dimension which is the same color with the color box.

Consequently the CFD domain of the investigated domestic refrigerator has been created with some assumptions which were specified in section 2.3.1.

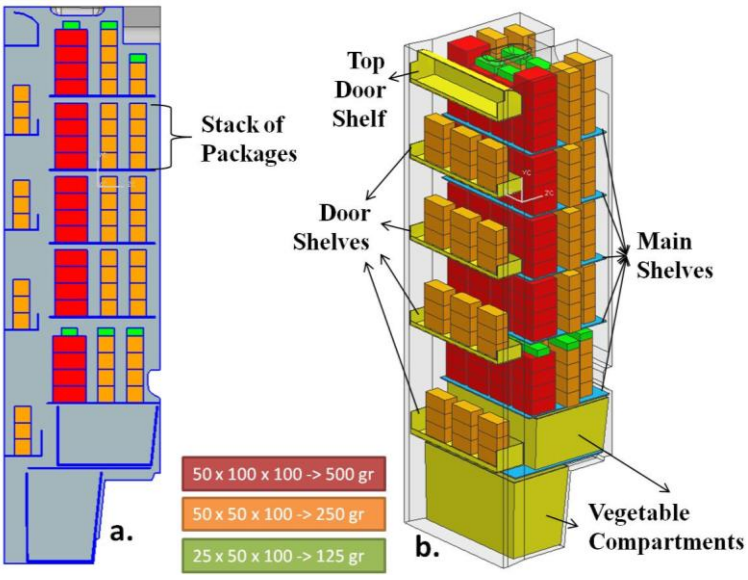

Figure 4.5 The CFD domain with test packages

4.2 Meshing

The created domain geometries have been divided to small control volumes for creating the computational grids in this step. The mesh structure consists of elements which represent the control volume. The element consists of nodes on

which the governing equation is discredited. Also average of the any properties of the nodes represents the connected element properties. So the mesh density which is the number of the elements and nodes has to be enough fine for the accuracy of the solution. For ensuring that, meshes have been created with different density.

The tetrahedral elements were used for generation the fluid domain mesh. However the boundary layers were created with pyramid and prism elements near the boundary surface of the fluid domain to calculate the boundary layer changes. For this way two generated mesh with different density have shown in Figure 4.6.a and b. Created meshes was named as “Mesh-01” (Figure 4.6.a) and “Mesh-02” (Figure 4.6.b) and the Mesh-02 is more density than the Mesh-01.

Then the fluid domain was divided two parts from near the shelf-5 to attained more fine mesh density (Figure 4.6.c). This mesh was named as “Mesh-03”. The domain which is above the shelf-5 is named as “Top Inner Air” while the other one is named as “Bottom Inner Air”. The more elements were created at the small gaps between the boundary surfaces where is in the bottom inner air comparing the other two mesh. The small gaps region have been specified with rectangular area and the created mesh in bottom inner air domain have been shown in Figure 4.7 with comparing Mesh-02.

The explained above mesh process were implemented for the “Domain Without Fan”. The last created fine mesh (Mesh-03) was also implemented for the “Domain With Fan”. Since the difference between two domains is only the presence of the discharge and suction grilles surfaces and those surfaces are in the top inner air, the mesh have been implemented only the top inner air. The bottom inner air mesh is the same for both of two domains. The difference of the mesh between with fan and without fan domain has shown in Figure 4.8 near the fan box boundary region of the domain.

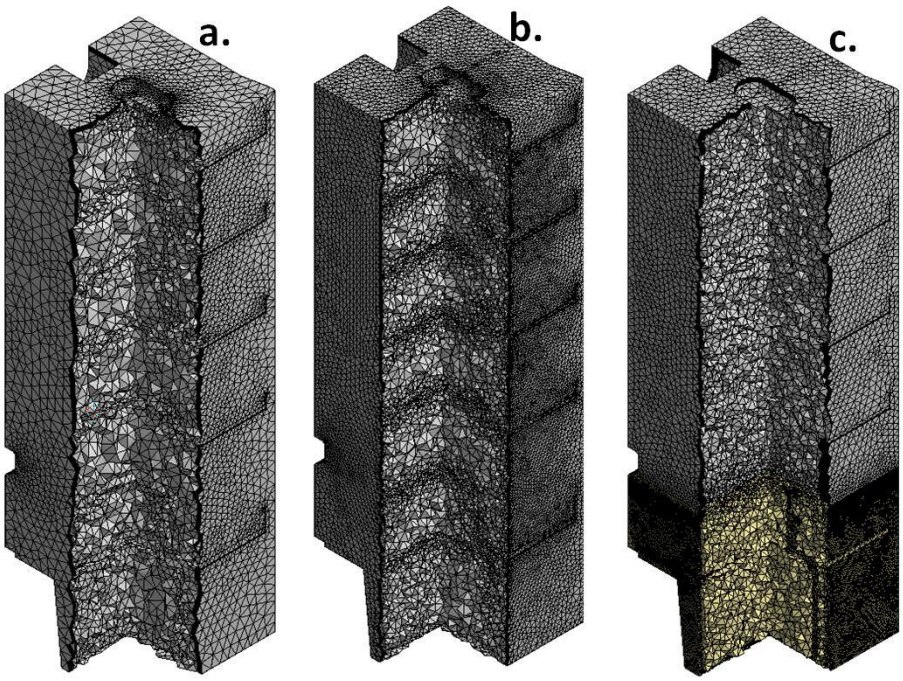

Figure 4.6 Section views of the meshes: (a) Mesh-01, (b) Mesh-02, (c) Mesh-03

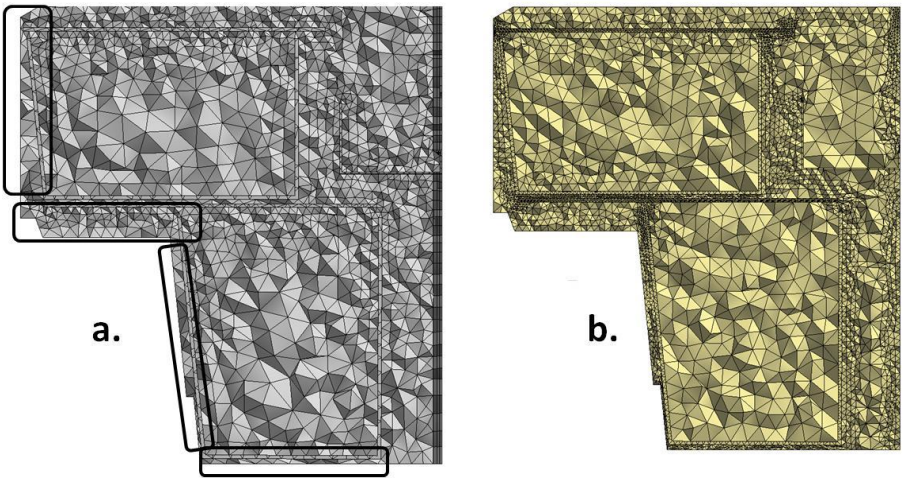

Figure 4.7 Mesh of the bottom inner air domains: (a) Mesh-02, (b) Mesh-03

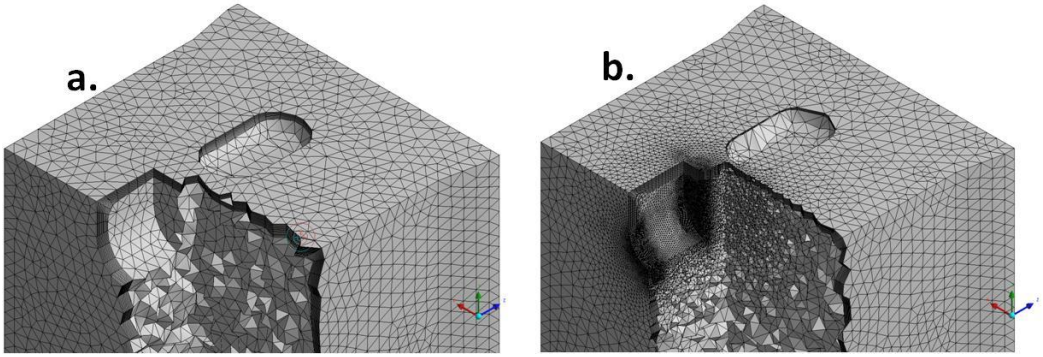

Figure 4.8 The section view of the mesh near the fan box boundary: (a) Mesh-03 without fan, (b) Mesh-03 with fan

All mesh properties which are the number of the elements and nodes have given in Table 4.1.

Table 4.1 Mesh properties of different mesh density of the fluid domain

Mesh No		Number of Nodes	Number of Elements
Mesh-01		105,604	399,708
Mesh-02		349,695	1,316,792
Mesh-03 without fan	Top Inner Air	147,497	486,686
	Bottom Inner Air	286,018	1,408,876
	Total	433,515	1,895,562
Mesh-03 with fan	Top Inner Air	362,455	1,574,288
	Bottom Inner Air	286,018	1,408,876
	Total	648,473	2,956,164

In addition hexahedral and tetrahedral elements were used for generation the solid domains mesh. The thickness of the solid domains was created with at least two elements. The solid domains have been used some numerical simulations and their mesh views are shown in Figure 4.9 and properties are reported in Table 4.2.

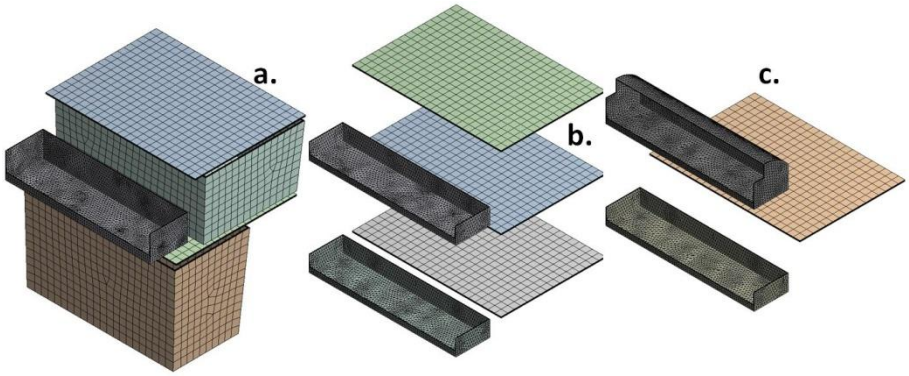

Figure 4.9 Solid domains mesh views: (a) Vegetable compartment baskets, bottom vegetable compartment lid, bottom door shelf and shelf-5, (b) Shelf-2, 3, 4 and middle door shelves, (c) Shelf-1 and top door shelves

Table 4.2 Mesh properties of solid domains

Solid Domain	Number of Nodes	Number of Elements
Main Glass Shelves	10,320	7,452
Door Shelves	46,213	192,506
Vegetable Compartments Baskets	10,640	8,232
Bottom Vegetable Compartment Lid	2,400	1,748
Total	69,573	209,938

Also for the loaded condition simulations, mesh processes were occurred as same density as Mesh-03 for fluid domains. Furthermore mesh processes were also occurred for domains of the test packages and the other solid parts. All created meshes for loaded condition are shown in Figure 4.10 and the properties of meshes are reported in Table 4.3.

Table 4.3 Mesh properties of domains for loaded condition simulations

Domain	Number of Nodes	Number of Elements
Shelves	27,538	99,577
Test Packages	127,714	96,668
Vegetable Compartments Baskets	13,040	9,980
Inner Air	849,739	3,290,528
Total	1,018,031	3,496,753

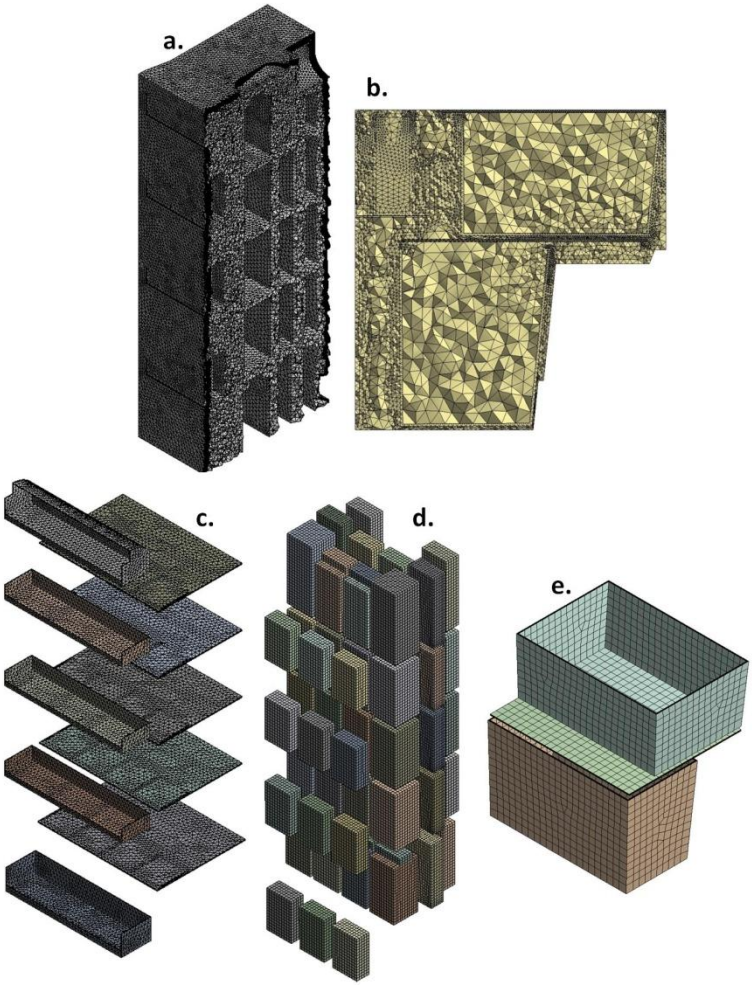

Figure 4.10 The mesh views of the domains for loaded condition simulations: (a) Upper inner air section, (b) Bottom inner air section, (c)The shelves ,(d) Test packages, (e) Vegetable baskets

4.3 Specification the Physics and Boundary Conditions

4.3.1 The Material Properties

For the fluid domains the thermo-physical properties was determined by the experimental results. The material properties which were determined in the Table 3.4 were used for all numerical simulations.

The solid material properties were used in Table 4.4 for the simulation which included solid domains.

Table 4.4 Thermal properties of solid material

Material	Density [g/cm^3]	Thermal Conductivity [W/m K]	Specific Heat [J/g C]	Emissivity
High Impact Polystyrene (HIPS)	1.04*	0.16*	1.97*	0.971**
Glass	2.05***	1.4***	0.75***	0.92****

*www.matweb.com – Categories: Polystyrene, Impact Modified
** See section 3.2.2
*** ANSYS CFX Material Library – Glass Plate Properties
**** http://www.infrared-thermography.com/material-1.htm

Also the test packages are represented the lean beef (ISO 15502, 2005). The thermal properties of the test packages were reported in Table 4.5 and this values were specified by Çengel (2007) (p. 17-20). The emissivity of the fat beef were used and specified by Saravacos & Kostaropoulos, (2002) (p. 285).

Table 4.5 Thermal properties of the test packages (represented the beef)

Material	Density [kg/m^3]	Thermal Conductivity [W/m C]	Specific Heat [kJ/kg C]	Emissivity
Beef (Test Packages)	1070*	0.41**	1.7***	0.971

* Average properties
** At 6 C
*** Below freezing

4.3.2 The Analysis Type

The steady-state assumption was made for all simulations. However for comparison between steady-state and transient analyses a transient analysis was

implemented with fixed evaporator temperature in the fifth thermostat stage with fan simulation. As emphasized in section 2.3.2 the time step and the initialization parameters were specified.

Value of the time step is calculated according to the equation (2.32) since the forced convection driven is occurred. Firstly, time step was calculated at ~0.19 s with usage maximum velocity of the discharge grille (4.68 m/s) and evaporator height (0.91 m). However time step value was used as 0.1 s for ensured more accuracy of the transient analysis.

The results of the steady-state analysis were used as initialization conditions to reduce computational time.

4.3.3 The Natural Convection Model

The gravity acceleration was specified at the –y direction for all numerical simulations. Also reference temperature and density were used at the average temperature in the Table 3.4 for Boussinesq approximation for calculation the equation 2.35.

4.3.4 Flow Condition Model

For the simulations with fourth thermostat stage and without fan, the flow was assumed laminar flow according to equation 2.36. For the calculation, the characteristic length (L) is 0.91 m which is the evaporator length, the temperature difference (ΔT) is calculated between the average inner air temperature (3.768 C) in Table 3.4 and the arithmetic average evaporator temperature (-3.16 C) in Table 3.3 and the air properties are in Table 3.4. Since Ra number has found approximately 6.88×10^8 which is less than the 10^9 (critical Ra number for the vertical plate) the flow condition has assumed laminar flow.

For simulations with fifth thermostat stage and without fan, the flow was assumed turbulence flow according to equation 2.36. The difference of the above calculation is the arithmetic average evaporator temperature (-6.727 C) in Table

3.10. Since Ra number has found 1.08 x 10^9 which is greater than the 10^9 the flow condition assumed turbulent. And the k-ε and Shear Stress Transport (SST) numerical turbulence models were used and the good agreement model with experimental result was selected.

For the simulations with fan, the flow assumed turbulent flow. Firstly the Re number (Eq. 2.37) was calculated where the characteristic length (L) is 0.91 m, characteristic velocity (U) is 4.68 m/s which is the highest velocity in Table 3.7 and the kinematic viscosity ($\nu=\rho/\mu$) is calculated according to the values in Table 3.4. Since the Re number has found 19.7 x 10^4 which is less than 5 x 10^5 (critical Re number for parallel flow over flat plate) the flow should have been assumed laminar. However the flow over a flat plate is not completely represent the flow in the domestic refrigerator. So the assumptions for the flow condition were investigated in the literature studies which were modeled fan effects in the refrigerator. Therefore the k-ε turbulence model was used in many studies (Ding, Qiao, & Lu, 2004; Foster, Madge, & Evans, 2005; Fukuyo, Tanaami, & Ashida, 2003; Navaz, Faramarzi, Gharib, Dabiri, & Modarress, 2002; Yang, Chang, Chen, & Wang, 2010). Consequently the k-ε turbulence model has been used for these type simulations.

4.3.5 Radiation Model

The radiation model assumptions have been explained in section 2.3.6. In addition the emissivity of the surfaces has to be specified. For that purpose the fluid surfaces which interacted the solid domains, were specified emissivity values which were listed in Table 4.4.

4.3.6 Boundary Conditions

The boundary conditions types have been explained in section 2.4.

For all simulations the wall boundary conditions have been the same value. The specified values in Table 2.2 were used for the heat transfer coefficients depend on the wall direction. The specified values in Table 3.2 were used for the

outside temperature. In addition the outside temperature for the bottom wall has been assumed at 25 C. Also the fan and light box boundaries (Figure 4.3) have been assumed as adiabatic wall. All walls are no-slip wall for the mass and momentum equations.

The created surface which is occurred by divided the domain (Figure 4.6.c) is an inner surface and interface surface.

The inner boundaries (Figure 4.3) have been assumed as adiabatic wall in simulations which have no solid domains. In opposite simulations those walls are interface surfaces.

The evaporator surface has been assumed as fixed temperature. For the fourth thermostat stage simulations with and without fan the temperature value which was specified in Table 3.3 was -3.16 C. For the fifth thermostat stage, the temperature was -6.727 C without fan simulations and -6.466 C with fan simulations and specified in Table 3.10.

For the simulations with fan the inlet and outlet boundary conditions were used respectively the discharge grilles boundary and suction grilles boundary (Figure 4.4). The specified velocities in Table 3.7 have been used on the inlet boundaries and shown in Figure 4.11.a. Also the static pressure have been specified as 0 Pa on the outlet boundaries and shown in Figure 4.11.b.

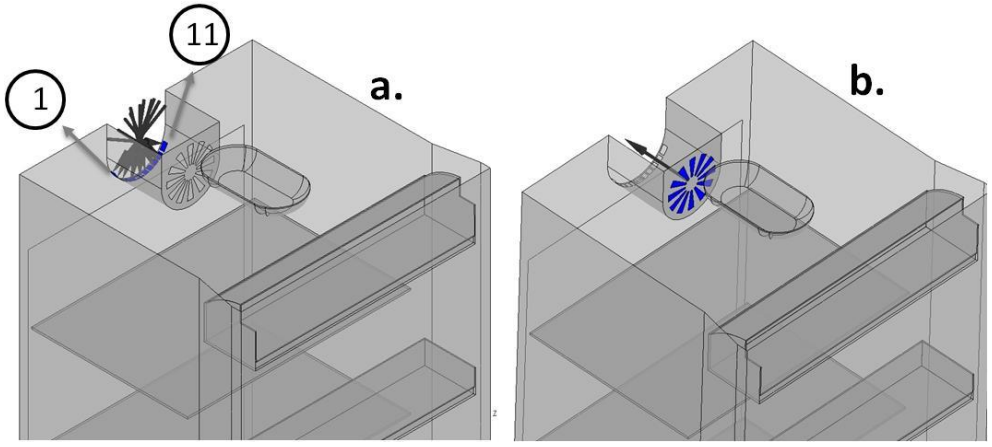

Figure 4.11 The inlet (a) and outlet (b) boundary conditions

4.4 Solver

The prepared CFD models which have been described the previous sections have been iteratively solved according to finite volume method. The iterative solutions have completed when the fluid domain energy, mass and momentum imbalances have reached in the range ±5%. The solid domains energy imbalance has been near the 0% in simulations which included solid domain.

In some solutions maximum residual values which have been near the 10^{-3} have been observed the energy and momentum equations for the fluid domain when energy imbalances have reached the desired range. Otherwise the fluid domain energy residuals have been smaller than the 10^{-4} in simulations which included solid domains.

4.5 Validation of the Numerical Results

4.5.1 The Fourth Thermostat Stage Simulations without Fan

4.5.1.1 The Effects of the Mesh Density

To investigation the mesh density effects, the CFD results with usage Mesh-01, 02 and 03 (see sec. 4.2) have been compared with experimental results without fan (Table 3.8) For that purposes the vertical line has been created between position S.5-0 and S.1-0 and named as “Vertical Line-0 (V.L-0)” and then temperature distributions on V.L-0 have been compared between numerical results and experimental results (Figure 4.12.a). Also the same comparison has implemented on “Vertical Line-1 (V.L-1)” (Figure 4.12.b) which has been created between position S.5-1 and S.1-1.

The comparison of the numerical results each other shows that the temperature distributions are almost same except the S.5 region on both lines. The results in this region are slightly changed especially on the V.L-1 (in range ~1 C) with altering the mesh density. Also the same observation was seen on the each main glass shelf boundary. It should be noted that the locations of sudden temperature changing are the location of the main glass shelves.

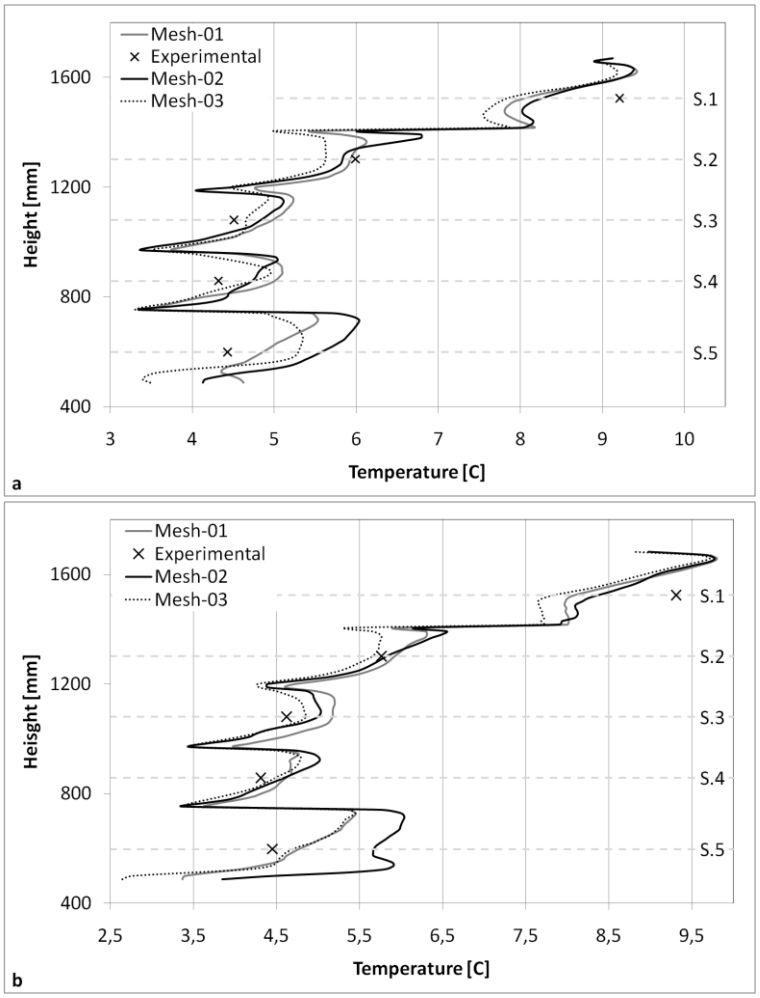

Figure 4.12 Temperature distributions on lines for different mesh densities and experimental results at fourth thermostat stage without fan case: (a) Vertical Line-0, (b) Vertical Line-1

The comparison between numerical results and experimental results shows that the maximum difference is ~1.5 C at the S.5 and S.1 on both lines. Result of Mesh-03 is the most good agreement at the S.5 while is the worst agreement at the S.1 in both lines comparing with experimental results. Also results are good agreement in the other region for all simulations.

The above conclusions were made for the fresh-food compartment. For the comparison temperature of vegetable compartments, volumes which are in each vegetable compartment were created in simulations. The average temperatures of those volumes were compared among each other and experimental results and reported in Table 4.6. As can be seen that, the top vegetable is colder than the bottom vegetable in the experimental result but the opposite situation is observed

in all numerical results. Also the differences between the experimental result and numerical results are so more especially in the top vegetable compartments. In addition temperature was increased with mesh density increasing and also the difference between experimental and numerical results was increased. Actually predicted result with Mesh-03 simulation had been expected good agreement with experimental result especially in the bottom inner air domain because of the generated more fine mesh in the bottom inner air (Figure 4.7.b). Otherwise the observed situation was the opposite from this expectation. This may be due to the fact that the conduction effects via solid parts have not been consideration.

Table 4.6 The average temperatures of vegetable compartments for different mesh densities and experimental results at fourth thermostat stage without fan case

Vegetable Compartment Position	**Average Temperature [C]**			
	Experimental	**Numerical Results**		
		Mesh-01	**Mesh-02**	**Mesh-03**
Top	6.86	10.09	10.54	11.97
Bottom	9.4	8.31	8.54	8.19

Therefore generated meshes are suitable for the numerical study according to the comparing with the experimental result in top inner air domain. However the observed results in the vegetable compartments were not good agreement with experimental result. The reason of this situation had been believed that the heat conduction via solid parts which were not considered in the simulations.

As a result of the mesh density investigation it was decided the usage Mesh-03 in all other simulations because of the fine mesh at the bottom inner air.

4.5.1.2 The Effects of the Solid Domains

The solid domains which are included all shelves and two vegetable compartments baskets and their lids have been added in the fluid domain to consideration the heat conduction via solid parts. This simulation’s aim is the improvement the accuracy of the numerical study.

The temperature distributions on the Plane-A are shown in Figure 4.13. It can be seen that temperature distribution is huge difference (~5 C) in some regions which are in top vegetable compartment, between the vegetable compartments

and back walls and in the top door shelf comparing between cases with and without solid domains. Also top of the domestic refrigerator was reduced approximately 2 C through removing the warm region in the top door shelf. Also temperatures in the small region near the shelf-3 and 4 were increased approximately 1 C via solid conduction in these shelves. Further the temperature of the S.2 region was increased approximately 0.5 C through heat transfer from warm air which was top of the domestic refrigerator to this region via shelf-1 conduction.

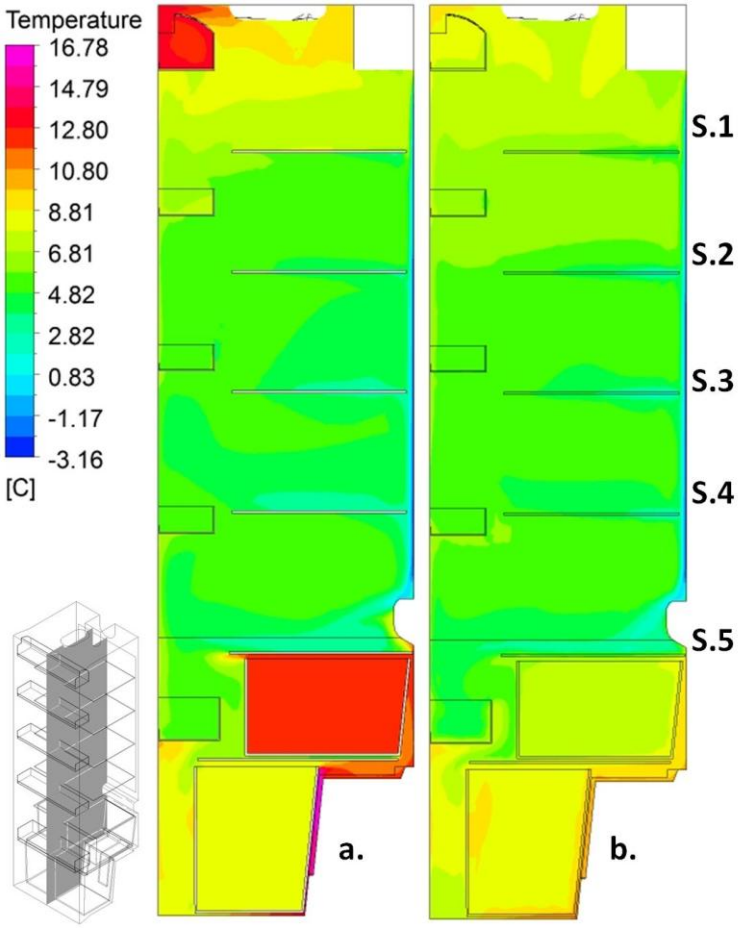

Figure 4.13 The temperature distribution on Plane-A for fourth thermostat stage without fan case: (a) Without solid domains, (b) With solid domains

This temperature difference between two cases is due to the fact that the heat conduction via the solid parts. Especially the solid domains which are the vegetable compartments baskets, the main glass shelf-5 and the glass lid of the bottom vegetable compartment are huge affected for the temperature distribution

in the bottom inner air fluid domain. Those effects are exhaustively shown in Figure 4.14. It can be seen that the heat transfers from the back walls near the vegetable compartments into the vegetable compartments via the vegetable baskets. Then the transferred heat into the top vegetable compartment compensate to the cold airflows which are above the shelf-5 and front of the compartment respectively via shelf-5 conduction and via basket conductions. The same transfer mechanism is observed to the bottom vegetable compartment but the top one is more effective than this one.

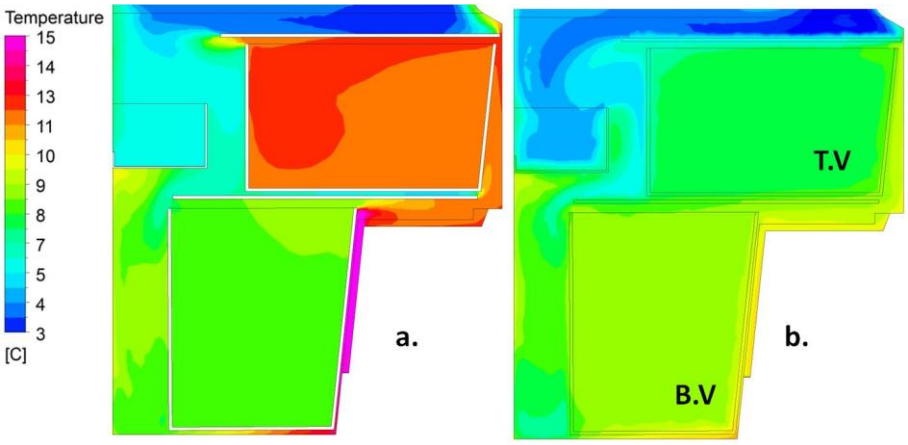

Figure 4.14 The temperature distribution of bottom inner air domain on Plane-A for fourth thermostat stage without fan case: (a) Without solid domains, (b) With solid domains

The comparison of the average temperature of vegetable compartments between the experimental and two numerical results is reported in Table 4.7. It shows that the improvement of the numerical result accuracy for vegetable compartment results with solid domains. Therefore the heat conduction effects have been emphasized. Also more accuracy numerical study was attained.

Table 4.7 The average temperatures of vegetable compartments for with and without solid domains simulations and experimental results at fourth thermostat stage and without fan case

Vegetable Compartment Position	**Average Temperature [C]**		
	Experimental	**Numerical Results**	
		Without Solid Domains	**With Solid Domains**
Top	6.86	11.97	7.56
Bottom	9.4	8.19	8.71

Consequently the solid domains should be considered when the following situation occurred:

- Nearly close cavity is occurred by the solid domains such as cavity of vegetable compartments, cavity of the top door shelve, gap between the vegetable compartment and the back wall.
- High temperature difference between two sides of the solid domain is occurred such as shelf-5 above and under region.

Also the inner surface temperatures were calculated at points which were specified in section 3.2.1. The calculated temperatures have been compared with experimental results (Table 3.5) and shown in Table 4.8. It can be seen that the top wall temperature was reduced through solid domains effects. The same result has been shown at top region for temperature distribution (Figure 4.13). However the difference between numerical and experimental result in the with solid domain case is greater than the without solid domain case. This situation is not meant that the accuracy of the numerical result is bad with solid domains. On the contrary it shows that the capability of the numerical study is as this temperature difference at top region. On the other hand the results of other walls were slightly changed with added solid domains and were good agreement with experimental study.

Table 4.8 The temperatures of inner walls for with and without solid domains simulations and experimental results at fourth thermostat stage without fan case

Inner Wall Position	**Experimental Result**	**Numerical Results**	
		Without Solid Domains	**With Solid Domains**
Top	10,99	9,29	8,15
Left	5,89	5,49	5,91
The Door	5,92	5,75	6,16

Finally the numerical results with and without solid domains and the experimental results are shown in Figure 4.15 as the same lines (V.L-0 and 1) which are explained in section 4.5.1.1. It can be shown that the solid domains are affected approximately 0.5 C except the top and bottom point of both lines between numerical results. The maximum difference between the numerical

result with solid domains and the experimental study is 0.8 C at the position S.1 on the V.L-1.

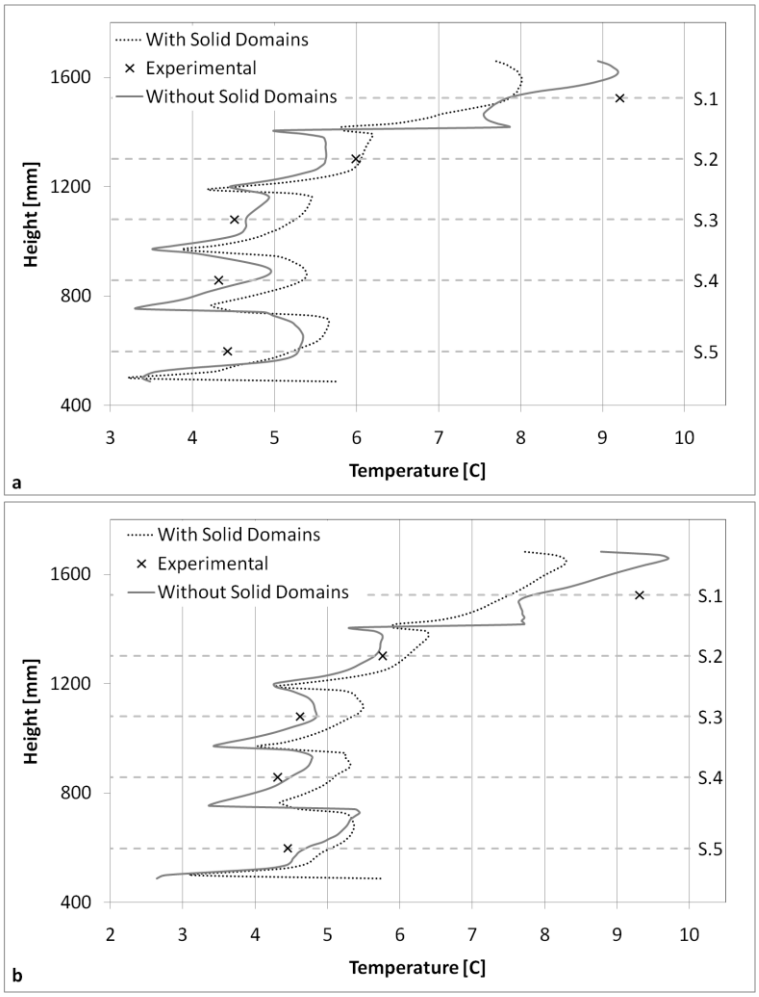

Figure 4.15 The temperature distributions on lines for simulations with and without solid domains and experimental results at fourth thermostat stage without fan case: (a) Vertical Line-0, (b) Vertical Line-1

4.5.2 The Fifth Thermostat Stage Simulations without Fan

4.5.2.1 The Effect of the Turbulence Model

As mentioned previous the flow was assumed turbulent (see sect. 4.3.4). For the specification of the turbulence model, two simulations with k-ε and SST turbulence models were implemented.

For comparison the numerical result the vertical lines were created the same way which was described in section 4.5.1.1. However in this situation three lines

which were the V.L-2, 3 and 4 according to the experimental set-up (see sec. 3.3.2) added. Therefore the temperature distributions on those lines were attained and also these numerical results were compared with experimental results and shown in Figure 4.16. It can be seen that the numerical results are slightly good agreement with experimental result in SST simulations for all lines comparing with the k-ε simulation. The maximum difference between experimental and numerical results is 2.89 C at S.5 position on V.L.4 and is 2.79 C at S.1 position on V.L.3 respectively in k-ε and SST model.

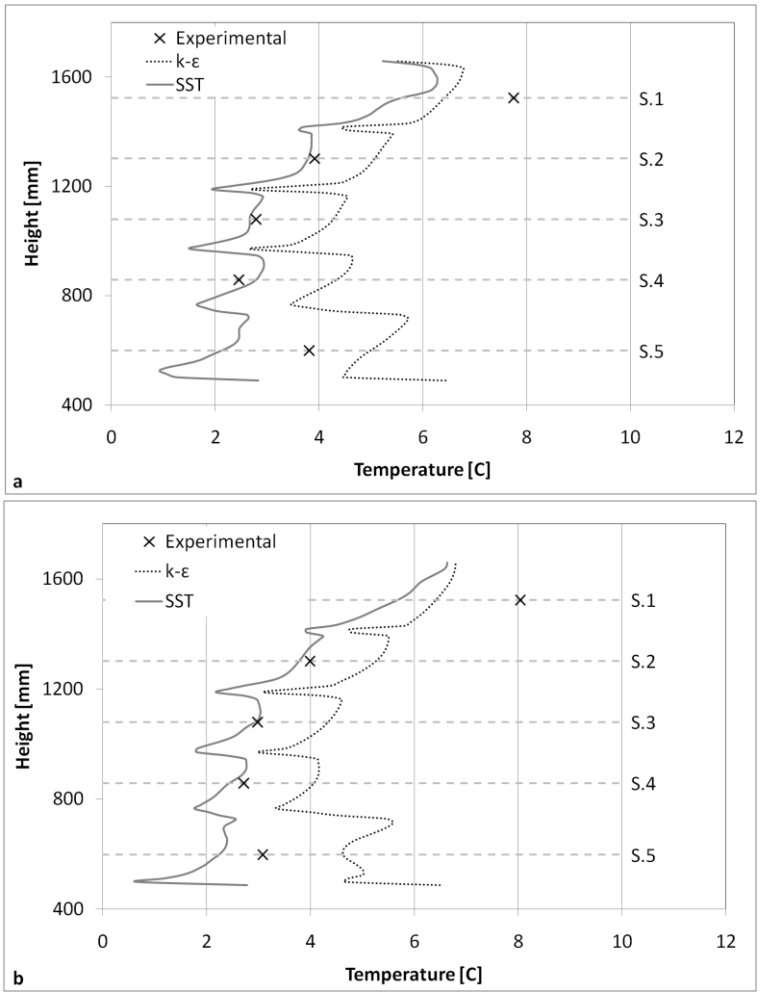

Figure 4.16 The temperature distributions on lines for simulations with k-ε and SST and experimental results for fifth stage thermostat stage and without fan case: (a) Vertical Line-0, (b) Vertical Line-1

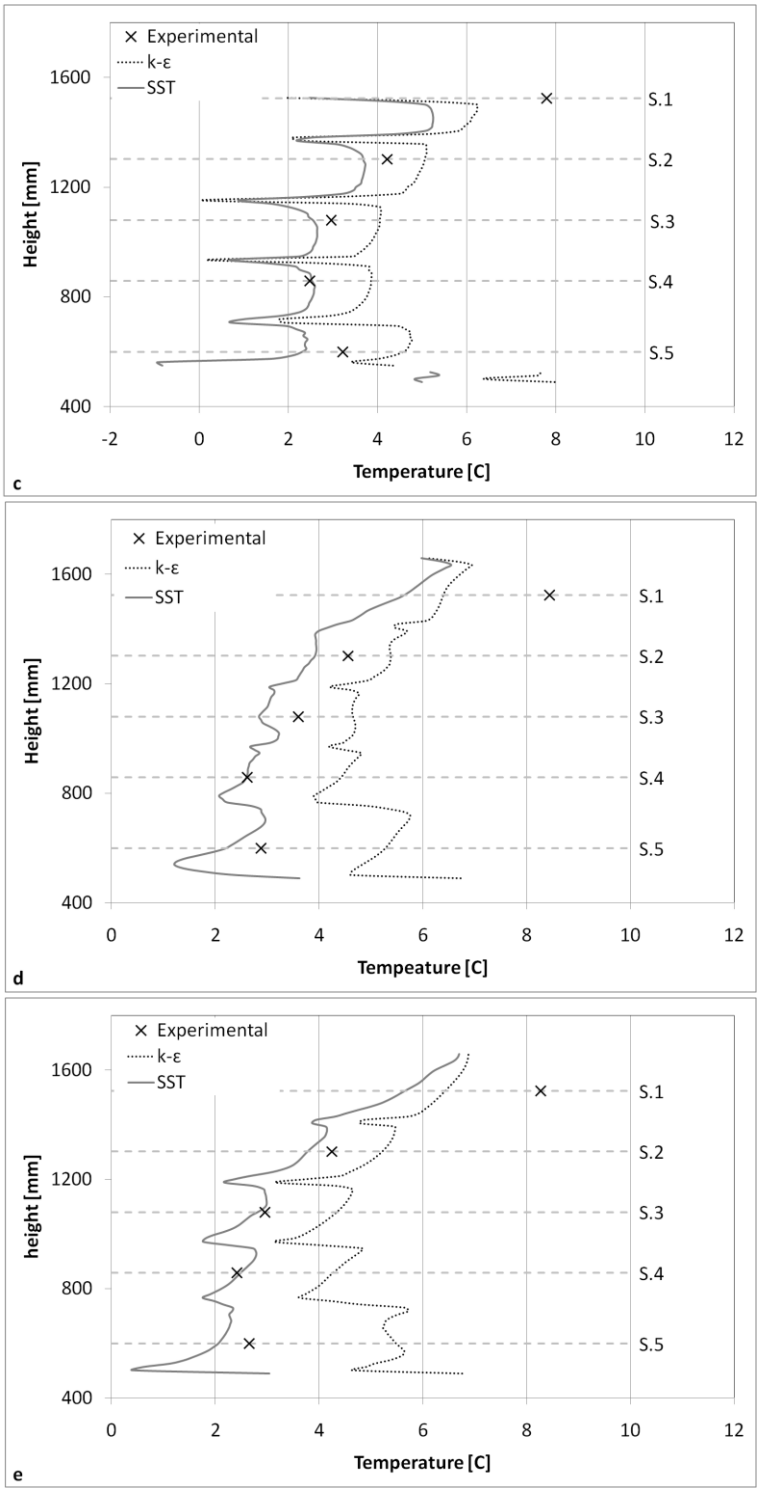

Figure 4.16 (continued) The temperature distributions on lines for simulations with k-ε and SST and experimental results at fifth thermostat stage without fan case: (c) Vertical Line-2, (d) Vertical Line-3, (e) Vertical Line-4

Also four points were created according to the experimental set-up position (see sec. 3.3.2) in vegetable compartments and calculated average temperatures

of that points for comparison of the vegetable compartments temperature and shown in Table 4.9 .The SST model is good agreement with experimental result in top vegetable compartment while the k-ε model is good agreement in bottom vegetable. However the difference (2.38 C) between the k-ε model and experiment results in the top vegetable is greater than the difference (1.32 C) between the SST model and experimental results in the bottom vegetable.

Table 4.9 The average temperatures of vegetable compartments for simulations with k-ε and SST and experimental results at fifth thermostat stage without fan case

Vegetable Compartment Position	**Average Temperature [C]**		
	Experimental	**Numerical Results**	
		k-ε Turbulence Model	**SST Turbulence Model**
Top	6.47	8.85	5.15
Bottom	8.3	9.45	6.8

In addition the streamlines (Figure 4.17) on the Plane-A was created for revelation the difference of the turbulence models. It can be seen that the flow in the k-ε model is more turbulent than the SST model. However the calculated Ra number (1.08×10^9) is slightly greater than the critical Ra number (10^9), so the flow is expected more smoothly. Due to this expectation and the above conclusion on the temperature distribution on lines the SST turbulence model is thought to be suitable.

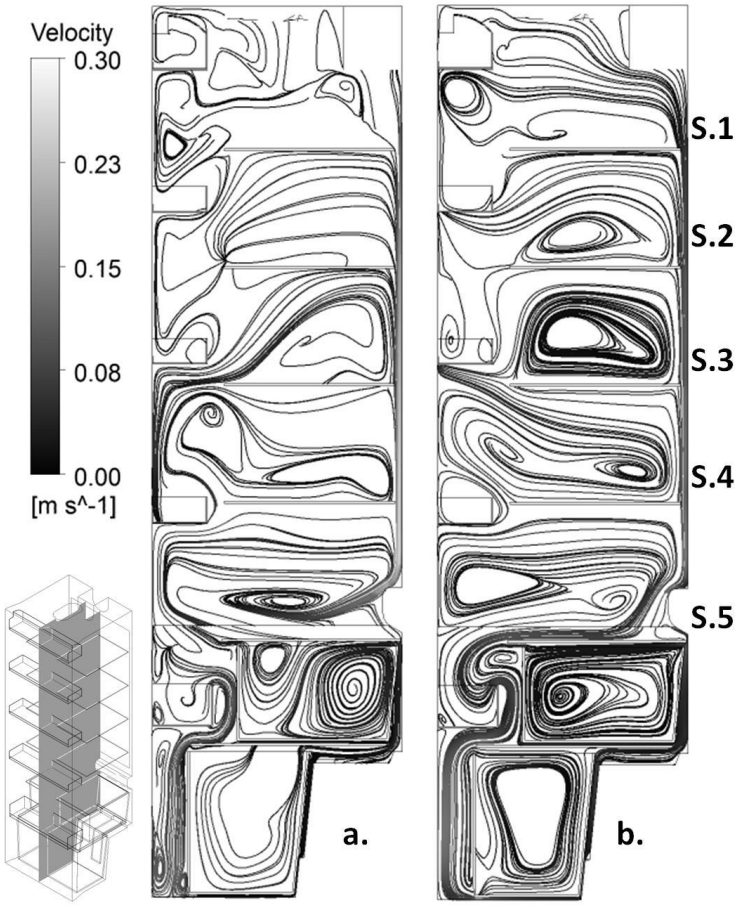

Figure 4.17 Streamlines on the Plane-A at fifth thermostat stage without fan case: (a) SST turbulence model (b) k-ε turbulence model

4.5.3 The Fourth Thermostat Stage Simulation with Fan

As emphasized in section 4.3.3, the k-ε turbulence model was used for simulations with fan. The suitability of this assumption was investigated. For that purposes, temperature distributions of two vertical lines (V.L-0, 1) which was specified in section 4.5.1.1 were obtained. Then numerical and experimental results were compared through these temperature distributions.

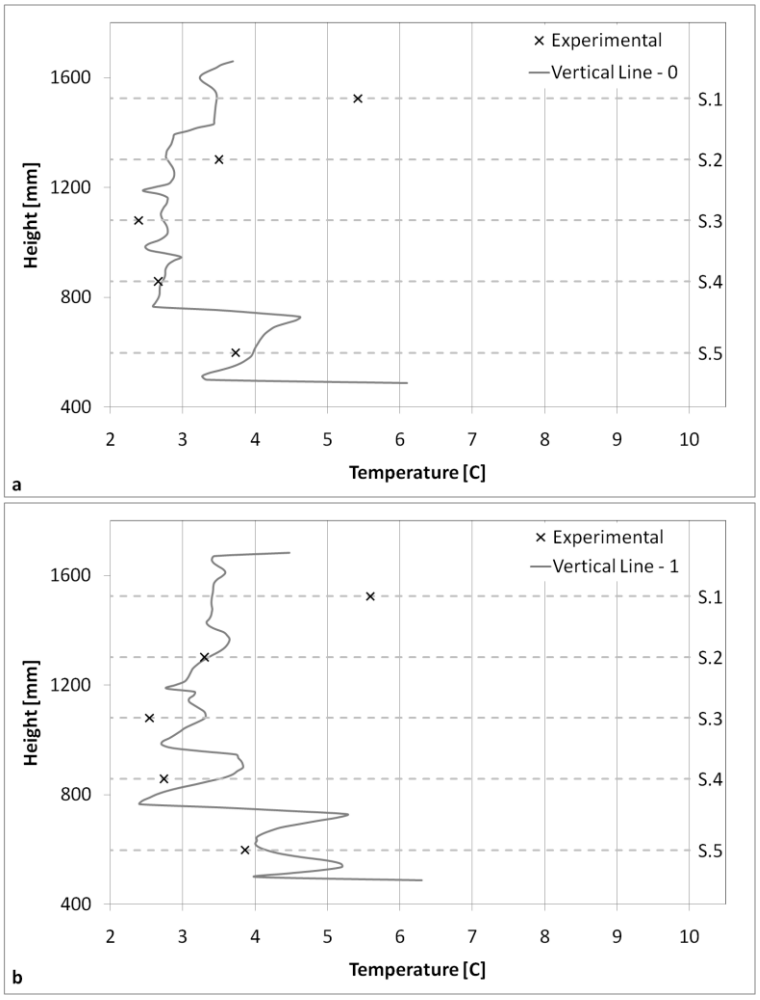

Figure 4.18 The temperature distributions on lines for simulations with k-ε and experimental results at fourth thermostat stage with fan case: (a) Vertical Line-0, (b) Vertical Line-1

Figure 4.18 is shown the temperature distribution on lines and experimental results which are reported in Table 3.8 for with fan case. It can be seen that numerical results are good agreement with experimental ones at the all positions except the S.1 positions in both lines. The maximum difference between numerical and experimental result was ~2.18 C at the S.1 position (top region) in V.L-1. This may due to the fact that the fan has been modeled continuously active. But in the real conditions, the fan activation time depends on the compressor on-off time. This situation causes that the numerical temperatures are colder than the experimental temperatures in these positions. As mentioned before that these positions are the most affected region by fan (see sec. 3.4.2).

Also the comparison of the average temperatures of the vegetable compartment positions is shown in Table 4.10. The temperature of the top vegetable compartments is colder than the bottom vegetable compartment both numerical and experimental results. The differences between numerical and experimental results are 2 C and 0.34 C respectively in top and bottom vegetable compartments.

Table 4.10 The vegetable compartments temperature for simulation and experimental results at fourth thermostat stage with fan case

Vegetable Compartment Position	**Average Temperature [C]**	
	Experimental	**Numerical**
Top	6.43	8.46
Bottom	8.81	9.15

Consequently, according to the above comparison the numerical study was validated through comparing with experimental results. Also for the turbulent flow simulations with fan case, the k-ε turbulence model is good agreement with experimental results by means of the temperature comparisons.

4.5.4 The Fifth Thermostat Stage Simulation with Fan

The predicted temperatures have been compared with experimental results with fan (see Table 3.9). The comparison was carried out on the same lines which were explained in section 4.5.2.1. Temperature distributions on those lines are shown in Figure 4.19.

The maximum differences between experimental and numerical results are observed at S.1 positions on all lines. Among the S.5 positions the maximum difference is observed on V.L-0 the other ones are good agreement with experimental result. In addition the temperature differences with experimental results are approximately 0.5 C on the other positions.

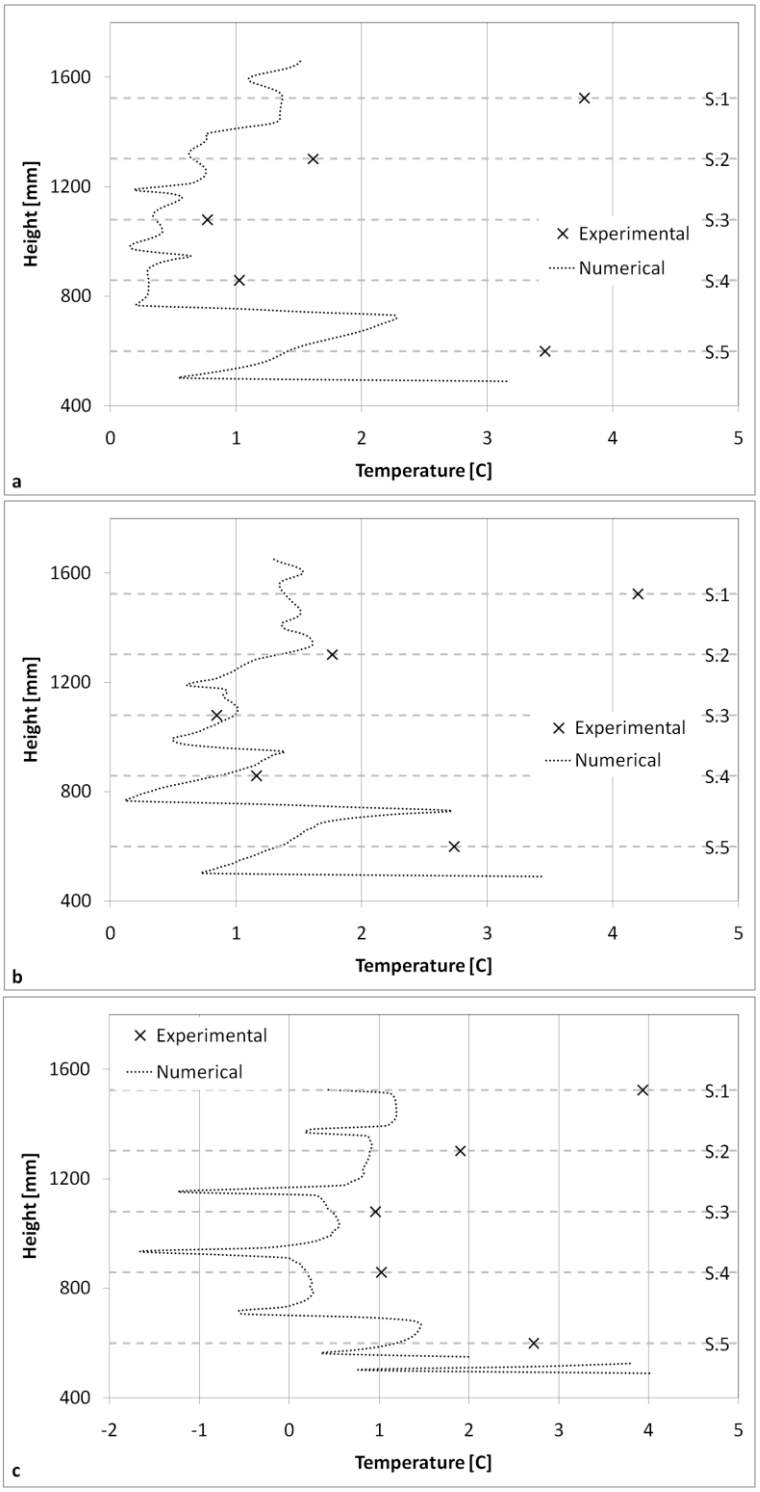

Figure 4.19 The temperature distributions on lines for simulation and experimental results at fifth thermostat stage with fan case: (a) Vertical Line-0, (b) Vertical Line-1, (c) Vertical Line-2

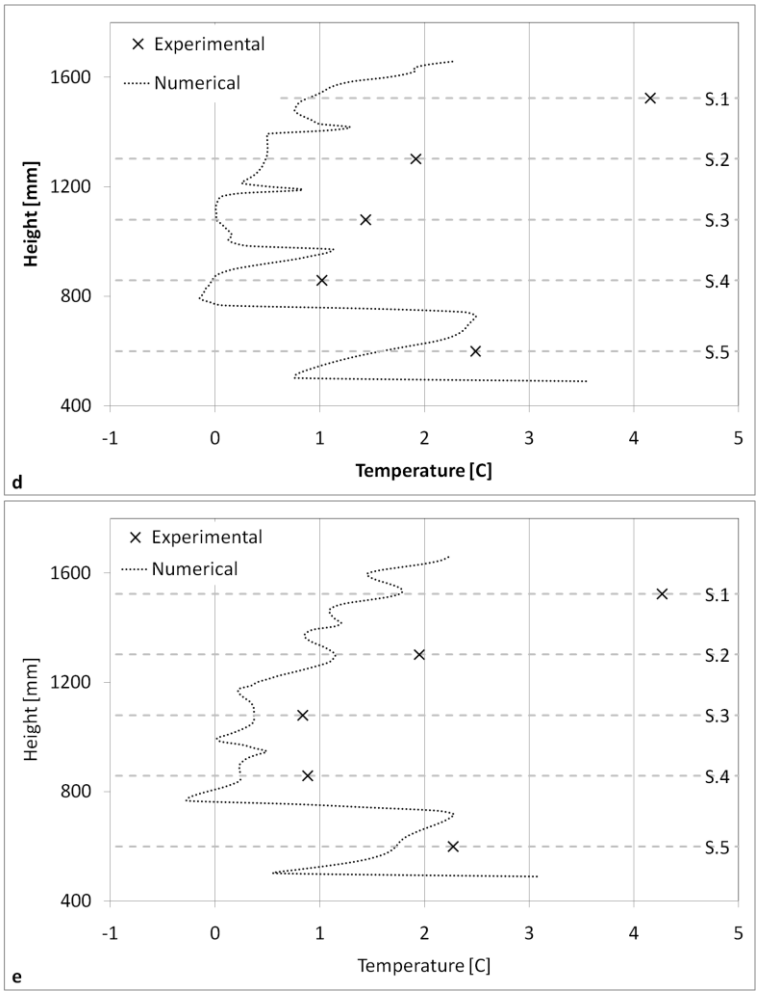

Figure 4.19 (continued) The temperature distributions on lines for simulation and experimental results at fifth thermostat stage and with fan case: (d) Vertical Line-3, (e) Vertical Line-4

The maximum difference is at 3.3 C on the S.1 position on the V.L-3. The mentioned above the all S.1 positions the worst agreement with experimental result on all lines. The same observation was made in section 4.5.3. As emphasized before, assumption of the fan modeling is caused this situation at the top region.

Also the comparison of the average temperatures of the vegetable compartment positions is shown in Table 4.11. The temperature of the top vegetable compartments is colder than the bottom vegetable compartment both numerical and experimental results. The differences between numerical and experimental results are 1.3 C and 1 C respectively in top and bottom vegetable compartments.

According to the above comparison the accuracy of the numerical results are validated for fifth thermostat stage and with fan case.

Table 4.11 The vegetable compartments temperature for simulation and experimental results at fifth thermostat stage with fan case

Vegetable Compartment Position	**Average Temperature [C]**	
	Experimental	**Numerical**
Top	6.2	4.9
Bottom	7.96	6.95

4.6 The Effect of the Transient Analysis

The transient analysis was carried out for investigating the effect of the transient assumption on the numerical results. For that purposes the fifth thermostat stage with fan case was solved with usage maximum 0.1 s time steps interval.

The temperature distributions on Plane-A were obtained for every 0.5 s. Then the animation was created with usage these temperature distributions. After the investigation the created animation, some periodic regions were observed. The periodic regions were shown in Figure 4.20. The temperatures except these regions were not changed during the animation.

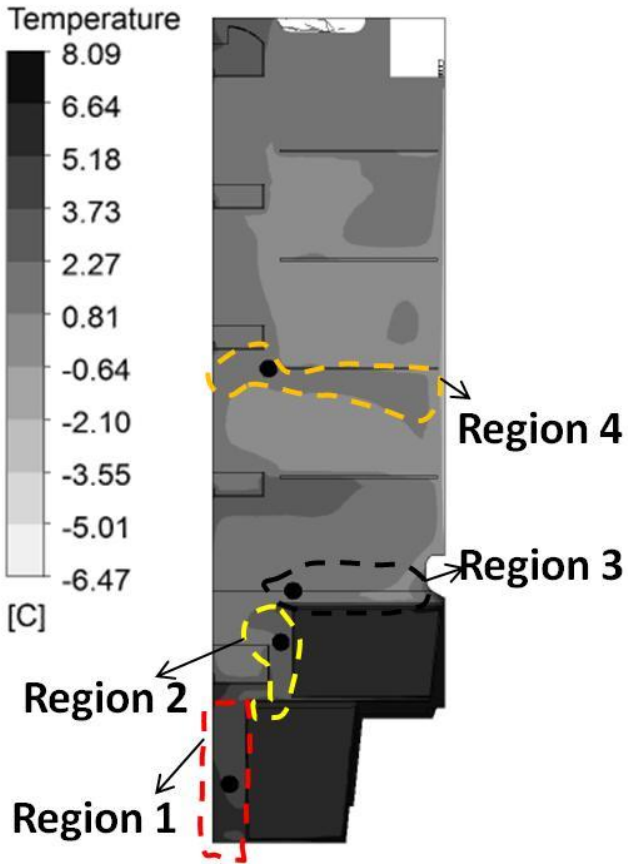

Figure 4.20 The periodic regions at transient analysis and its points

In addition to comparison the steady-state and transient results, time average temperatures were calculated in the transient results. For this purposes four points which were in periodic regions, were created and shown in Figure 4.20. The time average temperatures of these points were compared with the temperatures of the same points with steady-state analysis and reported in Table 4.12. It can be seen that the time average temperatures are good agreement with the steady-state temperature except region one. The maximum difference was observed in region-1 and was 0.81 C. This result showed that the temperature fluctuation range of the region-1 is greater than the other ones.

The temperature-time curves on points were obtained to observe the temperature fluctuations and shown in Figure 4.21. It can be seen that the maximum range observed in region one and this result explained why temperature difference is greater between average of the transient and steady

state results. Also the temperature is slightly fluctuated in region-3 and 4, so these temperatures may be assumed the constant.

Table 4.12 Temperature of the points for fifth thermostat stage with fan simulations

Region No	Average Transient Temperature Result [C]	Steady-State Result [C]	Absolute Difference
1	5,39	4,58	0,81
2	2,32	2,32	0,00
3	1,04	1,16	0,12
4	1,06	1,19	0,13

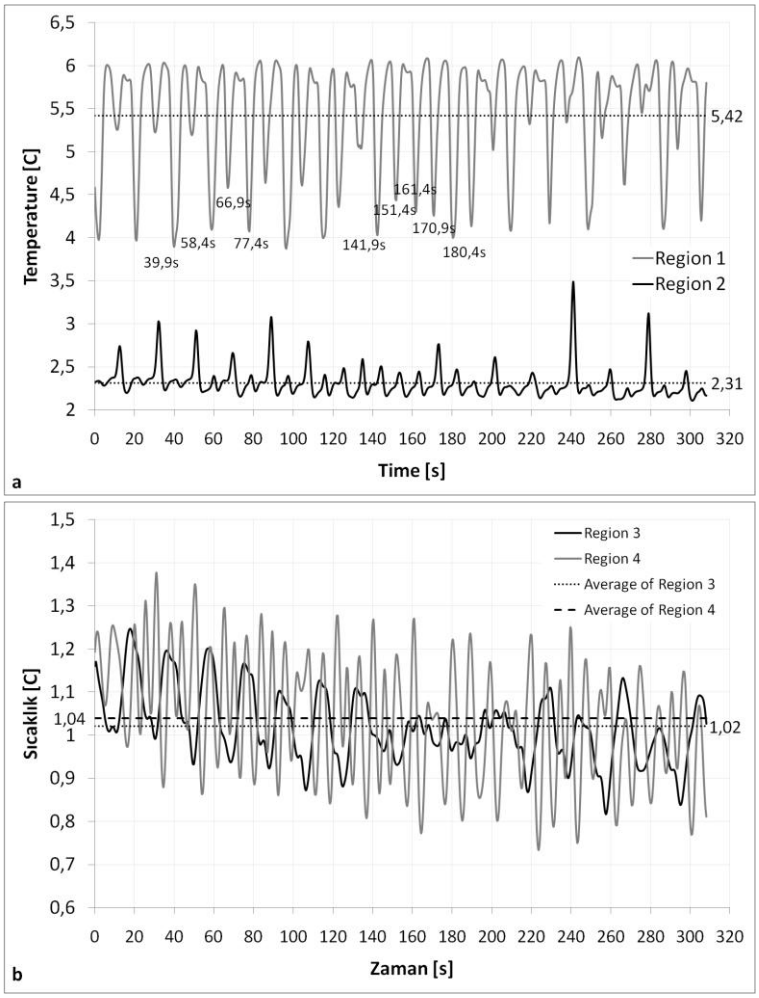

Figure 4.21 Temperature-time curves at region points for fifth stage with fan simulation: (a) Region 1 and 2, (b) Region 3 and 4

Consequently, the steady-state results may be assumed time average of the transient results for the domestic refrigerator. Since the temperature distribution except periodic region ones was not changed, the steady-state assumptions were suitable to investigation the temperature distribution for domestic refrigerator.

4.7 Summary

Firstly the mesh density study was implemented with three different meshes and so it showed that the numerical model was not influenced by changing mesh. Then the effects of the solid domains have been showed and so it decided that the solid domains added the numerical model. Also suitable numerical turbulence models have been selected for this study.

The all generated numerical studies have been validated according to comparison with experimental result. Also transient analysis was implemented with usage steady-state results and showed that the temperature distribution was not change in most regions. Therefore it shows that the implemented all assumptions are suitable for numerical study for investigated type domestic refrigerators.

CHAPTER FIVE

NUMERICAL RESULTS

5.1 The Mixed Convection Effects

To investigation the mixed convection effects, the fifth thermostat stage simulations with and without fan were implemented. The accuracy of the simulations has been validated in section 4.5. Also it should be noted that the fan effect is represented the mixed convection effect. In addition with fan domestic refrigerator is represented brewed type although without fan is represented the static type.

The comparison of the temperature distributions between with and without fan cases are shown in Figure 5.1 on the Plane-A. It can be seen that the top region is the most affected region from the fan effects. The temperature of that region was decreased approximately 5 C with fan. Also effects of the fan reduce from the top to bottom region. Furthermore it is clearly showed that the more uniform temperature was attained with fan effects inherently mixed convection effects in fresh-food compartment.

Therefore the warm zone region at the top of the domestic refrigerator in without fan case has been eliminated with fan. To understanding the improvement of the temperature distribution, the velocity vector maps were compared on the Plane-A (Figure 5.2).

The maximum velocity is 0.3 m/s and 4.68 m/s respectively in without fan and with fan cases. In the with fan case the maximum velocity is occurred bottom of the evaporator surface while in with fan case is occurred near the bottom of the fan box. The velocity scale in Figure 5.2 was taken between 0 – 0.25 m/s because the maximum velocity region was observed in small area of the domestic refrigerator and the more good comparison was made. Also the velocity vectors which were shown in Figure 5.2, were projections on the Plane-A. It can be seen that the stationary air was observed at the top region which was the warm zone in without

fan case. However the stationary air was gained movement with fan effects and this airflow was named as “top horizontal airflow”. Through this airflow, the warm zone which is observed without fan is removed.

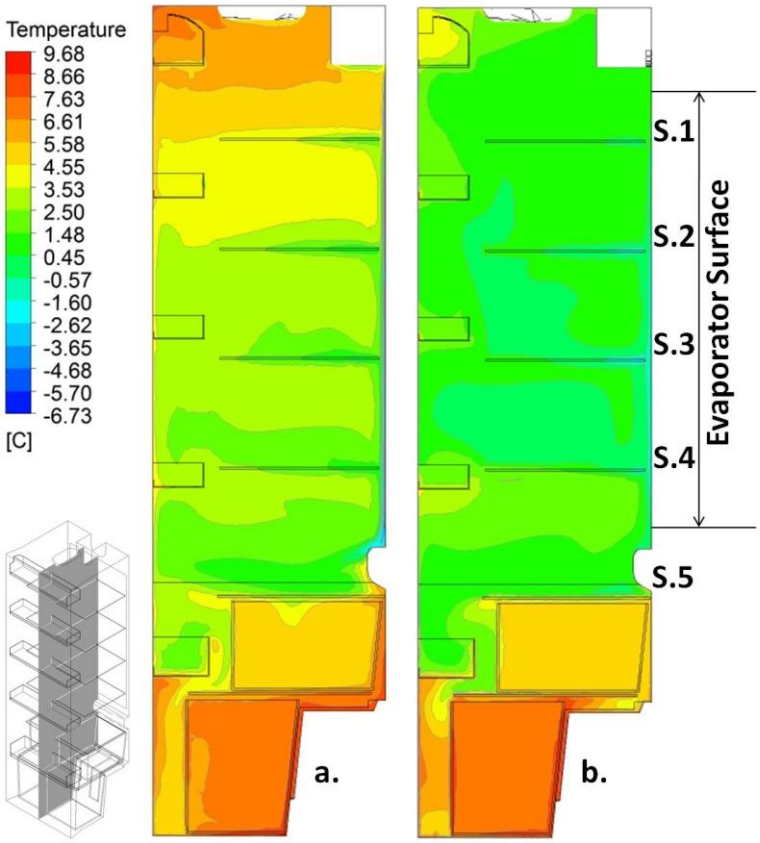

Figure 5.1 Temperature distributions on Plane-A for fifth thermostat stage: (a) Without fan case, (b) With fan case

Also the relatively cold air at the bottom region was moved from bottom to top region through the gaps between the main glass shelves and the door shelves in fan case and was named as “front airflow”. However in the without fan case this airflow is weak. Through this airflow in fan case, cold air which came above the shelf-5 was prevented flowing to front of the bottom vegetable basket. Therefore temperature of the region between the bottom vegetable basket and the door is slightly increased with fan effects.

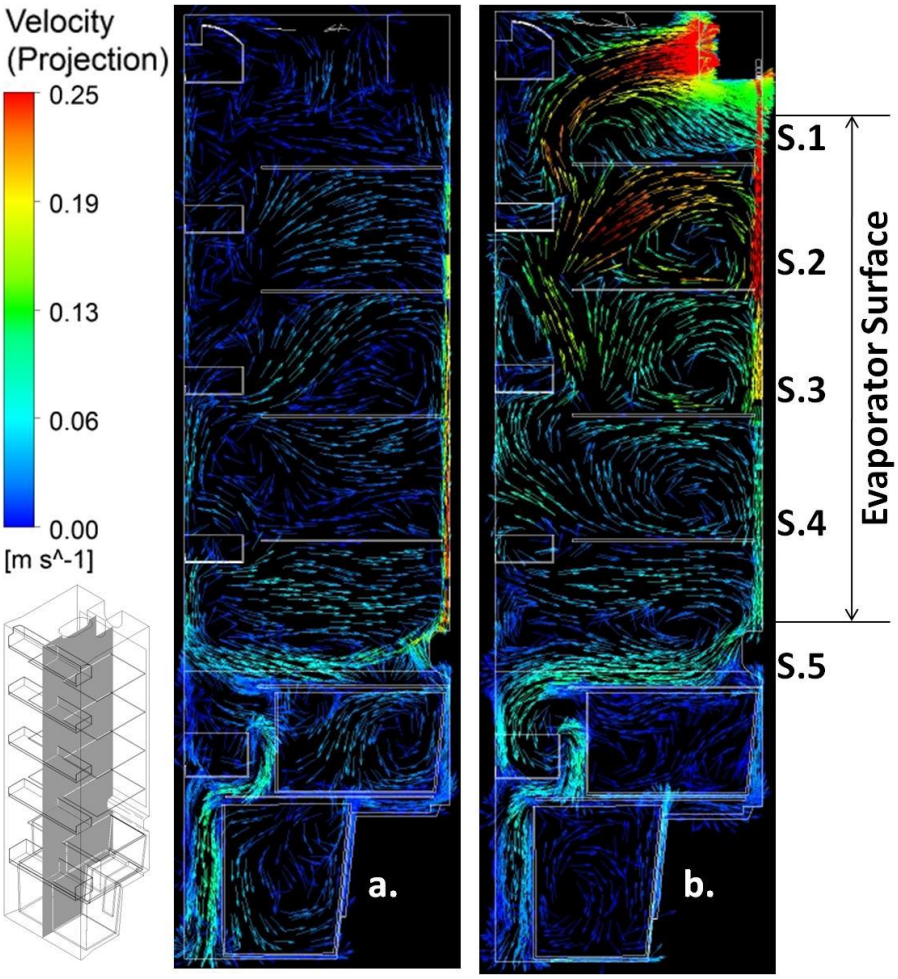

Figure 5.2 Velocity vector maps on Plane-A for fifth thermostat stage: (a) Without fan case, (b) With fan case

Through the described above two consecutive airflows which are the “front airflow” and the “top horizontal airflow”, warm zone at the top of the domestic refrigerator which observed in without fan case was removed in with fan effects.

In addition the speed of the cold airflow which is above the shelf-5 and was named as “bottom horizontal airflow” was increased with fan effects. So that cold airflow is more affected the vegetable compartment comparing with the without fan case. Therefore the small warm region which is the top vegetable compartment is removed with fan effects.

Also air flows from top of the evaporator to the bottom through the gap between the main glass shelves and the back wall in both cases. And this airflow was named as “main cold airflow”.

In addition the main air circulation which includes “main cold airflow”, “bottom horizontal airflow”, “front airflow” and “top horizontal airflow” was observed in both cases. But the main air circulation in fan case was observed clearly. This main airflow was indicated in the literature which was shown in Figure 1.12. Also indicated air recirculation at the bottom corner in Figure 1.12 was observed at the bottom door shelf in both cases (Figure 5.2) in this study.

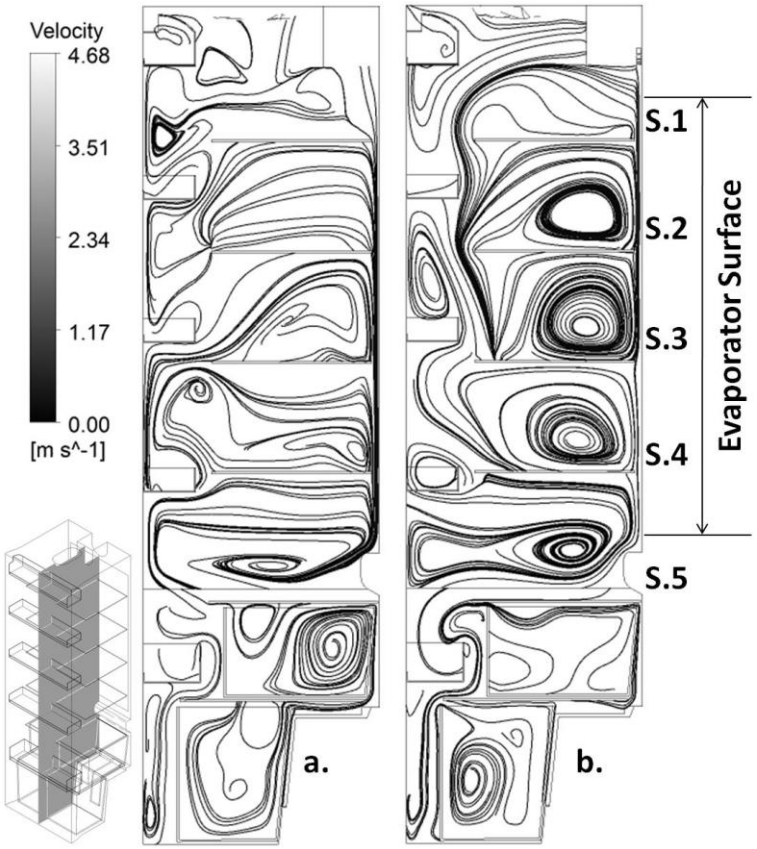

Figure 5.3 Streamlines on Plane-A for fifth thermostat stage: (a) Without fan case, (b) With fan case

When the temperature distribution is investigated in fan case, the very low temperatures which are near the 0 C are observed at shelf-2, 3 and 4 regions. This situation may cause the product freezing. So to find the reason of this low temperature, the streamlines were obtained both two cases and were shown in Figure 5.3. It can be seen that the air re-circulations were observed at these regions in fan case. And it believed that these air re-circulations are caused the more heat transfer from the evaporator surface and cold air flow is prevented from these regions to the other regions. So temperature of these regions is colder than the other

ones. This situation may be removed by increasing the gaps between the main glass shelf-2, 3 and 4 and back walls.

Also the investigation the v-velocity contour maps are agreed with the suggestion of increase the gaps. Figure 5.4 shows that the velocity gradients are greater than those gaps in fan case. So the “main cold airflow” is prevented in fan case. Otherwise in without fan case the gap between the main glass shelves and the back wall is suitable for the “main cold airflow”.

Consequently the undesirable situation which is the warm zone at the top of the domestic refrigerator is removed with mixed convection effects. And also more uniform temperature distribution is attained.

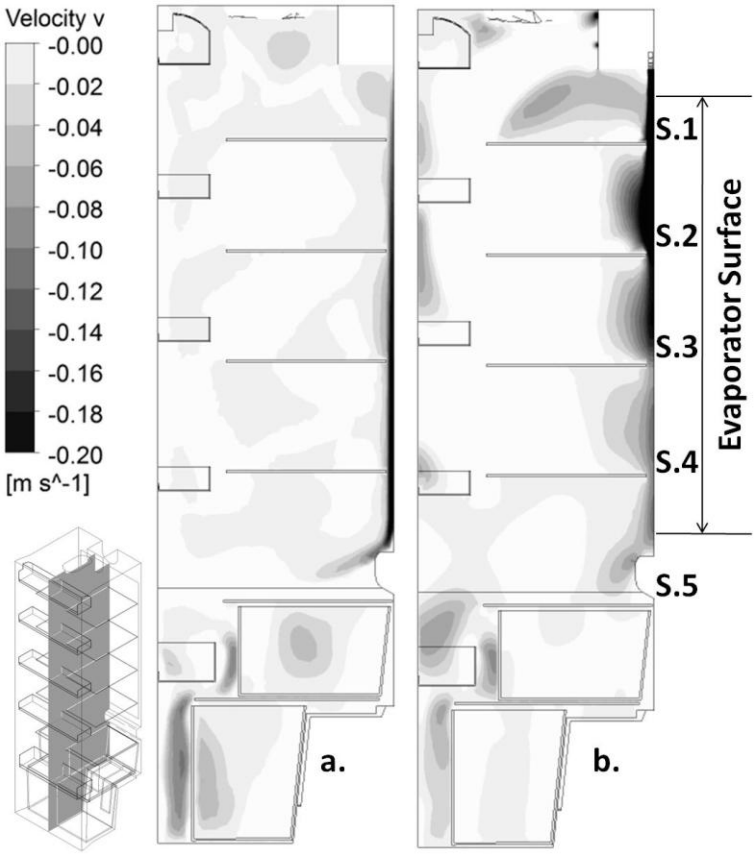

Figure 5.4 Velocity-v direction contour maps on Plane-A for fifth thermostat stage: (a) Without fan case, (b) With fan case

5.2 The Effects of the Evaporator Surface Temperature

To investigation the evaporator surface temperature effects, the without fan (static type) simulations were implemented for fourth and fifth thermostat stage cases. The evaporator temperature is -3.16 C (see Table 3.3) and -6.727 (Table 3.10) in fourth and fifth thermostat stage cases respectively.

The temperature distributions on Plane-A are shown in Figure 5.5. It can be seen that temperatures were decreased in whole domestic refrigerator with decreasing evaporator surface temperature. The temperature decrease is approximately 2 C in whole regions except the top region. Temperature decrease of the top region is approximately 1 C so this zone is the least affected region with evaporator temperature effects. Although temperatures are decreased with decreasing evaporator temperature, thermal uniformity in the fresh-food compartment is not attained. Also the maximum and average temperatures are reported in Table 5.1 for top inner air and bottom inner air domains. Table shows that temperatures are decreased approximately 2 C too.

Table 5.1 The maximum and average inner air temperatures for fourth and fifth thermostat stages for without fan

Domain	**Maximum Temperature [C]**		**Average Temperature [C]**	
	Fourth Stage (-3.16 C)	Fifth Stage (-6.727 C)	Fourth Stage (-3.16 C)	Fifth Stage (-6.727 C)
Top Inner Air	10.6	8.77	5.47	3.02
Bottom Inner Air	12.91	11.33	7.95	5.86

To comparison the velocity vector maps with fourth and fifth thermostat stages showed that the approximately same flow fields were observed (Figure 5.6). Only the “bottom horizontal airflow” was slightly changed. This may be due to the fact that the “main cold airflow” speed in fifth thermostat stage case is slightly higher than the fourth thermostat stage case. Increasing the “main cold airflow” is shown in Figure 5.7. The velocity distributions were occurred on the line which was middle line of the gap between the evaporator surface and the main glass shelves on Plane-A. And the top of the line is the top of the evaporator surface and bottom of the line is the water tray surface. The maximum velocity is occurred at the bottom

of the evaporator surface in both cases. Therefore the “main cold airflow” speed is increased with decreasing the temperature of the evaporator surface.

Also the v-velocity contour maps were shown in Figure 5.8. It can be seen that the velocity gradient thickness near the shelf-3 is slightly greater than the gap, so the “main cold airflow” is slightly affected. An inner design suggestion may be made that the gap between the shelf-3 and the back wall should be slightly increased.

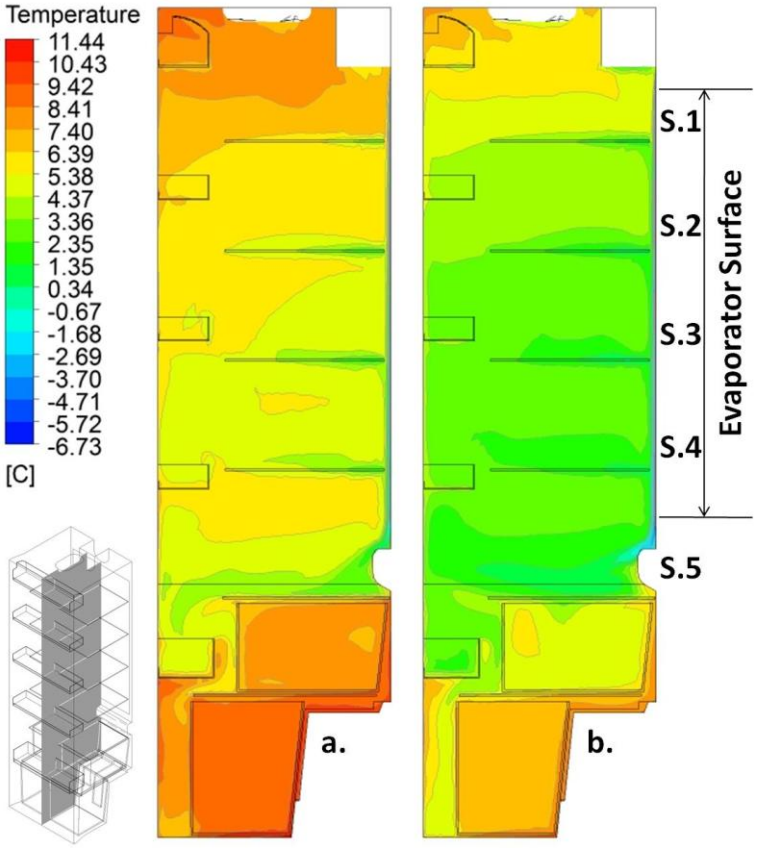

Figure 5.5 Temperature distributions on Plane-A for without fan: (a) Fourth thermostat stage case, (b) Fifth thermostat stage case

In addition observation of the streamlines on Plane-A (Figure 5.9) shows that the weak air re-circulations occur especially S.3, 4 and 5 regions with increasing the temperature of the evaporator surface. And this situation is a source of decreasing the temperatures of the inner air at these regions.

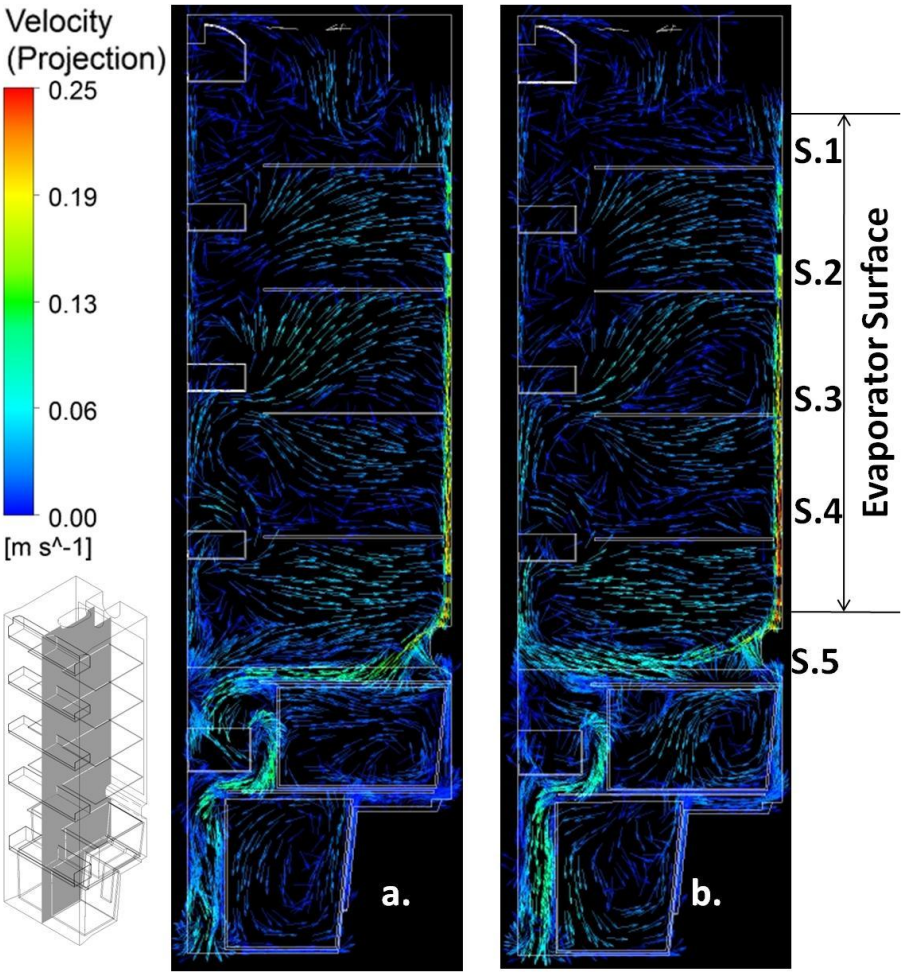

Figure 5.6 Velocity vector maps on Plane-A without fan: (a) Fourth thermostat stage case, (b) Fifth thermostat stage case

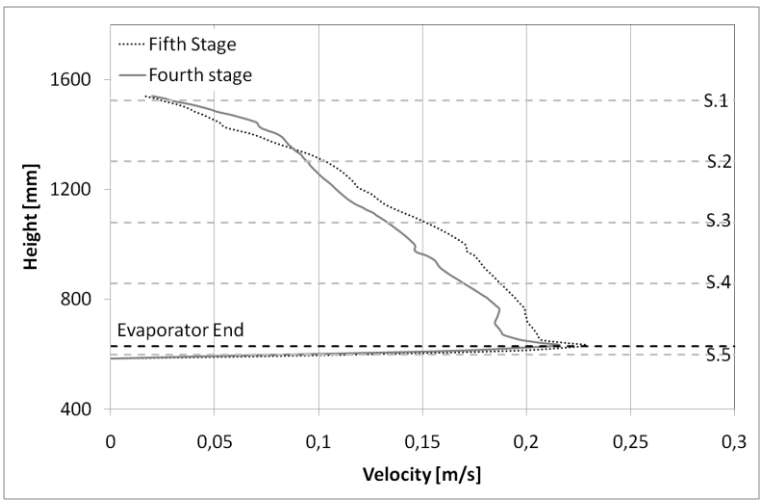

Figure 5.7 Velocity distributions on line near the evaporator surface on Plane-A for without fan case

Consequently temperatures are decreased with decreasing the evaporator surface temperature. However the uniform temperature distribution is not

attained with altering the temperature of the evaporator surface. Also maximum velocity is slightly increased with increasing the temperature of the evaporator surface.

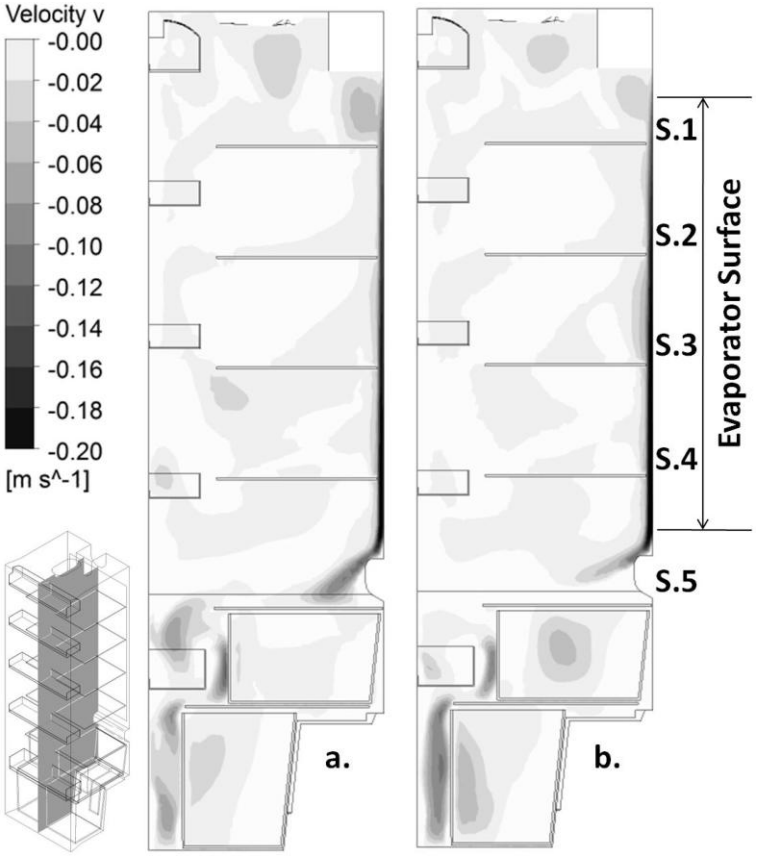

Figure 5.8 Velocity-v direction contour maps on Plane-A without fan: (a) Fourth thermostat stage case, (b) Fifth thermostat stage case

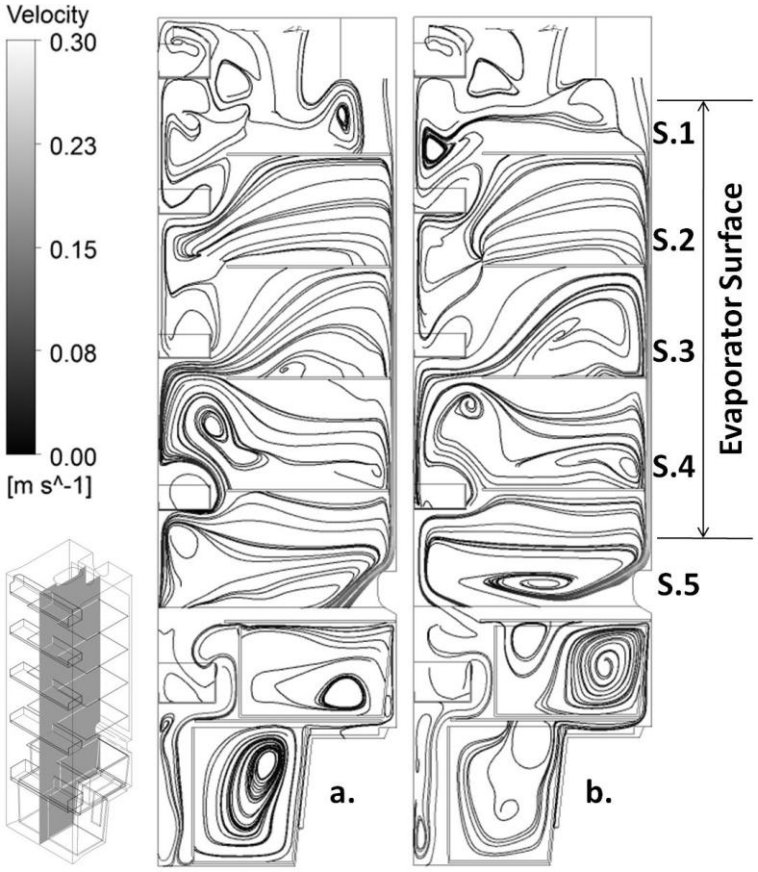

Figure 5.9 Streamlines on Plane-A without fan: (a) Fourth thermostat stage case, (b) Fifth thermostat stage case

5.3 The Effects of the Loaded Condition

The effects of the loaded condition were investigated for the fifth thermostat stage without fan cases. For those purposes the domestic refrigerator was stored with test packages according to the standard of ISO 15502 (2005) (Figure 4.5). It should be noted that this storage plain is an ideal situation so the real situation may be difference from this plain. To investigation of loaded condition effects, results of the simulations with the empty and loaded cases were compared.

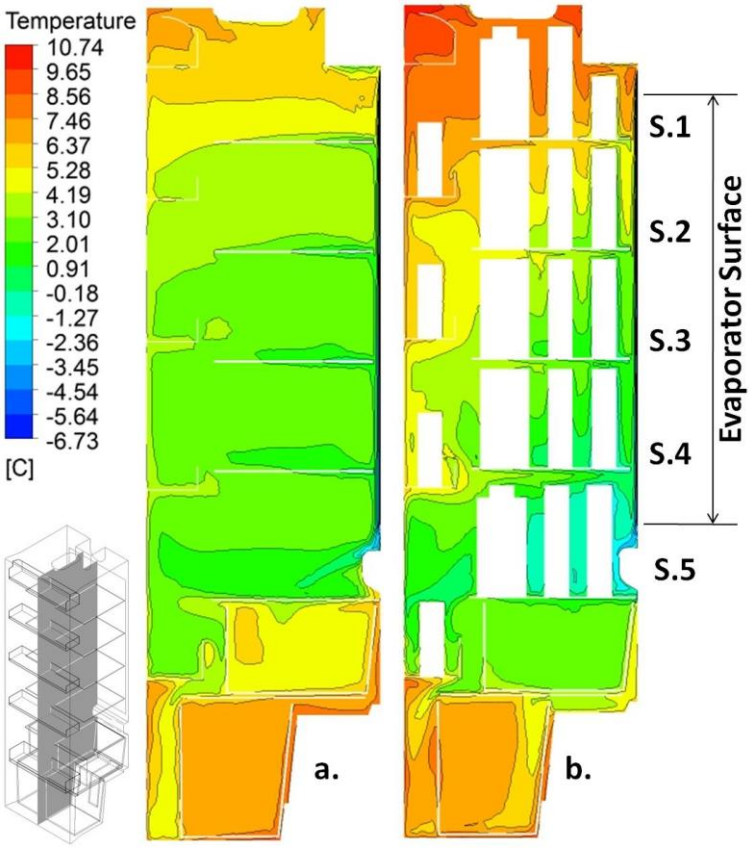

Figure 5.10 Temperature distributions for fifth thermostat stage without fan simulations: (a) Empty case, (b) Loaded case

Temperature distributions on plane which was situated 10 mm right side from Plane-A, were obtained and shown in Figure 5.10. The reason of the distance from Plane-A is to include the loads. It can be seen that the top region get warmer with loaded case. Temperatures of the top region were increased approximately 2 C. Otherwise in the S.5 region, temperatures were approximately decreased 2.5 – 3 C. The reason of the temperature decreases may be the prevention of the main cold airflow and keep it in S.5 region. Also temperatures of the top vegetable compartment were decreased by the keeping cold air in S.5 region. In addition the average temperature of the upper inner air domain is increased from 3 C to 5.25 C. These results show that thermal uniformity gets worse.

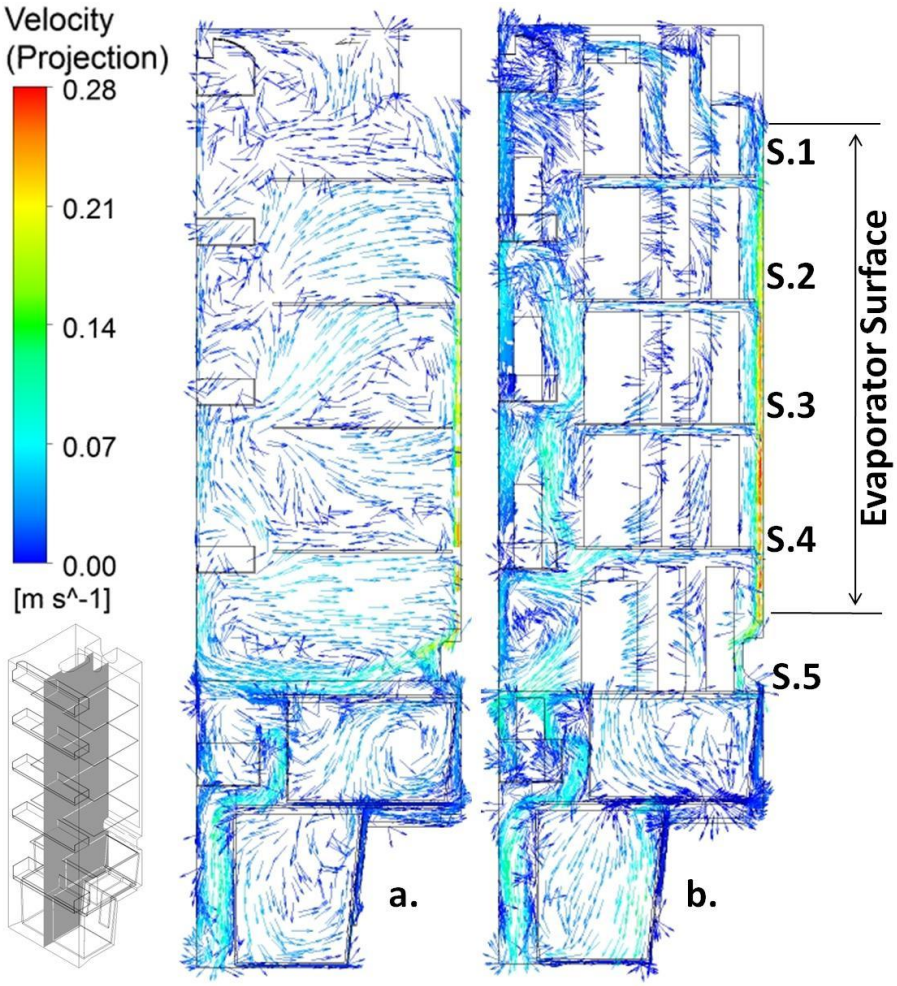

Figure 5.11 Velocity vector maps for fifth thermostat stage without fan simulations: (a) Empty case, (b) Loaded case

To more understanding the effects of the loaded conditions, velocity vector maps were created on same plane and shown in Figure 5.11. It can be seen that the main cold airflow were prevented by loads which were on the shelf-5. So the cold air was not flow to the other region and S.5 region temperatures were decreased. Also the maximum velocity is increased from 0.3 m/s to 0.4 m/s at the main cold airflow in whole compartment with loaded conditions. In addition the front airflow is higher in the loaded case. These situations are due to the occurring channel effects between the back wall and loads and between the door shelves and loads. Also the reason of the increasing temperature at the top region is warm airflow from bottom to top via front airflow. And coming warm air is collect at the top region because the prevention of the loads in shelf-1.

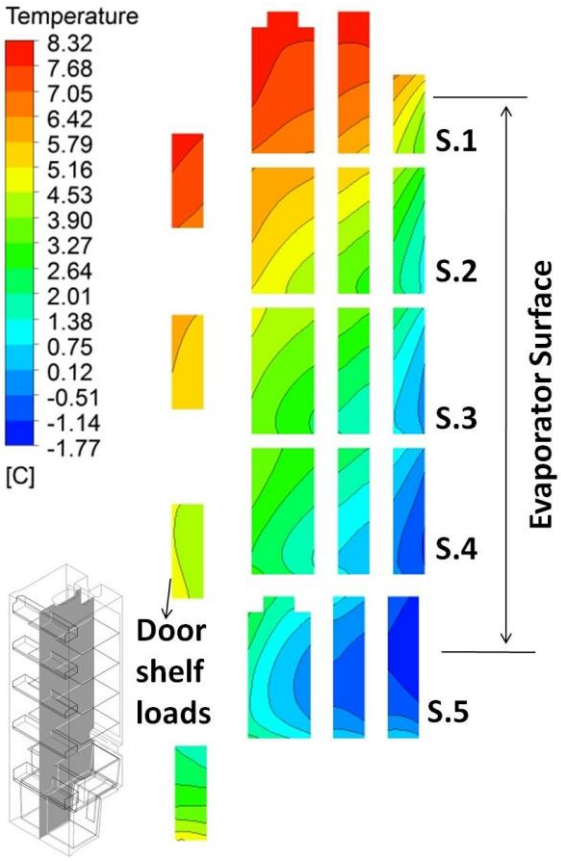

Figure 5.12 The temperature distribution of the loads for fifth thermostat stage without fan simulation

In addition temperature distribution on the loads on same plane was shown in Figure 5.12. It can be seen that the temperature of the loads on the shelf-5 is under the 0 C. So this situation may be occurred freezing of the products. The same situation is observed loads which are near the back wall on the shelf-3 and 4.

Consequently the thermal condition gets worse with loaded case. It should be noted that this investigation made for static type domestic refrigerators and maybe the thermal condition with loaded case will be improved by the mixed convection as the empty case situation in section 5.1. Also temperature distribution of the loads shows that the more perishable food is placed at the bottom of the refrigerator. In addition a suggestion is made that the S.5 region may be converted the chiller compartment with closed the front of the region.

5.4 Determination of the Most Effective Inner Design Parameters

The inner design parameters of the investigated brewed and static type domestic refrigerators have been determined according to the indicated conclusions in above sections.

5.4.1 The Gap Between the Main Glass Shelves and the Back Wall

Whatever the presence of fan and temperature of the evaporator surface, it shows that the “main cold airflow” which ensures desirable temperature in whole region, is moved the gap between the main glass shelves and the back wall (includes evaporator surface). So this gap is selected an inner design parameter. The suitable value of this gap is changed depend on the presence of the fan or evaporator surface temperature. The value of gap should be specified by observation of the temperature and velocity gradient on the back wall for each domestic refrigerator types.

5.4.2 The Gap Between the Main Glass Shelves and the Door Shelves

Especially in the brewed type (with fan case) the gap between the main glass shelves and the door shelves is importance for moving the “front airflow”. If this gap is close or very small value, the relatively cold air at the bottom region is not moved to top region and so the temperature difference between bottom and top region is increased and so thermal uniformity is not attained. The value of this gap should be specified by observation of the temperature contour and velocity vector maps or streamlines.

5.4.3 The Evaporator Surface Temperature

In both static and brewed type domestic refrigerators, the evaporator surface temperature is an important inner design parameter. This parameter is affected the velocity especially in the static type refrigerator. In other hand this parameter is affected more to ensuring the desirable inner air temperatures.

Also the refrigeration cycle system is connected with the numerical domain system via the evaporator surface temperature. So the specified evaporator surface temperature by the numerical investigation is directly affected the refrigeration cycle system design for both investigated static or brewed type domestic refrigerator.

In addition it should be noted that the calculated time average evaporator surface temperature by experimental study is used in the numerical investigation. As emphasized in section 3.4.1 that average temperature of the evaporator surface is depended on the maximum and minimum points of the fluctuation of the evaporator surface temperature. If the desirable conditions are attained with higher evaporator surface temperature compare with old one by numerical investigation, this means that the minimum temperature of the evaporator surface may be increased. In the other words, this means that difference between the evaporator and condenser temperature (inherently pressure difference) is reduced and work-input by the compressor is reduced and so the energy consumption is reduced. This situation was emphasized in section 1.2.8.1. The specified evaporator surface temperature by the results of numerical investigations should be evaluated this thought.

Actually increasing the evaporator surface temperature depends on the air side convective coefficient. If this coefficient is increased, the evaporator surface temperature is increased. The air side convective coefficient depends on the "main cold airflow" in investigated domestic refrigerator. The "main cold airflow" is affected by the gap between the main glass shelves and the evaporator surface and the presence of the fan. Consequently the evaporator surface temperature depends on the other inner design parameters.

5.4.4 The Evaporator Length (or Area)

The maximum velocity is observed at the bottom of the evaporator surface in the static type domestic refrigerator case. So it shows that the longer the evaporator length the higher the velocity. Also this length is directly depends on the evaporator area. And this area is related to the heat transfer. So this parameter is determined as an inner design parameter.

5.4.5 The Fan Box Location

Emphasized parameter in the section 3.4.3 which is the fan box location is determined as an important inner design parameter. The velocity vector map on plane which is the middle plane of the gap between the main glass shelves and the evaporator surface is shown in Figure 5.13. It can be seen that the inlet velocity from the discharge grilles is not uniform. This situation is obtained in experimental study (see sec. 3.2.3) too. The more airflow is moved left side instead of the evaporator surface. The air side heat transfer coefficient on the evaporator surface may be adversely affected this situation. So the fan box location is determined an important inner design parameter to improvement the air side heat transfer coefficient.

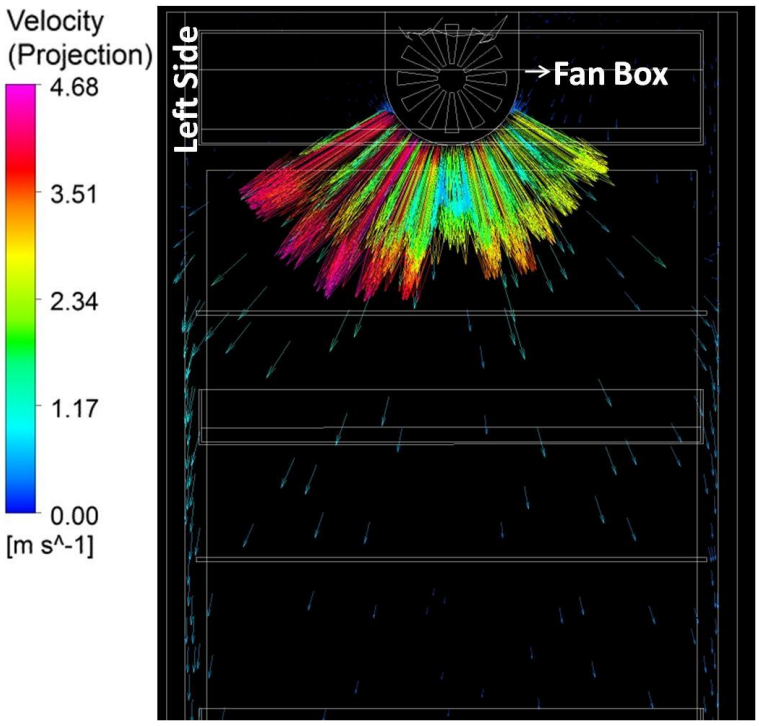

Figure 5.13 Velocity vector map on the fan box discharge grilles and following vectors on near the evaporator surface

5.5 Summary

Indicated the above comparisons and observations are collected as follows.

- Observed warm zone in the static type refrigerator is a problem for attaining the desirable temperature range and thermal uniformity.

- The added fan in static type domestic refrigerator is accomplished that problem via occurred mixed convection effects at problematic zone. Also thermal uniformity is achieved too.
- The decreasing the temperature of evaporator surface is slightly decreased the warm zone temperature but is still the warmest zone in domestic refrigerator. Also thermal uniformity problem is still continued. So changing the evaporator surface temperature is not a solution to improvement the thermal uniformity in investigated type domestic refrigerator.

Also the important inner design parameters are determined with described why are important. In addition it should be noted that the indicated parameters were also determined in literature (see Table 1.4). Furthermore it shows that the determined inner design parameters are affected each other. So the identified the best values should be tried different combinations of these parameters for attained desired conditions in the domestic refrigerator.

CHAPTER SIX

DESIGN STUDY

6.1 Design with Specification of the Best Values

The best values of the some determined inner design parameters were indicated by (Avcı, 2011) which was an optimization study on the same investigated domestic refrigerator in this study. It found the best values via usage numerical parametric study and Artificial Neural Network (ANNs) methods. Besides the determined inner design parameters the average velocity (V_{fan}) of the discharges grilles on the fan box was also determined as parameter. The other ones are: the gap between the main glass shelves and the back wall (t_b) (see Figure 3.2), the evaporator height (H), temperature of the evaporator surface (T_{evap}) and distance from centre of the fan to the left side wall (t_{fan}) (see Figure 3.2). It optimized according to the temperatures of the measurement points which are described in standard of ISO 15502 (2005).

The measurement points are placed at top (T_t), middle (T_m) and bottom (T_b) locations which are described in standard of ISO 15502 (2005) in the fresh-food compartment. In optimization study the following conditions which were the expected conditions during the energy test by standard of ISO 15502 (2005), were described and the best values were found complying with these condition.

- The temperatures of the measurement points are between 0 C and 8 C.
- The average temperature (T_{ave}) of the measurement points has not greater than the 5 C.

The simulations of the designs which were occurred different combinations of the inner design parameters were implemented as same conditions as the fourth thermostat stage with fan simulation (see sec. 4.5.3). Also the accuracy of the numerical study of the new design was assumed as the same value of the current state simulation.

The best values of the inner design parameters were specified according to the desired output conditions and reported in Table 6.1. It can be seen that the desired output conditions are attained with usage numerical study. It should be noted that the best values were specified for 25 C environment conditions.

Table 6.1 The optimized values of the inner design parameters and output conditions (Avcı, 2011)

Parameters	**Design Parameters**					**Output Parameters**			
	t_b [mm]	**H [mm]**	**t_{fan} [mm]**	**T_{evap} [C]**	**V_{fan} [m/s]**	**T_{ave} [C]**	**T_t [C]**	**T_m [C]**	**T_b [C]**
Optimized Design	22	665	140	-2	5.5	4.8	4.66	4.86	4.67

For investigation the suitability of the new design (Figure 6.1.a), temperature distribution on Plane-A was obtained and shown in Figure 6.1.b. It can be seen that temperatures were range between 3 C and 5 C in the fresh-food compartment. Also better thermal conditions should be attaining through adding more output parameters such as point temperature. In addition achieving better the thermal uniformity, the temperature difference between three points should be added as output parameters.

Consequently after the determined important design parameters, the optimum designs will be created according to the desired conditions by numerical studies. Thus a lot of designs are experienced prior the prototype manufacturing.

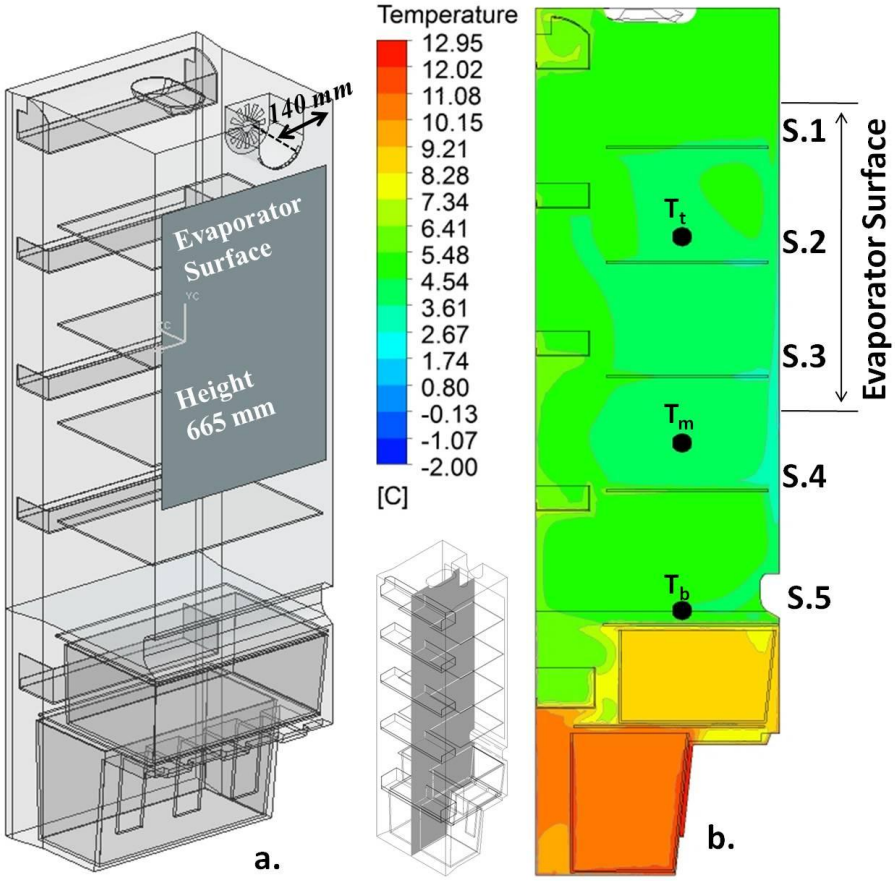

Figure 6.1 (a) New created design, (b) Temperature distribution of the new design on Plane-A (T_t: Top measured point, T_m: Middle measured point, T_b: Bottom measured point)

6.2 Design Suggestion of the Location of the Evaporator Surface

Problem of the static type domestic refrigerator (without fan case) is presence the warm zone region at the top of the domestic refrigerator. This region causes the non-uniform temperature distribution. The added fan which is changed the type of domestic refrigerator from static to brewed is accomplished this warm region and ensure thermal uniformity. The stationary region which is the top of the static type domestic refrigerator is got to move via the fan. So the solution of the problem which is the presence of warm zone in static type is movement of the top region air. So based on this thought, a suggestion is made that a part of the evaporator is located the top wall of the domestic refrigerator. So top air will cold and inherently the density will increase and air will get movement. The aim of this suggestion is that the desired conditions are attained via not usage the fan in the static type

refrigerator. Also heat gain by fan motor is determined at 6 % by (ASHRAE, 2006, chap. 48). The other aim is removing this heat gain.

However there is a problem of this suggestion design. It is the defrost water disposal from the top wall evaporator surface. The defrost water drops the fresh-food compartment and on the surface of food products. This problem may be accomplished via designed new water tray. So water tray is added at the top region in suggestion new design.

6.2.1 New Inner Design

The current and new design domains are shown in Figure 6.2. Evaporator surface was divided seven parts with no change the evaporator area. Five parts were placed on the top wall. Two parts are still on the back wall but separately placed. Also the top section views are exhaustively shown in Figure 6.3. New water tray was inclined placed for condensed water flow at 30 mm below to the top wall. The aim of this distance is prevention the frost on the water tray surface which interactions the inner air which is under the water tray. In addition the top door shelf was taken down to location the new water tray. Further the fan and light boxes are removed. It should be noted the light box was not added in new design but the light location in new design should be placed the under the side walls.

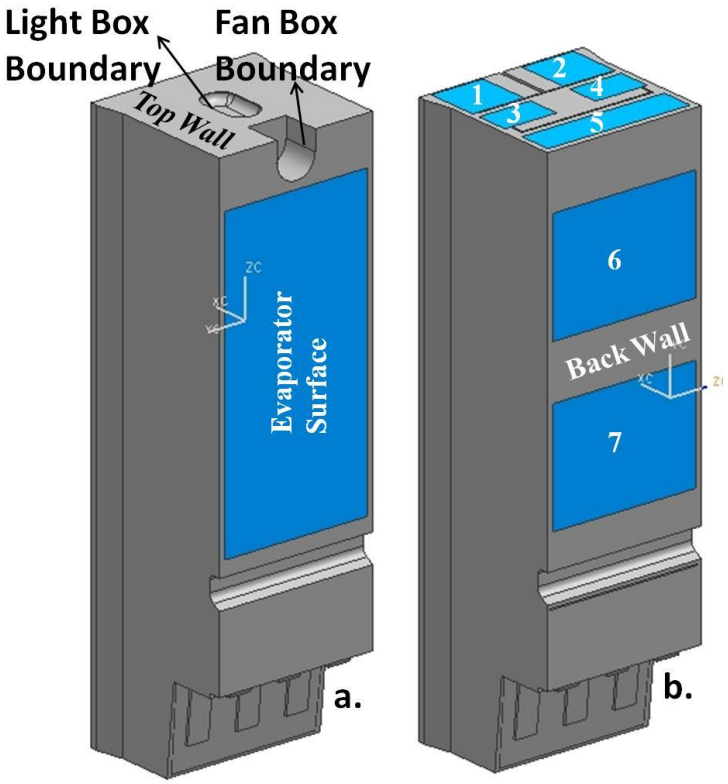

Figure 6.2 Comparing the models: (a) Current (b) New design

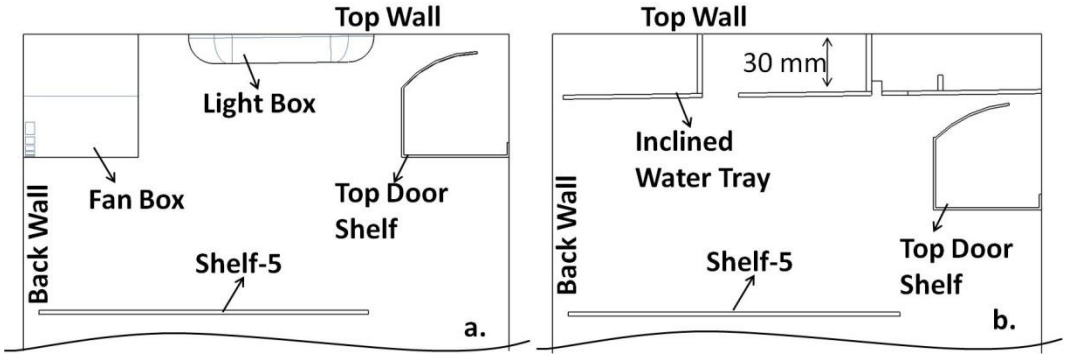

Figure 6.3 The detail section views of the models: (a) Current, (b) New

6.2.2 Water Tray Design

Designed water tray is shown in Figure 6.4. It consists of grilles, guide plates and water blocker. The grilles and guide plates locations were designed according to the observation of the flow fields of the more than one design trials. Water blockers were designed by estimation the defrost water flow line and noted that it is not modeled for the numerical simulations but it is shown schematically in Figure 6.5.

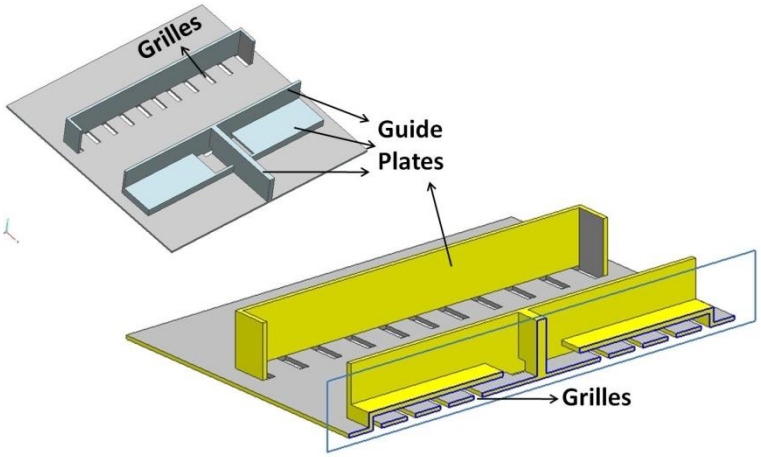

Figure 6.4 Designed water tray

Also water tray is placed inclined from front to back so ensure that frost water is flow to back wall and then it flows the bottom water tray via on the back wall surface. To better understand, inner airflow and defrost water flow are schematically shown in Figure 6.5. The white lines represent the inner airflow while the blue ones are defrost water flow. It should be noted that these flows are expected situation.

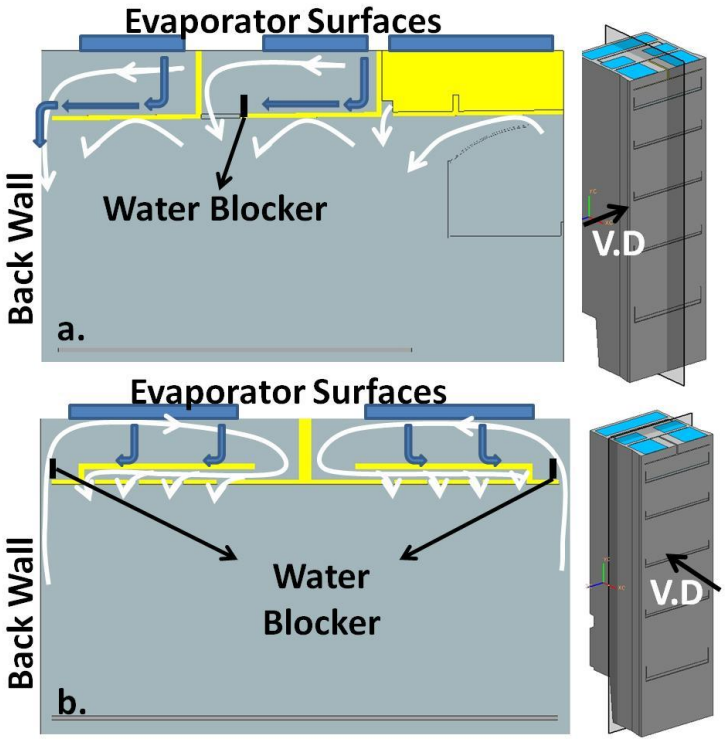

Figure 6.5 The expected inner air and defrost water flows near the water tray: (a) Side section view, (b) Front section view. (V.D: View Direction)

6.2.3 Results

The suggested new design was solved according to the fifth thermostat stage so the evaporator surface temperature assumed -6.727 C (see Table 3.10). Implemented assumptions which were used for the fifth thermostat stage simulation without fan (see sec. 4.5.2) were used too for this simulation. In addition the water tray material was assumed HIPS which is the same material of the inner plastic.

The obtained results have been compared with the current model simulation results which are the fifth thermostat stage with and without fan cases. For comparison, a volume which has warmer than the 5 C which is the desired average temperature in fresh food compartment by standard of ISO 15502 (2005) is created and named as "Warm Volume" and shown in Figure 6.6. It can be seen that the warm top region in the without fan case is removed via fan and new design. But the best case is still with fan case. Also the percentages of the warm volumes are reported in Table 6.2. It shows that the improvement of the new design is closed the fan case. Also it should be noted that this new design is investigated by terms of cooling time.

Table 6.2 Comparison the warm volume percents for fifth stage simulations

Case	**Warm Volume [m^3]**	**Percent of the Warm Volume [%]**
Without Fan	0.102	29.14
With Fan	0.047	13.43
New Design	0.068	19.43

In addition temperature distributions on Plane-A were created for comparison and shown in Figure 6.7. It can be seen that thermal uniformity of the new suggested design is better than the static type (without fan) but slightly worse than the brewed type (with fan) cases. The average temperatures of the upper inner air domain are 3 C, 1.91 C and 1.4 C for the without fan, new and with fan cases respectively.

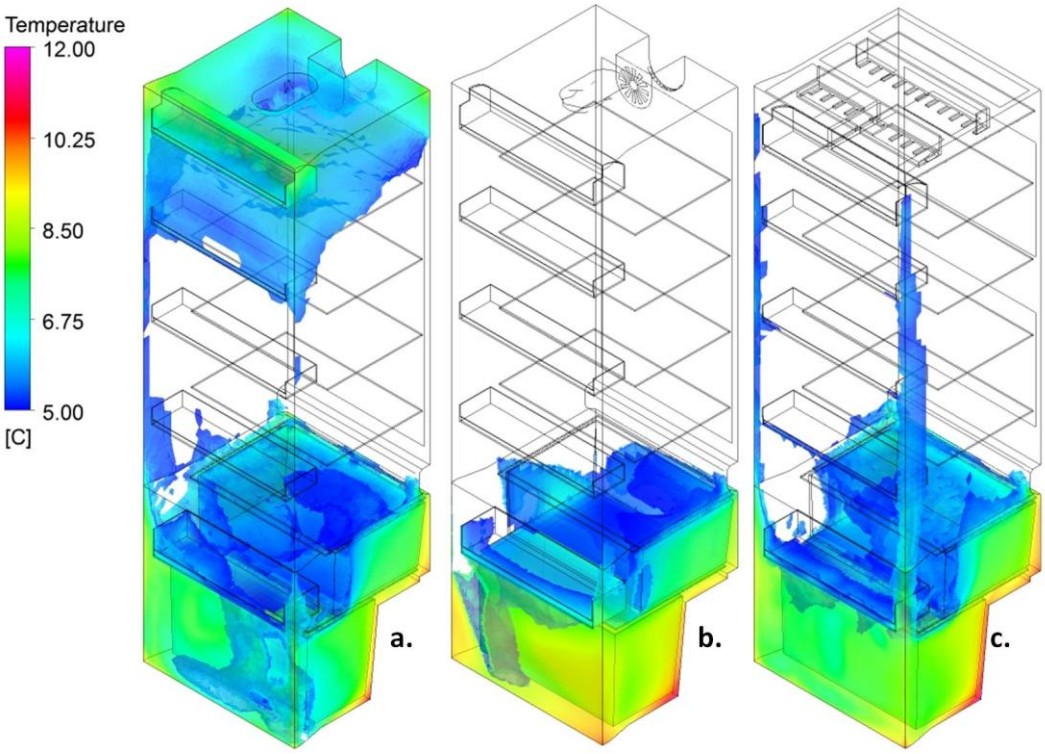

Figure 6.6 Temperature distributions in the warm volume for fifth stage simulations: (a) Without fan case, (b) With fan case, (c) New design case

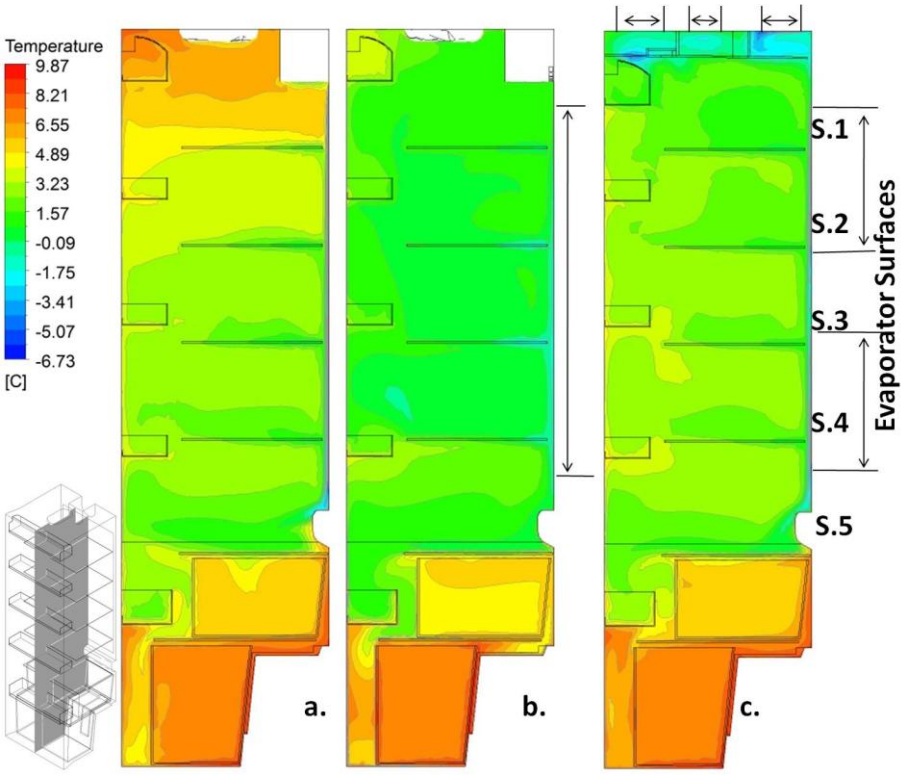

Figure 6.7 The temperature distribution on Plane-A for fifth thermostat stage: (a) Without fan case, (b) With fan case, (c) New case for without fan

Therefore location and reason of the problematic region will be specified with simulations of the current state. Then the suitability of made modifications which are removed the problematic region are investigated with numerical study instead of a lot of experimental studies.

CHAPTER SEVEN

CONCLUSION

Suitable thermal condition in the domestic refrigerator has to be attained for healthy food storage for a long time. This condition is achieved by proper inner air circulation. Inner air circulation also directly depends on the temperature and flow distributions. Also these distributions are attained by suitable inner design of the domestic refrigerator. So the temperature and flow distributions have to be investigated for proper design of the domestic refrigerator.

Design of the domestic refrigerator is expected achieving desired temperatures in different compartments, providing thermal uniformity and rapid cooling. Also design consists of refrigeration system design and inner design. The desired temperatures are achieved by both of the proper refrigeration system and inner designs while thermal uniformity and rapid cooling are achieved by proper inner design. Therefore the aim of this study is investigation of the temperature and flow distributions by means of the achieving desired temperature and providing thermal uniformity. For those purposes static and brewed (static with fan) type domestic refrigerators were investigated by experimental and numerical method.

Numerical studies were carried out with three-dimensional, the solid heat conduction and consideration of the heat transfers via natural convection and radiation. The “Boussinesq” approximation was used for modeling natural convection phenomena while the “Discrete Transfer” approximation was used for modeling the radiation heat transfer. The SST and k-ε turbulence models were selected for respectively in simulations of the static type domestic refrigerator and brewed type domestic refrigerator for turbulent flow. Also the heat gains from the environment were modeled by heat transfer coefficient boundary condition and the evaporator surface was modeled by fixed temperature boundary condition. Also inlet and outlet boundary conditions were used for modeling the fan effects in the simulation of the brewed type domestic refrigerator. In addition both steady-state and transient analyses were implemented and obtained that the results of the steady-

state analysis is time average results of the transient analysis to domestic refrigerators.

Experimental studies were implemented for four different cases which are fourth thermostat stage (-3.16 C evaporator surface temperature) with and without fan and fifth thermostat stage (~-6.5 C evaporator surface temperature) with and without fan. Numerical studies were carried out the same cases with experimental study. Mixed convection and evaporator temperature effects were determined by separately observed the experimental and numerical results. Two observation results were good agreement between each other. Also the predicted temperatures by numerical study were compared with measured temperatures by experimental study. The maximum temperature differences between each other were observed 2.18 C, 1.8 C, 3.3 C and 2.79 C for simulations with respectively fourth thermostat stage with, without fan, fifth thermostat stage with and without fan. All maximum differences were observed at the top region of the domestic refrigerator.

After the validation of the numerical study, results were exhaustively investigated for understanding the inner air circulation. For this purposes temperature and velocity contour maps, velocity vector maps and streamlines were created to investigate the mixed convection, evaporator surface temperature and loaded condition effects. Occurred mixed convection by the help of the fan was removed the warm zone which was observed at the top region of the static type domestic refrigerator and was caused non-thermal uniformity. Although decreasing temperature of the evaporator surface was decreased the whole temperatures, it was not ensured the thermal uniformity. In addition the thermal uniformity was get worse with loaded conditions in the static type domestic refrigerator. Also the warm zone which was stationary was get movement by the help of the fan and so the thermal uniformity was ensured through this movement.

In addition inner air circulation was described. So four airflows were observed: “main cold airflow” flows from top to bottom at the gap between the main glass shelves and the back wall (include evaporator surface), “bottom horizontal airflow” flows from the back wall to the door at the above of the top vegetable compartment lid (shelf-5), “front airflow” flows from bottom to top at the gap between the main

glass shelves and the door shelves and “top horizontal airflow” flows from the door to the back wall at the top region of the domestic refrigerator. Those airflows create the main air circulation. Also the small air recirculation was observed near the bottom door shelves. Described main air circulation and small air circulation are the characteristic of the static and brewed type domestic refrigerators and also these air circulations were determined in the literature for static type.

Also small air re-circulations were observed each space between the each main glass shelves in with fan cases. These air re-circulations caused decreasing the temperature near the 0 C which is occurred freezing of the foodstuffs, especially shelves - 2, 3 and 4. Also velocity gradients on the evaporator surface get greater than the gap between the main glass shelves and the back wall. So it showed that this gap is not suitable for the fan case (brewed type domestic refrigerator). On the other hand horizontal airflows were observed each space between the each main glass shelves in without fan cases. Otherwise air re-circulations were slightly begun through decreasing the temperature of evaporator surface in without fan case.

According to the all observation on the numerical results, the most important inner design parameters which are affected the temperature and flow distributions were determined for static and brewed type domestic refrigerators. These determined parameters are: the gap between the main glass shelves and the back wall, the gap between the main glass shelves and the door shelves, the evaporator surface temperature and the evaporator length (or area). Also the fan box location was determined an important parameter for the brewed type domestic refrigerators. In addition it showed that all inner design parameters were affected each other. So the best values should be specified with comparison of the different combination designs.

Also the two design studies were implemented for indicating the power of the numerical study. One of them was created according to the determined inner design for specification of the best values. The other one was a design suggestion to remove the problematic region which was warm zone for the static type refrigerator. Thus after the current state analyses, the suitability of the new designs

are investigated with numerical studies prior the experimental study or prototype manufacturing.

The new designs were not compared any experimental results. Hence the accuracy of the new design studies is assumed same as the current state simulation studies. So new design trials have to be carried out after the validation of the numerical studies.

The accuracy of the numerical study was validated comparing with measured temperatures through experimental studies. So the predicted of the flow fields were assumed validating. However it may be validated with comparing with flow field which is obtained by Particle Image Velocimetry (PIV) technique. In addition some studies were compared their numerical result of the flow fields with usage this technique in the literature.

Consequently the numerical models were developed for the static and brewed type refrigerators. It showed that the Computational Fluid Dynamics (CFD) with Heat Transfer analysis is suitable for investigation the design parameters of the domestic refrigerators. Also characteristic of inner air circulation was better understood via obtained temperature and flow distributions for the static and brewed type domestic refrigerators. In addition the mixed convection effects were exhaustively investigated. Finally examples of the design study were indicated with usage numerical study.

REFERENCES

Afonso, C., & Matos, J. (2006). The effect of radiation shields around the air condenser and compressor of a refrigerator on the temperature distribution inside it. *International Journal of Refrigeration (29)*, 1144-1151.

Ahlborn Mess - und Regelungstechnick GmbH. (2009). *ALMEMO Manual* (8th ed.).

Amara, S. B., Laguerre, O., Charrier-Mojtabi, M.-C., Lartigue, B., & Flick, D. (2008). PIV measurement of the flow field in a domestic refrigerator model: Comparison with 3D simulations. *International Journal of Refrigeration (31)*, 1328-1340.

American Society of Heating, Refrigerating and Air-Conditioning Engineers [ASHRAE]. (2006). ASHRAE handbook - Refrigeration.

ANALYSIS SYSTEM (ANSYS) CFX, Release 12.1. (2009). User's guide.

Anderson, E. (2004). *Refrigeration home & commercial* (5th ed.). WILEY.

Avcı, H. (2011). Computer aided analysis and experimental investigations towards optimizing the design parameters of domestic refrigerator. *M.Sc. thesis, Dokuz Eylül University graduate school of natural and applied sciences at Turkey*.

Azzouz, K., Leducq, D., & Gobin, D. (2009). Enhancing the performance of household refrigerators with latent heat storage: An experimental investigation. *International Journal of Refrigeration (32)*, 1634-1644.

Cao L.H. (2009) Experiment and numerical research on compression/injection hybrid refrigeration cycle in household refrigerators. *M.Sc. thesis, School of Energy Science and Engineering, Central South University at China*, (Chinese version).

Cortella, G., Manzan, M., & Comini, G. (2001). CFD simulation of refrigerated display cabinets. *International Journal of Refrigeration (24)*, 250-260.

Cortella, G. (2002). CFD-aided retail cabinets design. *Computers and Electronics in Agriculture (34),* 43-66.

Çengel, Y. A., & Boles, M. A. (2006). *Thermodynamics an engineering approach* (5th ed.). McGraw-Hill.

Çengel, Y. A., & Cimbala, J. M. (2006). *Fluid mechanics:Fundementals and applications.* McGraw-Hill.

Çengel, Y. A. (2007). *Heat and mass transfer:A practical approach* (3rd ed.). McGraw-Hill.

Çengel, Y., Akgün, E., & Arslantaş, S. (2009). Verimsiz eski buzdolaplarının yüksek verimli yenileriyle değiştirilmesi. *1. National Energy Efficiency Forum.* Istanbul.

D'Agaro, P., Cortella, G., & Croce, G. (2006). Two- and three-dimensional CFD applied to vertical display cabinets simulation. *International Journal of Refrigeration (29),* 178-190.

Dinçer, İ., & Kanoğlu, M. (2010). *Refrigeration systems and applications* (2nd ed.). WILEY.

Ding, G.-L., Qiao, H.-T., & Lu, Z.-L. (2004). Ways to improve thermal uniformity inside a refrigerator. *Applied Thermal Engineering (24),* 1827–1840.

Emissivity values for common materials. (n.d.). Retrieved July 7, 2011, from http://www.infrared-thermography.com/material-1.htm

Flir Systems. (2010, May 10). Installation manual - SC3XX and SC6XX series.

Foster, A. M., Madge, M., & Evans, J. A. (2005). The use of CFD to improve the performance of a chilled multi-deck retail display cabinet. *International Journal of Refrigeration (28),* 698-705.

RefrigeratorExpert (n.d) *French doors refrigerators*. Retrieved May 1, 2011, from http://www.refrigeratorexpert.com/french-door-refrigerators.html.

Fukuyo, K., Tanaami, T., & Ashida, H. (2003). Thermal uniformity and rapid cooling inside refrigerators. *International Journal of Refrigeration (26)*, 249-255.

Griffith, B. T., Arasteh, D., & Türler, D. (1995). Energy efficiency improvements for refrigerator/freezers using prototype doors containing gas-filled panel insulating systems. *46th International Appliance Technical.* Urbana.

Gupta, J. K., Gopal, M. R., & Chakraborty, S. (2007). Modeling of a frost-free refrigerator. *International Journal of Refrigerator (30)*, 311-322.

Hermes, C. J., Marques, M. E., Melo, C., & Negrao, C. O. (2002). A CFD model for buoyancy drıven flows ınsıde refrıgerated cabınets and freezers. Retrieved July 7, 2011, from http://www.ppgem.ct.utfpr.edu.br/lacit/publicacoes/congressos .

Incropera, DeWitt, Bergman, & Lavine (2007). *Fundementals of heat and mass transfer* (6th ed.). WILEY.

International Institue of Refrigeration [IIR]. (November, 2003). How to improve energy efficiency in refrigerating equipment. *Informatory Note on Refrigerating Technologies, (17)*. Retrieved July 7, 2011, from http://www.iifiir.org/en/doc/1015.pdf

International Organization for Standardization 15502 [ISO 15502]. (2005). ISO 15502 - Household refrigerating appliances - Characteristics and test methods. ISO

James, S. J., & Evans, J. (1992). The temperature performance of domestic refrigerators. *International Journal of Refrigeration , 15* (5), 313-319.

James, S. J. (November, 2003). Developments in domestic refrigeration and consumer attitudes. *Bulletin of the IIR* (5). Retrieved July 7, 2011, from http://www.iifiir.org/en/doc/1051.pdf

James, S. J., Evans, J., & James, C. (2008). A review of the performance of domestic refrigerators. *Journal of Food Engineering (87)*, 2-10.

Koury, R. N., Machado, L., & İsmail, K. R. (2001). Numerical simulation of a variable sped refrigeration system. *International Journal of Refrigeration (24)*, 192-200.

Lacerda, V. T., Melo, C., Barbosa Jr, J. R., & Duarte, P. O. (2005). Measurements of the air flow field in the freezer compartment of a top-mount no-frost refrigerator: the effect of temperature. *International Journal of Refrigeration (28)*, 774-783.

Laguerre, O., Derens, E., & Palagos, B. (2002). Study of domestic refrigerator temperature and analysis of factors affecting temperature: a French survey. *International Journal of Refrigeration (25)*, 653-659.

Laguerre, O., Amara, S. B., & Flick, D. (2005). Experimental study of heat transfer by natural convection in a clossed cavity: application in a domestic refrigerator. *Journal of Food Engineering (70)*, 523-537.

Laguerre, O., Amara, S. B., Moureh, J., & Flick, D. (2007). Numerical simulation of air flow and heat transfer in domestic refrigerators. *Journal of Food Engineering (81)*, 144-156.

Laguerre, O., Amara, S. B., Charrier-Mojtabi, M. -C., Lartigue, B., & Flick, D. (2008). Experimental study of air flow by natural convection in a closed cavity: Application in a domestic refrigerator. *Journal of Food Engineering (85)*, 547-560.

Liu, Y., Chen, K., Xin, T., Cao, L., Chen, S., Chen, L., et al. (2011). Experimental study on household refrigerator with diffuser pipe. *Applied Thermal Engineering (31)*, 1468-1473.

Lorentzen, G. (1971). The role of refrigeration in solving the world food problem. *Proceedings of the XIII International Congress of Refrigeration.* Washington.

Navaz, H. K., Faramarzi, R., Gharib, M., Dabiri, D., & Modarress, D. (2002, September). The application of advanced methods in analyzing the performance of the air curtain in a refrigerated display case. *Transactions of the ASME* , 756-764.

Overview of materials for polystyrene, impact modified. (n.d.). Retrieved July 7, 2011, from http://www.matweb.com/search/DataSheet.aspx?MatGUID=be2fb354bdd54f4ba07710a547e1cb02&ckck=1

Paljak, & Peterson. (1972). *Thermography of buildings.* Stockholm.

Saedodin, S., Torabi, M., Naserian, R. S., & Salehi, P. (2010). A combined experimental and three-dimensional numerical study of natural convection heat transfer in a domestic freezer for optimization and temperature prediction. *International Review of Mechanical Engineering (I.RE.M.E.) (6)*.

Saravacos, George D., Kostaropoulos, A. E. (2002). Handbook of food processing equipment. Kluwer Academic/Plenum

Sekhar, S. J., Lal, D. M., & Renganarayanan, S. (2004). Improved energy efficiency for CFC domestic refrigerators retrofitted with ozone-friendly HFC134a/HC refrigerant mixture. *International Journal of Thermal Sciences (43)*, 307-314.

Shixiong, B., & Jing, X. (1990). Testing of home refrigerators and measures to improve their performance. *International Institue of Refrigeration [IIR] - Comissions B2, C2, D2/3 - Dresden (Germany)*, 411-5.

Stoecker, W. F. (1998). *Industrial refirgeration hanbook*. McGraw-Hill.

Tao, W.-H., & Sun, J.-Y. (2001). Simulation and experimental study on the air flow and heat loads of different refrigerator cabinet designs. *Chemical Engineering Communications , 1 (186)*, 171-182.

Tian, Y. S., & Karayiannis, T. G. (2000). Low turbulence natural convection in an air filled square cavity. Part I: The thermal and fluid flow fields. *International Journal of Heat and Mass Transfer (43)*, 849-866.

Versteeg, H. K., & Malalasekera, W. (1995). *An introduction to computational fluid dynamics:The finite volume method.* Longman Scientific & Technical.

Victoria, R. (1993). Ne joues pas avec le froid. 50 millions de consommateur. *(267)* , 36-7.

Yang, K.-S., Chang, W.-R., Chen, I.-Y., & Wang, C.-C. (2010). An investigation of a top-mounted domestic refrigerator. *Energy Conversion and Management (51)*, 1422-1427.